ROBUST SMITH PREDICTOR DESIGN WITH FINITE DIMENSIONAL FILTERS

A DISSERTATION SUBMITTED TO

THE GRADUATE SCHOOL OF ENGINEERING AND SCIENCE

OF BILKENT UNIVERSITY

IN PARTIAL FULFILLMENT OF THE REQUIREMENTS FOR

THE DEGREE OF

DOCTOR OF PHILOSOPHY

IN

ELECTRICAL AND ELECTRONICS ENGINEERING

By

Mustafa Oğuz Yeğin

January 2024

ROBUST SMITH PREDICTOR DESIGN WITH FINITE DIMENSIONAL FILTERS
By Mustafa Oğuz Yeğin
January 2024

We certify that we have read this dissertation and that in our opinion it is fully adequate, in scope and in quality, as a dissertation for the degree of Doctor of Philosophy.

Hitay Özbay(Advisor)

Arif Bülent Özgüler

Ömer Morgül

Mehmet Önder Efe

İsmail Uyanık

Approved for the Graduate School of Engineering and Science:

Orhan Arıkan
Director of the Graduate School

ABSTRACT

ROBUST SMITH PREDICTOR DESIGN WITH FINITE DIMENSIONAL FILTERS

Mustafa Oğuz Yeğin
Ph.D. in Electrical and Electronics Engineering
Advisor: Hitay Özbay
January 2024

The time delay is a widely recognized inherent phenomenon present in practical control systems, and it has been a subject of extensive research over the past century. Unless managed appropriately, even a minor delay can deteriorate performance and potentially lead to instability. Therefore, incorporating a model for time delay and designing the controller to mitigate its effects are crucial steps to attain the desired robustness and performance criteria in control theory. Additionally, owing to its infinite-dimensional structure, the majority of predictor-based controllers comprise finite impulse response filters, necessitating approximation with finite-dimensional transfer functions for seamless integration into physical systems.

Controller designs based on the Smith predictor can effectively cancel out the impact of dead-time delay. This study introduces an extension of the Smith predictor to formulate stabilizing controllers for Linear Time Invariant (LTI) Single-Input Single-Output (SISO) systems with multiple unstable modes and time delay. The main contribution of this approach lies in the streamlining of previous predictor-based control designs intended for unstable plants. The main contribution of this methodology lies in the simplification of previous predictor-based control designs tailored for unstable plants. The predictor filters are crafted by solving a Nevanlinna-Pick interpolation problem to attain optimal robust stability. The process also upholds the fundamental essence of the Smith predictor scheme, allowing the design of a controller based on the non-delayed nominal plant. Despite the susceptibility of Smith predictor-based designs to uncertain delays, the robustness of the proposed configuration surpasses that of the $\mathscr{H}_\infty$ optimal controller design, as demonstrated in the relevant section.

The proposed design is also extensible to a category of distributed parameter SISO systems and Multi-Input Multi-Output (MIMO) plants. For distributed parameter SISO systems, it is assumed that the plant's transfer function can be expressed through coprime factorization. The fundamental idea underlying this approach is treating the infinite-dimensional inner factor of the plant as a “time delay,” and, in turn, determining the predictor structure accordingly. The modeling and controller design steps

expounded here are exemplified using a flexible beam model. Regarding MIMO systems, provided specific conditions are met, the tangential Nevanlinna-Pick interpolation technique can be employed to derive the controller and filters according to the proposed configuration.

While numerous studies have addressed model order reduction in the context of $\mathscr{H}_\infty$-norm error, achieving optimal $\mathscr{H}_\infty$ approximation remains a challenging and unresolved problem. This study introduces an alternative model reduction method that seeks to minimize the $\mathscr{H}_\infty$ norm of the difference between the reduced model and the original Finite Impulse Response (FIR) structure. The proposed method essentially reduces the order of a given function by one with the minimum $\mathscr{H}_\infty$-norm error, employing a high-order Pade approximation of the time-delay term. As the method reduces the order by one, an iterative algorithm is devised to recursively decrease the order of a given plant from n to a desired order of m, repeating the procedure $(n-m)$ times following the outlined steps. The main contribution of the proposed technique is that it provides a new perspective against $\mathscr{H}_\infty$-norm approximation by using Chebyshev equioscillation theorem on rational functions.

Various examples are provided to elucidate the methodology of the suggested controller design and the robust stability condition in the context of approximating the infinite-dimensional predictor structure. Furthermore, the proposed model order reduction method is compared with the most recent state-of-the-art techniques within the literature. Finally, potential avenues for further research are deliberated, encompassing both the controller structure and $\mathscr{H}_\infty$ approximation.

Keywords: Systems with Time Delay, Smith Predictor, Robust Stability, Coprime Factorization, MIMO Systems, Finite Impulse Response, Pade Approximation, $\mathscr{H}_\infty$-norm Approximation, Model Order Reduction.

ÖZET

SONLU BOYUTLU FİLTRELER İLE GÜRBÜZ SMITH ÖNGÖRÜCÜSÜ TASARIMI

Mustafa Oğuz Yeğin
Elektrik ve Elektronik Mühendisliği, Doktora
Tez Danışmanı: Hitay Özbay
Ocak 2024

Zaman gecikmesi, pratik kontrol sistemlerinde bulunan yaygın bir içsel fenomen olarak kabul edilmekte ve geçmiş yüzyıl boyunca geniş çaplı bir araştırma konusu olmuştur. Uygun bir şekilde yönetilmediği takdirde, küçük bir gecikme bile performansı kötüleştirebilir ve potansiyel olarak kararsızlığa yol açabilir. Bu nedenle, zaman gecikmesi için bir modelin dahil edilmesi ve bunun etkilerini azaltan bir kontrolörün tasarlanması, kontrol teorisinde istenen gürbüzlük ve performans kriterlerine ulaşmak için hayati adımlardır. Ayrıca, zaman gecikmesinin sonsuz boyutlu bir yapıya sahip olması nedeniyle, çoğu öngörücü tabanlı denetleyici, sonlu dürtü yanıtlı (FIR) süzgeç içermekte ve fiziksel sistemlere sorunsuz bir entegrasyon için sonlu boyutlu transfer fonksiyonları ile yaklaşım gerektirmektedir.

Smith öngörücüsü temelli denetleyici tasarımları, gecikmeli süreçlerin etkisini etkin bir şekilde ortadan kaldırabilir. Bu çalışma, Smith öngörücüsünün bir genişlemesini tanıtarak, çoklu kararsız modlara ve zaman gecikmesine sahip doğrusal zamanda değişmez (DZD) zaman gecikmeli tek girişli tek çıkışlı (TGTÇ) sistemler için kararlılık sağlayan denetleyiciler formüle etmektedir. Bu yaklaşımın temel katkısı, kararsız sistemler için tasarlanmış olan önceki öngörücü tabanlı kontrol tasarımlarının basitleştirilmesindedir. Öngörücü filtreleri, eniyi sağlamlığı elde etmek için, bir Nevanlinna-Pick interpolasyon problemi çözülerek oluşturulmuştur. Süreç aynı zamanda Smith öngörücü şemasının temel özünü koruyarak, gecikmesiz nominal sistem temelli bir denetleyici tasarlama olanağı sunar. Smith öngörücü temelli tasarımların, bilinmeyen gecikmelere karşı duyarlı olmasına rağmen, önerilen konfigürasyonun sağlamlığı, ilgili bölümde gösterildiği gibi, $\mathscr{H}_\infty$ eniyi denetleyici tasarımının önündedir.

Önerilen tasarım, aynı zamanda bir sınıf dağılmış parametreli TGTÇ sistemler ve çoklu girişli çoklu çıkışlı (ÇGÇÇ) sistemler için genişletilebilirdir. Dağılmış parametreli TGTÇ sistemler için, sistemin transfer fonksiyonunun aralarında asal çarpanlara ayırma aracılığıyla ifade edilebileceği varsayılmaktadır. Bu yaklaşımın

temel fikri, sistemin sonsuz boyutlu içsel faktörünü bir "zaman gecikmesi" olarak ele almak ve bu sayede öngörücü yapısını buna göre belirlemektir. Burada açıklanan modelleme ve denetleyici tasarım adımları, esnek bir çubuk modeli kullanılarak örneklenmektedir. ÇGÇÇ sistemler için ise, belirli koşullar sağlandığında, önerilen konfigürasyona göre denetleyici ve filtrelerin türetilmesi için teğetsel Nevanlinna-Pick interpolasyon tekniği kullanılabilir.

Çeşitli çalışmalar, $\mathscr{H}_\infty$-norm hatası bağlamında model derecesi düşürme konusuna odaklanmış olsa da, eniyi $\mathscr{H}_\infty$ yaklaşımını elde etmek hala zorlu ve çözümlenmemiş bir sorundur. Bu çalışma, azaltılmış model ile orijinal FIR yapısı arasındaki farkın $\mathscr{H}_\infty$ normunu en aza indirmeyi amaçlayan alternatif bir model derecesi düşürme yöntemi sunmaktadır. Önerilen yöntem, zaman gecikmesi teriminin yüksek dereceli Pade yaklaşımını kullanarak, verilen bir fonksiyonun derecesini minimum $\mathscr{H}_\infty$-norm hatası ile bir azaltır. Yöntem, dereceyi bir azalttığı için, belirli bir sistemin derecesini n'den istenen bir dereceye (m) kadar azaltmak için, adımları tekrarlamak üzere tasarlanmış yinelemeli bir algoritma içerir. Önerilen tekniğin temel katkısı, Chebyshev eşsalınımlık teoreminin kullanımı ile $\mathscr{H}_\infty$-norm yaklaşımına karşı yeni bir bakış açısı sunmasıdır.

Önerilen denetleyici tasarımının metodolojisini ve sonsuz boyutlu öngörücü yapısının yaklaşımı bağlamında önerilen gürbüzlük koşulunu açıklamak amacıyla çeşitli örnekler sunulmuştur. Ayrıca, önerilen model derecesi düşürme yöntemi, literatürdeki en güncel yöntemlerle karşılaştırılmıştır. Son olarak, hem denetleyici yapısı hem de $\mathscr{H}_\infty$ yaklaşımını kapsayan ileriye yönelik potansiyel araştırma alanları üzerinde durulmuştur.

Anahtar sözcükler: Zaman Gecikmeli Sistemler, Smith Öngörücüsü, Gürbüz Kararlılık, Asal Çarpanlara Ayırma, ÇGÇÇ Sistemler, Sonlu Dürtü Yanıtı, Pade Yaklaşımı, $\mathscr{H}_\infty$-norm Yaklaşımı, Model Derecesi Düşürme.

Acknowledgement

First of all, I would like to express my sincere thanks to my supervisor, Prof. Hitay Özbay for his patience, unwavering guidance, motivational influence, invaluable suggestions and continuous support throughout my academic journey. This work would have been impossible without his assistance on multiple fronts.

I am indebted to the distinguished members of my thesis jury Prof. Arif Bülent Özgüler, Prof. Ömer Morgül, Prof. Mehmet Önder Efe and Assoc. Prof. İsmail Uyanık for accepting to serve as jury members in my PhD thesis defense and their guidance.

I wish to convey my profound gratitude to Prof. Orhan Arıkan, who had been my advisor throughout my undergraduate education, for his unwavering guidance and steadfast support during the entirety of my academic career.

I extend my sincere appreciation for the invaluable knowledge and support imparted by all my instructors during both my undergraduate and graduate studies. Additionally, I express gratitude to the Electrical and Electronics Engineering Department at Bilkent University for their financial support, alongside their commitment to delivering high-quality education. I am also thankful to ABMN for providing the opportunity to pursue my PhD studies. Lastly, I wish to convey my sincere thanks to my colleagues at ABMN for their understanding and cooperative spirit.

Additionally, I am very thankful to the current and former members of our research group, Bahadır Çatalbaş, Burak Çatalbaş, Ali Nail İnal, Caner Odabaş, Hasan Eftun Orhon, Dilan Öztürk Şener, and Ahmet Safa Öztürk for our wonderful times at Bilkent University.

I express my gratitude to Mürüvet Parlakay, Aslı Tosuner, Aydan Gençel, and Armağan Gürsoy for their contributions to administrative tasks. Additionally, I appreciate the technical support provided by Ergün Hırlakoğlu, Onur Bostancı, Metin Kayabaşı, and Ufuk Tufan.

I would like to thank The Scientific and Technological Research Council of Turkey (TÜBİTAK) for their financial support through the scholarship for PhD Students between 24.01.2018 - 23.01.2022, National Scholarship Program (2211/A). Furthermore, during the last two months of my PhD study, I was supported by a scholarship through TÜBİTAK-ARDEB 1001 project 123E233.

I wish to extend my appreciation to Hamdi Armağan Gürdal for his abundant assistance, thoughtful advice, and guidance throughout the entirety of my academic tenure.

Finally, I am grateful to my parents Haluk, Ayşenur, my brother Emre for their endless support and encouragement throughout my life. Furthermore, I wish to extend my appreciation to my brother's wife, Ecem, for her support, providing assistance as though she has been a longstanding presence among us.

Contents

List of Figures

List of Tables

Acronyms

CSP Classical Smith Predictor. 5, 6

FIR Finite Impulse Response. iv, 4–6, 8, 21, 29, 43, 80

FSP Filtered Smith Predictor. 6

HNA Hankel Norm Approximation. 4, 7, 75, 80

IIR Infinite Impulse Response. 8

IRKA Iterative Rational Krylov Algorithm. 7, 76

LFT Linear Fractional Transformation. 21

LMI Linear Matrix Inequality. 2

LTI Linear Time Invariant. iii, 11, 40, 79

MIMO Multi-Input Multi-Output. iii, 3, 5, 9, 10, 53, 79, 81

MSP Modified Smith Predictor. 6

PDE Partial Differential Equation. 7, 40, 41

RHP Right Half Plane. 70

SISO Single-Input Single-Output. iii, 3, 4, 8, 24, 40, 79

USP Unified Smith Predictor. 6

Chapter 1

Introduction

1.1 General Scope of the Thesis

Almost in any field, engineers encounter the phenomenon called time-delay, which in most cases needs to be taken into consideration to provide the optimal solution according to desired specifications. In control design systems, the limitations of the actuator, processing of the signals through sensors, and the process itself are some of the main sources of such delays. Since time delay occurs in many control applications, delay systems have been an active area of research for around 80 years. Due to its infinite dimensional nature, even a small amount of delay may complicate the modeling of the system, and the analytical aspects of controller design. Therefore, throughout the last century, various features of time-delay systems such as robust stability and design of optimal controller, have been focused by different methods. Solutions by using Linear Matrix Inequality (LMI) and improvements on Smith predictor designs are some of the latest research activities in this area within the last 20 years.

In 1957, Smith published an astonishing method that is even being focused on today to be improved for the sake of designing robust controllers on dead-time delay systems. The block diagram of the proposed design back then is given in Fig. 1.1. If the model proves to be highly accurate, this configuration results in a closed-loop transfer function, effectively excluding time delay from the feedback loop, i.e. the internal controller K is designed to stabilize P_o such that K does not depend on the time delay h.

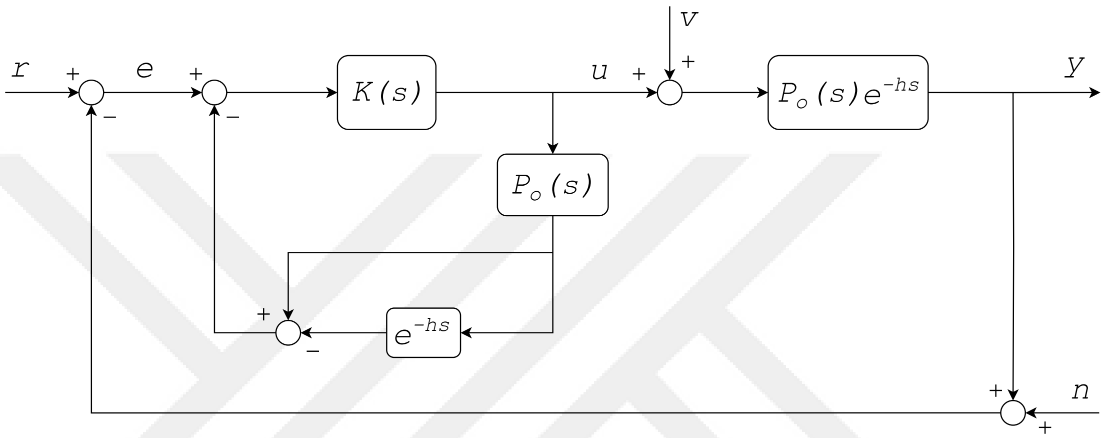

Figure 1.1: Classical Smith Predictor Structure for Stable P

This thesis introduces a new simplified controller design procedure based on Smith principle that focuses on robust stability. Typically, the block diagram of the generalized Smith predictor design appears as shown in Fig. 1.2 in the literature. Apart from the related works, the proposed method employs Nevanlinna-Pick interpolation for Single-Input Single-Output (SISO) dead-time systems in order to design the haptic filter, $H_2(s) = H(s)$, which is also used to derive the predictor filter as

$$H_1(s)P_o(s) := \left(1 - H(s)e^{-hs}\right) P_o(s). \tag{1.1}$$

The design process is also extended to Multi-Input Multi-Output (MIMO) systems by applying tangential Nevanlinna-Pick interpolation. The main contribution of this method is that both the design of predictor and haptic filters, and the robust stability analysis are simplified compared to related works in the literature, which are explained in detail in section 1.2. Additionally, this controller structure preserves the original spirit of the Smith predictor, that aims to provide a smooth design procedure for the internal controller in which only the unstable modes of the non-delayed part of the plant are taken into consideration during stabilization and optimization of given design criteria such as tracking performance, disturbance rejection, etc.

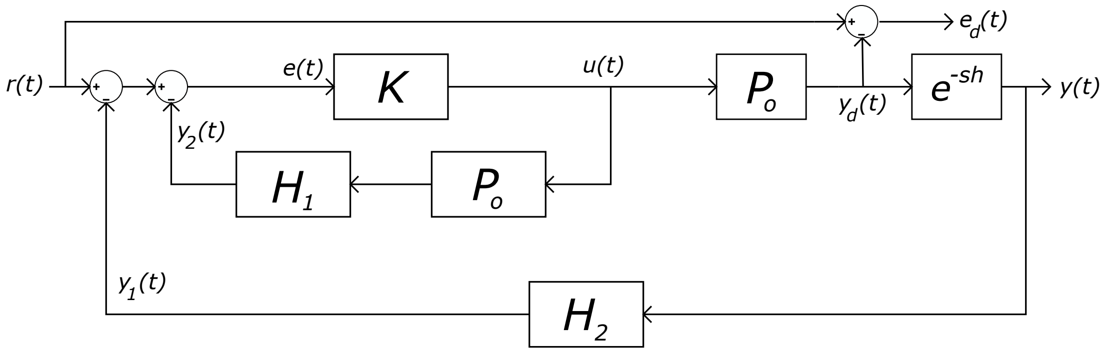

Figure 1.2: Generalized Smith Predictor Scheme for Possibly Unstable P_o

Predictor based controller structures mostly contain a Finite Impulse Response (FIR) component in the case of a time-delay, due to its infinite dimensional characteristic. This circumstance entails the necessity of an approximation method to be used on filter to obtain a finite order model to require fewer memory elements during implementation on physical systems. Even though there exist numerous papers on approximating FIR structures, derivation of the optimal solution is still an open problem. Furthermore, in the proposed method, the filter H_1P_o consists of both an FIR and an additive stable function. With the objective of representing H_1P_o by a low order rational function, while preserving robust stability condition, the rest of this thesis focuses on model order reduction techniques in $\mathscr{H}_\infty$. A new method is proposed by using eigenvalues, which has similarities with the Hankel-norm approximation, and minimax algorithm to reduce high order finite dimensional stable transfer functions. In addition to classical methods such as balanced truncation and optimal Hankel Norm Approximation (HNA), several state-of-the-art methods are used to compare resulting $\mathscr{H}_\infty$-norm error through two different examples. Existing research results in this field are explained in detail in section 1.3.

In the second chapter, the proposed design for SISO unstable systems with time delay is described by taking various aspects of the overall system in consideration: the closed loop stability, robustness condition, disturbance rejection capabilities, etc. Moreover, it is shown how similar but more complex methods may lead to the same configuration through an example. Furthermore, a conservative bound on robust stability condition for the approximation of the predictor filter is given. Lastly, this chapter compares the time domain responses of the proposed design with the closed loop system obtained by $\mathscr{H}_\infty$ optimal controller on several dead-time delay plants with variance on time delay. The third chapter extends the scope of covered systems within the configuration, to MIMO plants and to infinite dimensional systems with Blaschke products. The $\mathscr{H}_\infty$ approximation methods on the infinite dimensional predictor filter, which can be decomposed into an FIR and a stable function, are compared within the fourth chapter. A new method on $\mathscr{H}_\infty$ approximation for model order reduction is also explained. Finally, further developments on the proposed design to extend the set of applicable systems, such as MIMO systems with internal delays, are given in the conclusion chapter.

1.2 Literature Survey of Improvements on Smith Predictor

The Classical Smith Predictor (CSP) approach employs a distinctive control structure in which the free part of the controller is designed only for the non-delayed plant [52]. The main contribution of this method was to compensate the dead-time by using the so-called Smith predictor, and hence provide a design procedure solely for the non-delayed component of the system. Even though the idea behind this structure was groundbreaking, the initial setup was only valid for stable systems. Moreover, an accurate model was mandatory due to its robustness. Therefore, starting from 1980s, efforts have been undertaken to expand its potential domains and enhance its versatility across various fields, to broaden the applicability of this method. Numerous approaches, based on Smith's principle, have been proposed to improve feedback loop performance. These include improving disturbance rejection capabilities, reducing steady-state error for diverse periodic signals, and simplifying the structure of the controller.

Watanabe and Ito [56] proposed a design to enhance system performance and relax observability conditions on the plant states. Matausek and Micic [36] refined the Smith predictor design, particularly for systems with long dead time. Léchappé et al. [31] adapted the predictor scheme to improve performance in the presence of unknown disturbances, employing the Arstein reduction method.

Several researchers, including those previously mentioned, have dedicated their research efforts in exploring the application of the Smith predictor in systems featuring unstable modes. Special attention is required when implementing controllers for such systems to ensure the stability of the inner loop of the predictor, as emphasized in [44]. The Modified Smith Predictor (MSP), initially proposed by Meinsma and Zwart [37], has undergone further generalization by Mirkin and Raskin [39]. In their approach, two FIR filters were introduced to identify the observer-predictor structure of all stabilizing controllers. Additionally, Zhong [60], and Zhong and Weiss [61] introduced the Unified Smith Predictor (USP), utilizing both CSP and MSP to simplify numerical computations, particularly for systems with high-frequency modes. Normey-Rico and Camacho [43] extended USP and introduced the Filtered Smith Predictor (FSP), where a low-pass filter was designed to filter the measured time-delay output. Garcia and Albertos [19] proposed another controller structure using coprime factorization to design FIR and haptic filters, focusing on discrete-time systems. This work was subsequently extended to continuous-time systems by Sanz et al. [48]. The primary drawback of these methods (except for [48, 56]) lies in the fact that the internal finite-dimensional controller design depends not only on the non-delayed unstable plant but also on the specific value of the time delay, thereby deviating from the original concept of the Smith predictor scheme. In [48], the internal controller design is independent of the delay value; however, the design steps are intricate, making robustness analysis a challenging task. The robust stability of predictor based systems in case of parametric uncertainties is deeply investigated in [28].

1.3 Literature Survey of Model Order Reduction

Modeling plays a crucial role in examining and handling practical systems within computational environment. In the field of control theory, these models need to accurately depict the physical attributes of systems to meet stability conditions and performance criteria. Nevertheless, this requirement leads to an increase in the scale and complexity of these models, often resulting in cost-inefficiency. Furthermore, as time delays are prevalent in many physical systems, the majority of controller designs based on predictors involve structures with infinite dimensions. To employ these designs in practical control systems, it is necessary to represent them using finite order transfer functions. Consequently, numerous researchers have directed their efforts toward model order reduction, which essentially seeks to reduce the dimensions of the system representation with the primary goal of minimizing the error on a specified basis.

The proposed methods under model reduction may be categorized as system-theoretic and Partial Differential Equation (PDE) approaches [9]. The system-theoretic approach relies on a state-space representation, and its goal is to minimize the number of states to a level where the error between output signals is considered "low", which is the class of methods covered within this thesis. [2, 46, 49] comprehensively address a variety of methodologies proposed for the reduction of model order. Apart from the techniques described within these references, It is noteworthy to highlight curve-fitting methods, which aim to minimize the least squares error between frequency responses of the original system and the reduced-order model [23]. There also exists an abundance of procedures for the minimization of approximation errors, with only a limited selection detailed in [4, 11]. Considering the numerous approaches reducing model order and the specific focus of this thesis on modeling the infinite-dimensional stable transfer functions with low order rational functions, only the following methods have been emphasized.

- Truncation of states that have negligible effect on outputs: Balanced reduction and HNA are the most commonly used techniques under this category [3, 24, 40].
- Data-driven approaches that enforce suitable interpolation conditions: Zero-moment matching algorithms [50] and Iterative Rational Krylov Algorithm (IRKA) [3] are some of the recent works used within this area.
- Minimization of the $\mathscr{H}_2$ or $\mathscr{H}_\infty$ norm of the approximation error: Most of the procedures including data-driven approaches employ optimization techniques in order to minimize the approximation error according to a specified norm. For example, HinfIRKA, which is an extension of IRKA to minimize $\mathscr{H}_\infty$-norm error can be found in [3]. Furthermore, the MATLAB commands `fitfrd` and

`ssest`, which are used in section 4.3, extracts a model with desired order according to the frequency response of the given system under certain conditions. Lastly, `systune` can be used to reduce the order of a high order finite dimensional structures by applying non-smooth optimization techniques.

Beyond the references mentioned earlier, works such as [7, 38, 42, 57] delve into related topic, concentrating on the approximation of FIR structures to low-order Infinite Impulse Response (IIR) designs through diverse methodologies.

1.4 Key Contributions

One of the primary drawbacks of modified Smith predictor structures is the requirement for a precise model, leading to their application being specifically associated with dead-time delays. Hence, ensuring robustness in such configurations becomes a crucial consideration in the controller design process. One of the main contributions of this work is the novel design that is based on Smith predictor, in which the design process of the filters and robust stability analysis are less complex. This new design is able to keep the original essence of the Smith predictor design, where the inner controller block is solely designed to stabilize the non-delayed component of the plant, according to specified tracking and robustness performances. Hence, when the nominal model precisely represents the plant, the performance of the nominal closed loop aligns with the overall structure's performance. In this design, the haptic filter relies solely on the unstable modes of the plant and the time delay, leading to the resolution of interpolation conditions through Nevanlinna-Pick interpolation. This requirement results in the haptic feedback being an all-pass filter, simplifying the analysis of robust stability.

This research also demonstrates the applicability of the proposed design to a category of distributed parameter SISO systems with time delay. Illustrated with an example of a flexible beam, it is revealed that if the plant can be expressed in terms of coprime factors, such as $P = MN/D$, where M is the inner factor, N is the outer factor, and D is a rational stable factor, the inner factor M can be considered as a "time delay." Even when N is infinite-dimensional, a finite-order approximation of it can be used to derive a predictor-like filter using the proposed methodology.

Under certain commutativity conditions, the suggested design is also applicable on MIMO systems. In this case, as shown through an example, tangential Nevanlinna-Pick interpolation method is used to derive the haptic filter $H(s)$.

Given the requirement for a finite-order representation of the predictor filter, a novel approach to $\mathscr{H}_\infty$ approximation has been developed. Inspired by the principles of Nevanlinna-Pick interpolation and the Chebyshev equioscillation theorem, a set of equations has been formulated. One of the primary contributions of this formulation is to introduce a fresh perspective on $\mathscr{H}_\infty$ approximation techniques, an area of active research for the past four decades. It also highlights how Hankel norm approximation is often regarded as an effective model order reduction technique in the $\mathscr{H}_\infty$-norm context.

Chapter 2

Smith Predictor Based Controllers for SISO Unstable Systems with Dead-Time

One of the main disadvantages of the Smith-predictor based configurations is the necessity of an accurate model for the stability of the overall system. Therefore, a robust design is mandatory in such designs to avoid any instability caused by parametric uncertainties. Especially, since $H(s)$ strongly relies on initial time-delay, such structures mostly cannot be applied on systems with uncertain time-delays. In order to enhance the scope of appropriate systems to be used within this design, the main motivation behind our proposed method is to simplify both the design process and the robustness analysis of the overall feedback loop.

In the first section, the set of covered systems are explained, which can also be extended to MIMO cases as in the next chapter, and the problem is defined. The second section illustrates the proposed structure and shows the stability conditions of the closed loop system. The reason behind using Nevanlinna-Pick interpolation on haptic filter design and the robustness analysis of the overall system are given in the third section. Due to the structure of the predictor filter, to implement it on practical systems, an approximation method needs to be used. The fourth section derives a boundary on the approximation error to meet the robust stability condition. Finally, the responses of the dead-time delayed plants with the proposed controllers and filters, and with the optimal $\mathscr{H}_\infty$ controller in time domain are compared in the fifth section.

The notation used here is standard. In particular, $\mathscr{H}_\infty$ denotes the Hardy space of bounded analytic functions on

$$\mathbb{C}_+ := \{s \in C : Re(s) > 0\}.$$

For $F \in \mathscr{H}_\infty$, we have

$$\|F\|_\infty = \text{ess} \sup_{Re(s)>0} |F(s)|.$$

For the classes of transfer functions considered in this thesis, the norm of $F \in \mathscr{H}_\infty$ is achieved on the imaginary axis:

$$\|F\|_\infty = \sup_{\omega \in \mathbb{R}} |F(j\omega)|.$$

The standard feedback system with LTI controller C and LTI plant P, shown in Fig. 2.1, is denoted by $(C,P)_{CL}$, and it is stable if and only if $S = (1 + PC)^{-1}$, PS, and CS are in $\mathscr{H}_\infty$.

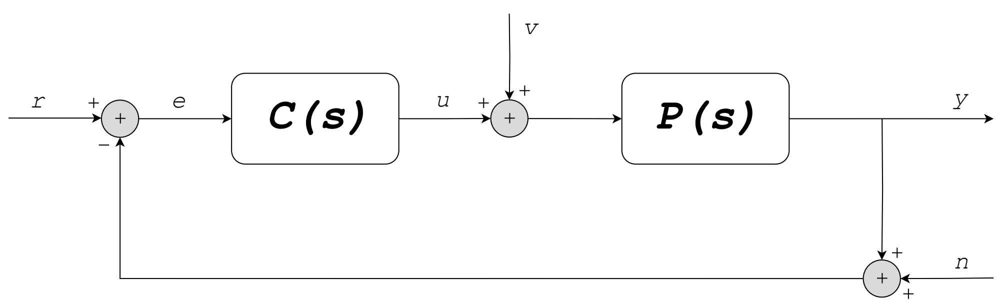

Figure 2.1: Standard Feedback System

2.1 Problem Formulation

The general closed loop configuration of the predictor-based control scheme is shown in Fig. 2.1, where $P_o(s)$ represents the delay-free plant with a limited amount of unstable modes and h is the time-delay. The closed right half plane poles of the plant are denoted as $p_i \in \mathbb{C}_+$, $i = 1,\ldots,m$. For the sake of simplicity in the presentation, it is assumed that p_i's are distinct, and P_o does not have any poles on the Im-axis.

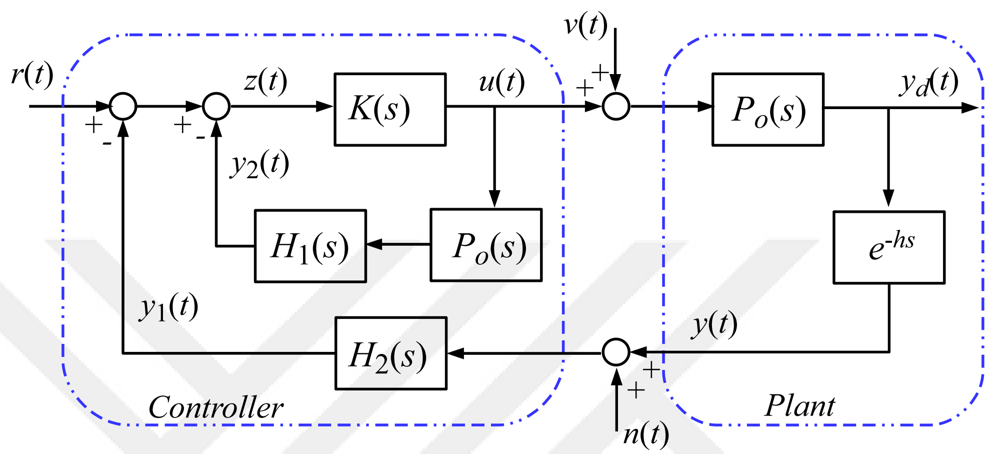

Figure 2.2: General configuration of the predictor-based controller design

As mentioned in the previous chapter, the main contribution of Smith predictor structure is to eliminate high dead-time delay during the design of the internal controller $K(s)$, implying that this configuration allows $K(s)$ to be designed for stabilizing solely the non-delayed component $P_o(s)$. Furthermore, most of the performance capabilities of the closed loop $(K,P_o)_{CL}$ are preserved within the overall closed loop.

In case the system $P_o e^{-hs}$ is stable and $H_1(s) = 1 - e^{-hs}$, $H_2(s) = 1$, this configuration leads to a stable closed loop system with transfer function from r to y being $T_{ry}(s) = e^{-hs}T_o(s)$, where $T_o = P_oK(1+P_oK)^{-1}$, i.e, time delay is taken out of the feedback loop. Many contributions in the literature, as mentioned above, dealt with various extensions by investigating how K, H_1 and H_2 should be designed in Fig. 2.1 when P_o is unstable. When $r \neq 0$ and $v = n = 0$, the signals in the loop satisfy

$$Y_1(s) = H_2(s)P_o(s)e^{-sh}U(s) \quad (2.1)$$

$$Y_2(s) = H_1(s)P_o(s)U(s) \quad (2.2)$$

$$Z(s) = R(s) - (H_1(s) + H_2(s)e^{-sh})P_o(s)U(s) \quad (2.3)$$

Assume that K is a stabilizing controller for P_o, and choose

$$H_1(s) = 1 - H_2(s)e^{-sh}. \quad (2.4)$$

Then, $Y_d(s) = T_o(s)R(s)$, i.e., time delay is taken out of the loop as in the classical Smith predictor. Now the question is how to choose H_2 so that the feedback system is stable.

In [39] the haptic filter H_2 of Fig. 2.1 is not used, but H_1 is designed in a special way, and K stabilizes a transformed version of the non-delayed part of the system (the design of K depends on the delay h, as well as P_o). In [43] authors have suggested a method in which $H_2(s)$ is designed as a low pass filter. Lastly, [48] uses coprime factorizations to construct $H_2(s)$. In the present work, $H_2(s)$ is designed by using Nevanlinna-Pick interpolation, that guarantees feedback system stability and optimizes the robustness margin, in the sense to be seen below.

Under the structure of Fig. 2.1, transfer functions from r to z and from r to y are

$$S := T_{rz} = \frac{1}{1+P_oK(H_1+H_2e^{-sh})}\,, \qquad T := T_{ry} = \frac{P_oKe^{-sh}}{1+P_oK(H_1+H_2e^{-sh})} \tag{2.5}$$

respectively. By using (2.4), we obtain $S = \dfrac{1}{1+P_oK} =: S_o$ and

$$T(s) = \left(\frac{P_o(s)K(s)}{1+P_o(s)K(s)}\right)e^{-sh} = T_o(s)e^{-sh}, \tag{2.6}$$

respectively, where T_o represents the complementary sensitivity function of non-delayed feedback system formed by the controller K and plant P_o.

To recapitulate, the problem is reduced to the following: let the controller K be designed by using conventional methods to stabilize the non-delayed plant P_o, then, design the predictor elements $H_1(s)$ and $H_2(s)$ such that the overall feedback system is stable, and a robust stability condition is satisfied (by considering uncertainties in the plant model and time delay).

2.2 Proposed Design

The conventional Smith predictor structure is not applicable to unstable systems without appropriate modifications, given that the delay-free part of the plant model serves as a multiplicative factor in the filter design within the controller, indicating that the unstable modes of the plant would lead to an unbounded controller output. To address this concern, we suggest a novel design in which the filter $H_1(s) = 1 - H_2(s)e^{-hs}$ is formulated from $H_2(s) =: H(s)$, based on a Nevanlinna-Pick interpolation. The efficacy of this method on both simplification of internal controller design and robustness analysis is highlighted within this section.

In the proposed configuration in accordance with the Smith predictor, as illustrated in Fig. 2.3, there exists a haptic feedback which is denoted by $H(s)$, and a main feedback controller

$$C_o(s) = \frac{K(s)}{1+(1-e^{-sh}H(s))P_o(s)K(s)}. \tag{2.7}$$

in which the internal controller K, as mentioned in problem formulation, is designed such that the closed loop $(K, P_o)_{CL}$ is both robustly stable and able to meet the specifications such as tracking performance.

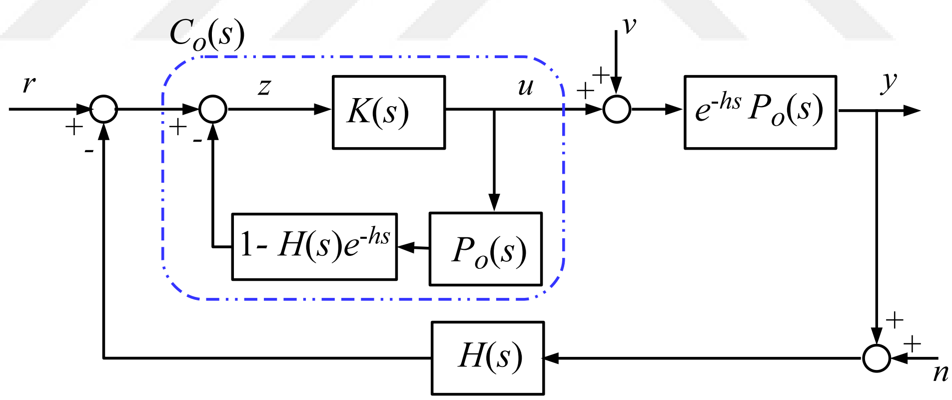

Figure 2.3: Proposed configuration of the Smith predictor based controller design

The filter H needs to be derived prudently to stabilize overall configuration, and to fulfill the main idea behind the Smith predictor, which is mathematically represented as in (2.6). Within the proposed setup, these conditions may only be satisfied when both the filters $F(s) := H_1(s)P_o(s)$ and $H(s)$ are stable, and $H_1(s)$ is defined as in (2.4). In order to guarantee stability of $F(s)$, unstable poles of the nominal plant $P_o(s)$, which are denoted as p_i, need to be canceled internally. When $H(s)$ is stable, this operation would remove all unstable poles of $F(s)$ and lead to a stable filter $F(s)$. Therefore, the following interpolation conditions must be satisfied:

$$H(p_i) = e^{hp_i}, \quad i = 1, \ldots, m, \tag{2.8}$$

where p_i denotes the unstable poles of the nominal plant $P_o(s)$.

Under previously defined conditions, the 9 transfer functions from external signals,

- r: Input Signal,
- v: Disturbance Signal,
- n: Measurement Noise Signal,

to internal signals,

- z: Error Signal of the Internal Controller,
- u: Output Signal of the Main Controller,
- y: Output Signal of the Closed Loop System,

can be derived as

$$T_{nz} = -HT_{rz} = -HS_o, \tag{2.9}$$

$$T_{nu} = -HT_{ru} = -H\left(KS_o\right), \tag{2.10}$$

$$T_{vu} = T_{ny} = -HT_{ry} = -H\left(T_o e^{-sh}\right), \tag{2.11}$$

$$T_{vz} = -H\left(P_o S_o e^{-sh}\right), \tag{2.12}$$

$$T_{vy} = P_o S_o e^{-sh} + T_o e^{-hs}\Big((1 - He^{-hs}P_o)\Big). \tag{2.13}$$

The closed loop system, given in Fig. 2.3, is stable if and only if the poles of all these transfer functions are located on the open left half-plane. When H is a stable transfer function, and K stabilizes the non-delayed plant P_o, meaning that both T_o and S_o are stable, it is guaranteed that all of the transfer functions above are stable, except T_{vy}. In order to assure the stability of T_{vy}, the predictor filter

$$F(s) = H_1(s)P_o(s) = (1 - H(s)e^{-hs})P_o(s) \tag{2.14}$$

also needs to be stable. This condition is satisfied by the construction of $H(s)$ from the interpolation conditions in (2.8).

At this point, establishing a stable H that fulfills (2.8) can be framed as a Lagrange interpolation problem. Nevertheless, as depicted in the next section, to meet the robust stability condition, it is crucial to derive a viable H that also meets an $\mathscr{H}_\infty$-norm criterion. Therefore, the Nevanlinna-Pick interpolation is a suitable technique to be used during the design of $H(s)$. The optimal Nevanlinna-Pick interpolation return in an all-pass H, as illustrated in the next section. It is crucial to emphasize on a similarity between the proposed configuration in Fig. 2.3, and the controller design appears in [37], where the authors use $P_o(s)(F(s)-e^{-hs})$ in the feedback path of C_o. The proposed structure within this paper would be equivalent to our design when $F=1/H$ and K/F stabilizes P_o. However, in the work presented by [37], the main emphasis is on H_∞ controllers, while in this context, our focus lies on the design of H.

Another thing to highlight before closing this section is that when the plant has only a single pole at the right half-plane, (i.e., $m=1$), the same controller structure appears in [45]. Similarly, when $m=1$, the configuration proposed within this thesis is basically equivalent to the one introduced in [56], where $H(s)$ is equal to a constant, within an analogous control system framework.

In addition, the design approach outlined in [48] bears a resemblance to the proposed structure and design procedure here: in [48], both the predictor filter F and the haptic feedback H are designed by coprime factorization and through the definition of an entire function. The present work relies on an alternative design for H_1, incorporating H to stabilize the predictor. A detailed examination of the distinctions and parallels with [48] will be presented in the fourth section through a numerical example.

2.3 Robustness Analysis

The differences between the mathematical model and the actual plant may cause an instability, which leads to an unbounded controller output that mostly harms the physical system. The main reasons behind this discrepancy may be summarized as poor estimation of the model, uncertainties within the plant, or the time-varying modes of the system. In order to keep the external signals bounded, one of the paramount objectives in controller design is to guarantee stability robustness in such instances. This is especially pertinent in predictor-based structures, where addressing potential delay mismatches between the actual plant and the nominal plant model becomes a critical concern, as discussed in [1], [16], [27], and related references. Furthermore, in interpolation-based procedures, uncertainty regarding the location of unstable poles may result in a delicate design. Therefore, one of the main objectives of the proposed method is to assure robust stability considering these two crucial aspects. This section focuses on robustness against multiplicative plant uncertainties, which consist of both the delay mismatch and possible variations of the unstable pole locations. It also captures the unmodeled dynamics.

Consider a set of uncertain plants denoted as $\mathscr{P}_\Delta$ whose elements are structured as

$$P_\Delta(s) = (1+\Delta_m(s))P_o(s)e^{-hs} \tag{2.15}$$

where Δ_m denotes the multiplicative plant uncertainties, such that P_Δ and P_o both have m-unstable poles (not necessarily at the same locations) and

$$|\Delta_m(j\omega)| < |W_m(j\omega)|, \ \forall\ \omega, \text{ for all } P_\Delta, \tag{2.16}$$

with a known fixed uncertainty bound $W_m(s)$. The multiplicative uncertainty Δ_m represents the unmodeled dynamics in the delay-free part of the plant, as well as the delay mismatch and imprecise unstable pole locations.

Let K and H be designed such that K stabilizes the nominal feedback system, as described in the previous section, where $H \in \mathscr{H}_\infty$ fulfills the interpolation conditions defined in (2.8). The nominal open loop transfer function of this structure is

$$G_o = HC_oP_oe^{-sh}, \tag{2.17}$$

which, by using (2.7), can be rewritten as

$$G_o = \frac{HKP_o e^{-sh}}{1+KP_o(1-He^{-hs})}. \tag{2.18}$$

Because that the nominal plant P_o is assumed to be strictly proper, the number of unstable poles of G_o is finite. In addition, by the nominal system stability, the number of encirclements of (-1) in the counter-clockwise direction in Nyquist graph of $G_o(j\omega)$ is the same as the amount of unstable poles of G_o. Under the uncertain plant, the open loop transfer function becomes

$$G_\Delta := HC_oP_\Delta, \tag{2.19}$$

where P_Δ can be replaced with (2.15), which leads to

$$G_\Delta = G_o(1+\Delta_m). \tag{2.20}$$

Note that the number of anti-stable poles of both G_Δ and G_o are equal. Moreover, the Nyquist plots of $G_\Delta(j\omega)$ and $G_o(j\omega)$ have the same number of clockwise and counter-clockwise encirclements of (-1), when the following condition is satisfied,

$$\left|\frac{G_o(j\omega)W_m(j\omega)}{1+G_o(j\omega)}\right| \leq 1 \quad \forall\ \omega,$$

due to the definition of W_m in (2.16). The condition above is mandatory, i.e., if it is not satisfied a Δ_m that destabilizes the closed loop system can be found, see e.g. [17].

It is a simple exercise to show that

$$\frac{G_o}{1+G_o} = \frac{KHP_o e^{-hs}}{1+KP_o} = H\ T_o\ e^{-hs}.$$

Thus, the proposed structure is robustly stable if and only if

$$\|W_m\ H\ T_o\|_\infty \leq 1. \tag{2.21}$$

Hence, when the condition

$$\|H\|_\infty \leq \frac{1}{\|W_m\ T_o\|_\infty} =: \rho \tag{2.22}$$

is satisfied, (2.21) is also guaranteed. Therefore, one way to design H is to meet the following three criteria:

- $H \in \mathscr{H}_\infty$,
- $H(p_i) = e^{hp_i}$, $i = 1,\ 2,\ \ldots,\ m$,
- $\|H\|_\infty \leq \rho$

This poses a Nevanlinna-Pick interpolation problem, as discussed in [17], and its feasibility is contingent upon the parameter ρ, which, in turn, relies on the magnitude of the multiplicative uncertainty W_m (assuming that K has been previously designed to determine T_o). If $W_m(s) = \alpha \widetilde{W}_m(s)$ where $\alpha > 0$ is a variable gain and $\widetilde{W}_m(s)$ is a fixed function, then, to optimize the degree of uncertainty represented by α, the aim is to design a stable H that satisfies (2.8) with the minimal attainable ∞-norm. A simplified solution for this optimal Nevanlinna-Pick interpolation problem can be found in [45]. This method returns the optimal H in the form

$$H_{opt}(s) = \gamma_{opt}\, M_o(s), \tag{2.23}$$

where M_o is an $(m-1)$-order all-pass transfer function, meaning that $|M_o(j\omega)| = 1$ for all ω, and the poles of M_o are in $\mathbb{C}_-$, and the zeros are located in $\mathbb{C}_+$ such that their locations are symmetrical to poles' with respect to imaginary axis. This resulting $H(s)$ is determined uniquely from a set of linear equations. The inner function M_o and the smallest achievable norm γ_{opt} depend on the problem data

$$\{p_1, \ldots, p_m\} \to \{e^{hp_1}, \ldots, e^{hp_m}\}. \tag{2.24}$$

The above discussion can now be summarized with the following results.

Proposition 1 *Consider the controller illustrated in Fig. 2.3, incorporating a predictor and configured with $H = H_{opt}$ determined through optimal Nevanlinna-Pick interpolation, as outlined in [45]. When the condition $\gamma_{opt} \leq \rho$ is satisfied, the feedback system remains stable for all uncertain plants characterized by the structure denoted as P_Δ in equation* (2.15). □

Remark 1 *It is worth highlighting the fact that the value of γ_{opt} solely depends on the location of unstable poles, and the nominal value of the time delay, h, due to the* *interpolation conditions $H(p_i) = e^{hp_i}$. Nevertheless, ρ defined in* (2.22) *is evaluated according to the upper bound of the multiplicative uncertainty, denoted as W_m, and the nominal closed loop transfer function $T_o = P_oK(1+P_oK)^{-1}$. Hence, if the robust stability criterion $\gamma_{opt} \leq \rho$ is not satisfied for a specified W_m, it becomes necessary to revisit and modify the design of K. One way to guarantee this condition is to define $W_t = \alpha W_m$, where $\alpha > 1$ and construct K according to the upper bound W_t recursively while increasing the value of α at each iteration. Certainly, the minimum achievable value for ρ can be derived through $\mathscr{H}\infty$ optimization for the controller K as discussed in [17]. Although it is feasible to directly formulate an H_∞ controller when prioritizing robust stability alone, as demonstrated in works such as [37, 45], this approach fundamentally entails a coupled design of K and H. Consequently, it positions us beyond the scope of the original Smith predictor framework as introduced in [56].*

Proposition 2 *Let ρ_{max} be the maximum attainable value of $\rho = 1/|W_mT_o|_\infty$ for all stabilizing controllers K of P_o. This is subject to a coprime factorization $P_o = N/D$ where N and D belong to $\mathscr{H}_\infty$. Consider an inner-outer factorization for N, denoted as N_iN_o, where N_i is the inner factor and N_o is the outer factor. Consequently, the reciprocal of ρ_{max} represents the smallest achievable $\mathscr{H}_\infty$-norm for the Nevanlinna-Pick interpolation problem associated with the data*

$$\{p_1,\ldots,p_m\} \to \left\{\frac{W_m(p_1)}{N_i(p_1)},\ldots,\frac{W_m(p_m)}{N_i(p_m)}\right\}. \tag{2.25}$$

Specifically, $\rho_{max} \leq \left(\max_\ell \left|\frac{W_m(p_\ell)}{N_i(p_\ell)}\right|\right)^{-1}$, and $\gamma_{opt} \geq \max_k |e^{hp_k}|$. Thus, a necessary condition for $\gamma_{opt} \leq \rho_{max}$ is

$$\max_k |e^{hp_k}| \leq \left(\max_\ell \left|\frac{W_m(p_\ell)}{N_i(p_\ell)}\right|\right)^{-1}.$$

Proof. Let $X, Y \in \mathscr{H}_\infty$ be such that they satisfy the Bezout identity $NX + DY = 1$. Subsequently, the parametric representation of the controller for K results in $W_mT_o = W_mN(X+DQ)$, where Q is a free parameter such that $Q \in \mathscr{H}_\infty$. By employing the inner-outer factorization of N as N_iN_o, ρ_{max}^{-1} is derived from the one-block problem

$$\inf_{Q\in\mathscr{H}_\infty} \|W_mN(X+DQ)\|_\infty = \inf_{Q_1\in\mathscr{H}_\infty} \|W_mN_oX + DQ_1)\|_\infty.$$

It is important to observe that the transfer function D has zeros located in the right half-plane ($\mathbb{C}+$) at p_ℓ, and at these points, $X(p_\ell)$ corresponds to $1/N(p_\ell)$ for $\ell = 1,\ldots,m$. Therefore, the solution to the one-block problem can be attained through Nevanlinna-Pick interpolation utilizing the data presented in (2.25). For additional insights, refer to [17]. □

Remark 2 *In the event that $\gamma_{opt} < \rho$, an alternative to the optimal interpolant H may be employed, which is a sub-optimal solution presented in the form of a Linear Fractional Transformation (LFT):*

$$H_\phi(s) = \rho \, \frac{\Theta_{11}(s)\phi(s) + \Theta_{12}(s)}{\Theta_{21}(s)\phi(s) + \Theta_{22}(s)}. \tag{2.26}$$

where $\Theta_{11}, \Theta_{12}, \Theta_{21}, \Theta_{22}$ are uniquely determined through a set of linear equations, which exclusively rely on the problem data given in (2.24)*. Moreover, $\phi \in \mathscr{H}_\infty$ with $\|\phi\|_\infty \leq 1$ serves as a free parameter, as detailed in [6]. In this case, the flexibility to adjust ϕ provides the capability to accommodate additional design objectives.*

Remark 3 *As previously stated, the interpolation conditions specified in* (2.8) *ensure the stability of the predictor $F(s) = (1 - H(s)e^{-hs})P_o(s)$ (the internal feedback in the main controller block C_o of Fig. 2.3). This transfer function can be expressed as a finite-dimensional strictly proper term alongside an infinite-dimensional transfer function, where the impulse response is confined to the interval $[0,h]$. An FIR function of this kind is inherent in other predictor-based controllers, exemplified in sources such as [39, 60, 48] (the associations with [39] and [48] will be illustrated in the following section). As discussed within section 1.3, there exist many effective approximation techniques for the practical implementation of the infinite dimensional FIR filter.*

Remark 4 *Evidently the reference tracking properties of the proposed system remain unaffected by the parameter H, specifically characterized by $T_{ry} = e^{-hs}T_o(s)$, where $T_o = P_oK/(1+P_oK)$, as in the original Smith predictor design. The aforementioned construction of H ensures a high degree of robustness against uncertainties in the plant. Conversely, when evaluating properties related to disturbance rejection, it is necessary to examine* (2.13)*:*

$$T_{vy} = P_oS_oe^{-sh} + T_oe^{-hs}\ (\ P_o(1 - He^{-hs})\ ).$$

The haptic feedback has no effect on the first term $P_oS_oe^{-hs}$, which is the transfer function from the disturbance signal v to the response of the plant, y, when employing a classical controller that is not based on prediction. On the other hand, the predictor F is a multiplying factor of the second term. In order to achieve proficient disturbance rejection, it is essential to minimize the magnitude of

$$\Psi := T_oP_o(1 - He^{-hs}),$$

in the frequency range where the disturbance is effective. Nevertheless, once the inner controller K is predetermined and the optimal Nevanlinna-Pick solution is used to design $H = H_{opt}$, the function Ψ becomes fixed. To consider the balance between robustness and disturbance rejection, it is possible to select $\rho > \gamma_{opt}$ as outlined in Remark 2. Following this, the free parameter ϕ in (2.26) can be manipulated in an effort to minimize the value of $|\Psi|$.

2.4 On Finite Dimensional Approximations of the Controller

Most of the predictor-based designs used for systems with time-delay contain a predictor filter which has an infinite dimensional structure. In order to integrate such structures into practical systems, many researchers focused on approximation methods, as discussed in section 1.3. The predictor filter $F(s)$, defined in (2.14), designed within the suggested configuration is a stable infinite dimensional transfer function, which can be decomposed into an FIR filter and an additive stable function. Although this structure can be approximated with a high order finite dimensional transfer function that returns low amount of error, in practical systems it is desired to have a low order representation in order to provide a cost efficient controller design. Therefore, in this section, a bound on the approximation error is given to preserve stability.

Let Δ_F denote the approximation error of the predictor filter $F = H_1P_o$ illustrated in Fig. 2.1, i.e.

$$\Delta_F(s) := F(s) - F_r(s) \tag{2.27}$$

where $F_r(s)$ is the r^{th} order approximation of F. When K, F and H are designed according to the previously described method, the closed loop system is stable. Then, the nominal open loop transfer function $G_o(s)$ is defined as

$$G_o(s) = \left(\frac{K(s)}{1+F(s)K(s)}\right) P_o(s)e^{-hs}, \tag{2.28}$$

and the nominal closed loop transfer function can be written as

$$T_o(s) = \frac{G_o}{1+G_oH}. \tag{2.29}$$

Due to the stability, the poles of T_o, i.e. the roots of the denominator of T_o, which is represented as $dT_o = 1+G_oH$, must be in $\mathbb{C}_-$. Therefore, the roots of the characteristic equation

$$dT_o := 1+G_oH = 1+KF+KP_oe^{-hs}H = 0 \tag{2.30}$$

are in the open left half-plane. When the approximation $F_r(s)$ is used instead of $F(s)$, the characteristic equation becomes

$$dT_r := 1+KF_r+KHP_oe^{-hs} = 0. \tag{2.31}$$

In order to use Δ_F in (2.27), dT_r can be rewritten in the form

$$\begin{aligned}
dT_r &= 1+KF_r+KHP_oe^{-hs}+KF-KF, && (2.32)\\
dT_r &= 1+K(F_r-F)+KHP_oe^{-hs}+FK, && (2.33)\\
dT_r &= 1-K\Delta_F+KF+KHP_oe^{-hs}, && (2.34)\\
dT_r &= dT_o-K\Delta_F, && (2.35)\\
dT_r &= dT_o\left(1-\frac{K\Delta_F}{dT_o}\right). && (2.36)
\end{aligned}$$

Then, because that the roots of $dT_o = 0$ lie on the open left half-plane, and by applying the small gain theorem, a sufficient condition to guarantee the stability of T_r is

$$\left|\Delta_F(j\omega)\left(\frac{K(j\omega)}{dT_o(j\omega)}\right)\right| = |\Delta_F(j\omega)|\left|\frac{K(j\omega)}{dT_o(j\omega)}\right| < 1 \;\; \forall\, \omega \tag{2.37}$$

Due to the definition in (2.30), this condition can also be represented as

$$|\Delta_F(j\omega)|\left|\frac{K(j\omega)}{1+K(j\omega)F(j\omega)+K(j\omega)H(j\omega)P_o(j\omega)e^{-hj\omega}}\right| < 1 \;\; \forall\, \omega \tag{2.38}$$

Note that $F = (1 - He^{-hs})P_o$. By replacing F in the inequality in (2.38), and by applying proper algebra, the condition is simplified to

$$|\Delta_F(j\omega)| \left| \frac{K(j\omega)}{1 + K(j\omega)P_o(j\omega)} \right| < 1 \ \ \forall\, \omega. \tag{2.39}$$

Then, if an upper bound is set, denoted as W_a, such that

$$|\Delta_F(j\omega)| < |W_a(j\omega)| \ \ \forall\, \omega, \tag{2.40}$$

the condition in (2.39) can finally be revised as

$$|W_a(j\omega)| \left| \frac{K(j\omega)}{1 + K(j\omega)P_o(j\omega)} \right| \leq 1 \ \ \forall\, \omega. \tag{2.41}$$

This result shows that, regarding the stability of the closed loop system, the upper bound on the approximation error between F and F_r solely depends on the design of K and the non-delayed component of the plant. Although that it is a conservative bound, due to the application of small gain theorem, if the condition defined in (2.39) is fulfilled, it is guaranteed that approximation F_r with order r can be used to stabilize the closed loop system. In the fourth chapter, several examples based on $\mathscr{H}_\infty$ model order reduction methods are given.

2.5 Example and Similar Techniques

In order to highlight the advantages of the proposed design, an example on SISO unstable systems are given in this section. The system considered here has two unstable poles with parametric uncertainty as shown in (2.42). Initially, the proposed technique is applied to derive the closed loop system and corresponding controller, predictor and haptic filter. In the second subsection, similar works on the literature are summarized, and their differences with the proposed method are explained. The third subsection compares the time domain responses of several systems obtained by the proposed technique and the optimal $\mathscr{H}_\infty$ controller. Finally, a discussion on disturbance rejection and robustness properties of the proposed design is given.

Consider the class of uncertain plants in the form

$$P_\Delta(s) = \frac{1}{s^2 - as + b} e^{-\widetilde{h}s} + \delta \tag{2.42}$$

where $\widetilde{h} \in [0.2\ ,\ 0.3]$, $a \in [1.95\ ,\ 2.05]$, $b \in [2.0\ ,\ 2.25]$, and $\delta \in [10^{-4}\ ,\ 10^{-3}]$.

As mentioned in the previous section, Smith predictor based controller structures are mainly applied on dead-time delay systems due to the necessity of an accurate model, i.e. the nominal plant. Hence, the parametric uncertainties outlined in (2.42), particularly the variance of the time delay, offer a concise recapitulation of the aforementioned analyses conducted throughout this section.

According to these uncertainties, let the nominal plant be formed as

$$P_o(s) = \frac{1}{s^2 - 2s + 2} e^{-hs}, \quad p_{1,2} = 1 \pm j\ , \quad h = 0.25. \tag{2.43}$$

Fig. 2.4 illustrates that the multiplicative uncertainty bound given below successfully bounds these parametric uncertainties:

$$W_m(s) = \frac{0.11(1 + s/0.6)(1 + s/11)^2}{(1 + s/1.8)}.$$

2.5.1 Proposed Design

By using Nevanlinna-Pick interpolation data in (2.24), according to the unstable poles of the nominal plant illustrated in (2.43), $\gamma_{opt} = \sqrt{\lambda_{max}(A^{-1}B)}$ can be computed from the 2×2 matrices A, B defined as

$$[A]_{i,j} = (\overline{p}_i + p_j)^{-1}\ , \quad [B]_{i,j} = e^{h(\overline{p}_i + p_j)}(\overline{p}_i + p_j)^{-1}$$

The resulting optimal value is $\gamma_{opt} = 1.6404$, and the corresponding optimal haptic feedback (2.23) is in the form

$$H_{opt}(s) = \gamma_{opt} M_o(s) = \gamma_{opt} \frac{s - a}{s + a}\ ,$$

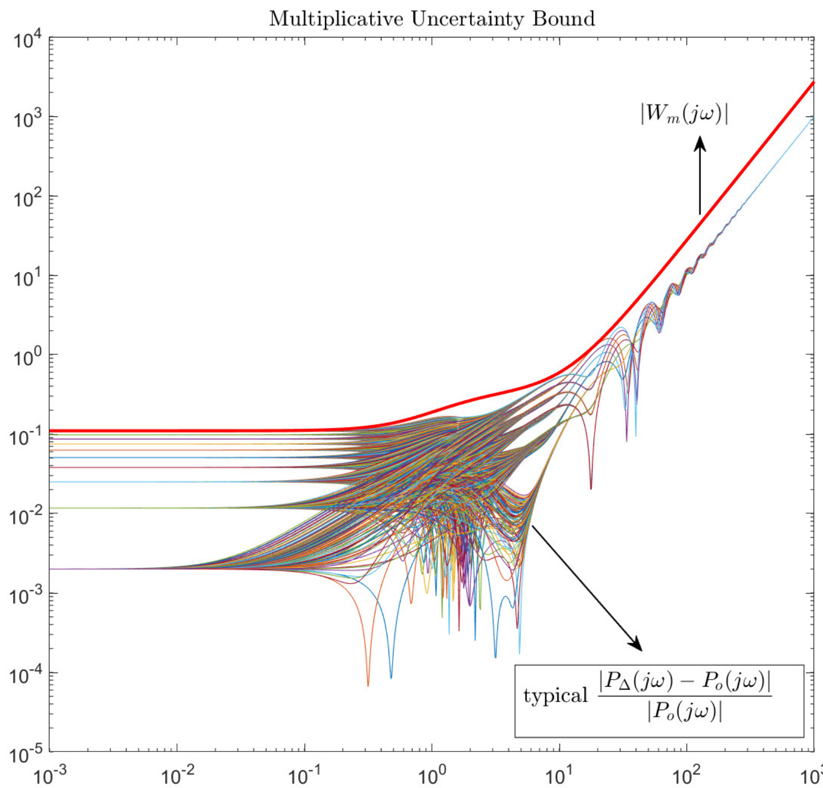

Figure 2.4: Magnitude of multiplicative uncertainties and the upper bound $W_m(s)$

where $a > 0$ is evaluated as

$$a = p_1 \left(\frac{\gamma_{opt} - e^{hp_1}}{\gamma_{opt} + e^{hp_1}} \right) = 0.2475$$

(typically, M_o is calculated based on a set of $(m-1)$ linear equations, in this case $m = 2$, [45]). Hence, the filters presented in Fig. 2.1 constructed by applying the proposed technique are

$$H_1(s) = 1 - e^{-0.25s} H(s), \tag{2.44}$$

$$H_2(s) = H(s) = 1.6404 \left(\frac{s - 0.2475}{s + 0.2475} \right). \tag{2.45}$$

The internal controller $K(s)$ depicted in Fig. 2.3 is derived through a mixed sensitivity minimization that incorporates P_o with an integrator in the sensitivity weight. This compels the inclusion of integral action in K to facilitate the tracking of step-like references, and results in

$$K(s) = \frac{189.37(s^2+0.592s+0.64)}{s(s+30)}. \tag{2.46}$$

Now that the haptic filter $H(s)$, predictor $F(s) = H_1(s)P_o(s)$, and the sub-controller $K(s)$ are constructed, it can be demonstrated that the value of ρ derived from K and W_m fulfills the robust stability condition specified in (2.22),

$$\rho = \left\| W_m \frac{P_o K}{1+P_o K} \right\|_\infty = 0.5165 < 0.6096 = \frac{1}{\gamma_{opt}}.$$

Then, the nominal closed loop transfer function from the reference signal r to system response y is obtained as

$$T_o(s) = \frac{189.37(s^2+0.592s+0.640)\ e^{-0.25s}}{(s+22.49)(s+3.994)(s^2+1.518s+1.349)}. \tag{2.47}$$

2.5.2 The Similarities of the Proposed Method with Related Works

Due to its Smith predictor based structure, there naturally exists similarities between the proposed method and related works on such designs. In this subsection, the most recent techniques within the literature that use Smith principle are summarized. Moreover, it is shown how the same closed loop systems may be designed through an example.

Both methods outlined in [39] and [48] incorporate a free parameter, labeled as $Q(s)$, that can be chosen such that the resulting closed-loop transfer functions align with (2.47). The connections between the proposed approach and the aforementioned methods are illustrated through the example provided in this subsection. Although the technique given in [48] uses a similar configuration with the design proposed within this thesis, the construction process of the haptic filter, and therefore the predictor differs. As described in the subsequent page, compared to the proposed method within this thesis, the design of the controller structure is relatively complex.

Initially, the approach outlined in [48] uses the subsequent decomposition to design filters within the predictor framework (employing the terminology introduced in [48]):

$$P_o(s) = \frac{N^+(s)N^-(s)}{D^-(s)D^+(s)} = \Gamma(s)\tilde{G}(s) = P_o(s)$$

where $N^+(s)$ and $N^-(s)$ denote polynomials incorporating the anti-stable and stable zeros of the plant respectively. The same notation is used to define $D^-(s)$ and $D^+(s)$, regarding the roots of the denominator. In this approach, the polynomials N^- and D^- are further decomposed as $N^- = N^-_\Gamma N^-_{\tilde{G}}$, $D^- = D^-_\Gamma D^-_{\tilde{G}}$. Hence, this technique employs the following decomposition to represent $P_o(s)$:

$$\Gamma(s) = \frac{N^+(s)N^-_\Gamma(s)}{D^-_\Gamma(s)} Q_w(s),\ \tilde{G}(s) = \frac{N^-_{\tilde{G}}(s)}{D^+(s)D^-_{\tilde{G}}(s)} \frac{1}{Q_w(s)},$$

where the transfer function $Q_w(s)$ is a free-parameter, ensuring that $\tilde{G}(s)$ is strictly proper while $\Gamma(s)$ is a proper function. The state space representation of $\tilde{G}$ is

$$\tilde{G}(s) = \tilde{C}(sI - \tilde{A})^{-1}\tilde{B} = \frac{N_{\tilde{G}}(s)}{D_{\tilde{G}}(s)}.$$

Also, another transfer function $\tilde{G}^*(s)$ is defined as

$$\tilde{G}^*(s) = \tilde{C}e^{\tilde{A}h}(sI - \tilde{A})^{-1}\tilde{B} = \frac{N_{\tilde{G}^*}(s)}{D_{\tilde{G}^*}(s)}$$

for further steps of the design proposed in [48].

To match our design with this controller structure, the unconstrained parameter $Q_w(s)$ must be chosen in a manner that

$$H(s) = \frac{N_{\tilde{G}^*}(s)}{N_{\tilde{G}}(s)},$$

$$H_1 P_o = (1 - e^{-hs}H(s)) = P_o(s) = \left(\tilde{G}(s) - e^{-sh}\tilde{G}^*(s)\right)\Gamma(s).$$

By applying proper linear algebra, these conditions lead to

$$Q_w(s) = \frac{c}{s + 0.2475} \tag{2.48}$$

where $c \in \mathbb{R}$ is an unrestricted constant. In essence, if the factorizations as carried out as demonstrated earlier, and the selection of the unconstrained parameter according to (2.48), the controller derived in [48] coincides with ours, assuming uniformity in the choice of controller K in both approaches.

Drawing comparisons between the setup in [39] and the methodology introduced in this thesis is more challenging than the earlier comparison, primarily due to variations in structures and the derivation of filters.

Within the configuration of [39], the plant is defined as

$$P = \begin{bmatrix} P_{11} & P_{12} \\ P_{21} & P_{22} \end{bmatrix} = \begin{bmatrix} P_{11} & P_{12} \\ P_{21} & -P_o H \end{bmatrix}.$$

Since the controller structure only depends on $P_{22}(s)$ and desired pole locations, the definition of $P_{22}(s)$ in terms of $P_o(s)$ and $H_2(s)$, and determination of closed loop poles are sufficient to obtain the FIR filter $\Pi_2(s)$, state-feedback F, observer L and the free-parameter $Q(s)$. Therefore, the design process can be summarized as, for a strictly proper plant whose state space representation is given as

$$P_{22} = C_2(sI - A)^{-1} B_2, \tag{2.49}$$

the predictor based controller of [39] is in the form

$$C_{mr} = (I + K_{mr}\Pi_2)^{-1} K_{mr} \tag{2.50}$$

where

$$K_{mr} = J_{11} + J_{12} Q (I - J_{22} Q)^{-1} J_{21}, \tag{2.51}$$

$$J = \left[\begin{array}{c|cc} A + B_2 F + e^{Ah} L C_2 e^{-Ah} & -e^{Ah} L & B_2 \\ \hline F & 0 & I \\ -C_2 e^{-Ah} & I & 0 \end{array}\right], \tag{2.52}$$

$$\Pi_2 = C_2 e^{-Ah} (I - e^{-(sI-A)h})(sI - A)^{-1} B_2, \tag{2.53}$$

and, F and L are formulated in a way that ensures the matrices $A + B_2 F$ and $A + LC_2$ are Hurwitz, whose eigenvalues constitute a portion of the closed loop system poles. It is important to highlight that the generator of all controllers, denoted as J, is dependent on the time delay, h.

To align this controller with our framework, the vectors F and L must be selected in such a way that they ensure alignment of the closed-loop system poles with those presented in (2.47). Moreover, the association between $P_o H_1$ and Π_2 is

$$H_1(s)P_o(s) = (1 - e^{-hs}H(s))P_o(s) = R_H(s) - \Pi_2(s), \tag{2.54}$$

where $R_H(s)$ represents a finite order strictly proper transfer function with poles derived from $H(s)$, and it is acquired through the application of partial fraction expansion.

The desired closed-loop poles are designated to coincide with the poles of $T(s)$. Nevertheless, it is essential to note a disparity in the orders of the closed-loop transfer functions, with $T_{mr}(s)$ in [39] being of sixth order while our counterpart, $T(s)$ is of fifth order. To reconcile this discrepancy, the remaining free pole can be fixed as the pole of $H(s)$. Despite the flexibility of placing the final residual pole anywhere on the left half of the complex plane ($\mathbb{R}_-$), empirical observations indicate that setting the free pole as the pole of $H(s)$ leads to a reduction in the order of $Q(s)$ in (2.51). Hence, the desired closed loop system poles are chosen as

$$p_{1,2}^d = -0.7592 \mp 0.8792j, \quad p_3^d = -22.49,$$

$$p_4^d = -3.994, \quad p_5^d = p_6^d = -0.2475.$$

This pole placement results in the state feedback and observer gains as

$$F = [-1.759,\ -0.1101,\ 0.0805], \tag{2.55}$$

$$L = [180.6,\ 16.45,\ -73.85]^T. \tag{2.56}$$

The connection between the suggested filter and Π_2 in this example can be established through systematic algebraic manipulation of (2.54), yielding

$$H_1(s)P_o(s) = \frac{0.338}{s+0.2475} - \Pi_2(s). \tag{2.57}$$

Then, the free-parameter in the design of [39], denoted as $Q(s)$, can now be determined by equating the controllers from both designs as expressed in (2.7) and (2.50). Through the use of (2.55)-(2.57), the generator matrix J can be derived, and Q can be calculated as

$$Q = 189.37,$$

which is equivalent to the high frequency gain of $K(s)$ in this specific example.

2.5.3 Comparison Between the Proposed Design with $\mathscr{H}_\infty$ Optimal Controller

In this subsection, in order to emphasize on the differences between the proposed design and $\mathscr{H}_\infty$ optimal controller, the responses of the closed loop systems obtained by both techniques are compared in time domain.

First of all, the design procedure of the $\mathscr{H}_\infty$ optimal controller is explained. During the construction of this system, to provide a fair comparison, the same multiplicative uncertainty bound W_m and sensitivity weight $W_s = 1/s$ are selected as used during the mixed sensitivity minimization to find the internal controller $K(s)$ within the proposed method in subsection 2.5.1. By using the software described in [58], which essentially uses Toker-Özbay formula [54], the infinite dimensional optimal controller $C_{opt}(s)$ is obtained, whose Bode plot is given in Fig. 2.5, where the optimal performance level, γ_{opt}, is

$$\gamma_{opt} = \left\| \begin{bmatrix} W_s(1+PC_{opt})^{-1} \\ W_m PC_{opt}(1+PC_{opt})^{-1} \end{bmatrix} \right\|_\infty = 1.11086\ . \tag{2.58}$$

In order to obtain responses of both closed loop systems in time domain through Simulink, the infinite dimensional structures in both configurations need to be approximated by finite order transfer functions. In the proposed design, the predictor filter $F(s) = H_1(s)P_o(s)$, where $H_1(s)$ is designed as (2.44) and has infinite order. To obtain a finite dimensional predictor structure, the 5^{th} order Pade approximation of $e^{-0.25s}$ is used, instead of more complicated approximation techniques on $\mathscr{H}_\infty$ approximation. Application of these methods and comparison of the corresponding errors are given in chapter 4.

After approximate pole/zero cancellation, the resulting finite order predictor,

$$F_a(s) = \frac{1.3\left(1-0.16\left(\frac{s}{24}\right)+\left(\frac{s}{25}\right)^2\right)\left(1-0.3\left(\frac{s}{77}\right)+\left(\frac{s}{77}\right)^2\right)}{\left(1+\frac{s}{29}\right)\left(1+\frac{s}{0.25}\right)\left(1+1.8\left(\frac{s}{30}\right)+\left(\frac{s}{30}\right)^2\right)\left(1+1.1\left(\frac{s}{34}\right)+\left(\frac{s}{34}\right)^2\right)}, \tag{2.59}$$

becomes a 6^{th} order stable transfer function. Bode plots of $F(s)$ and $F_a(s)$ are given in Fig. 2.6. Hence, the main feedback controller defined in (2.7) becomes an 8^{th} order

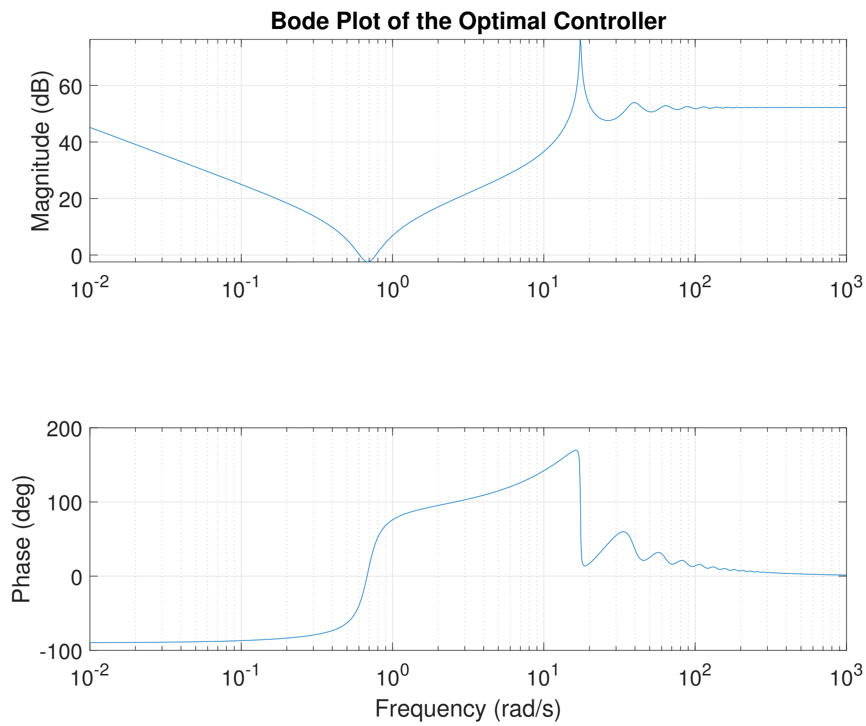

Figure 2.5: Bode plot of the optimal $\mathscr{H}_\infty$ controller

transfer function. Note that there also exists a haptic filter $H(s)$, which is first order as shown in (2.45).

The optimal controller whose frequency response is as shown in Fig. 2.5 is approximated by two different controllers: 11^{th} order $C_{11}(s)$ and 15^{th} order $C_{15}(s)$. The Bode plots of all these three controllers are given in Fig. 2.7. During the approximation, the procedure explained in [58] is used, in which the infinite dimensional term within $C_{opt}(s)$ is approximated automatically by applying `fitfrd` command in MATLAB.

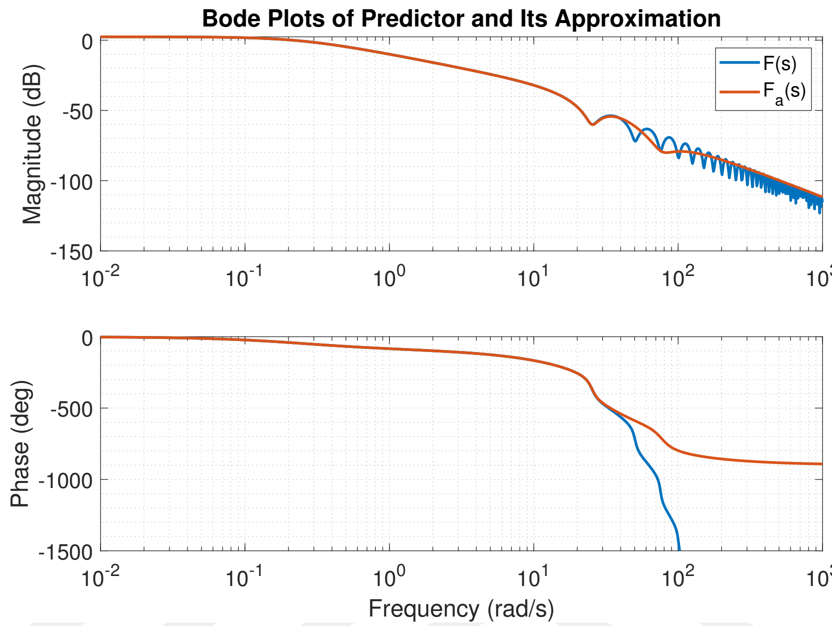

Figure 2.6: Bode plots of $F(s)$ and $F_a(s)$

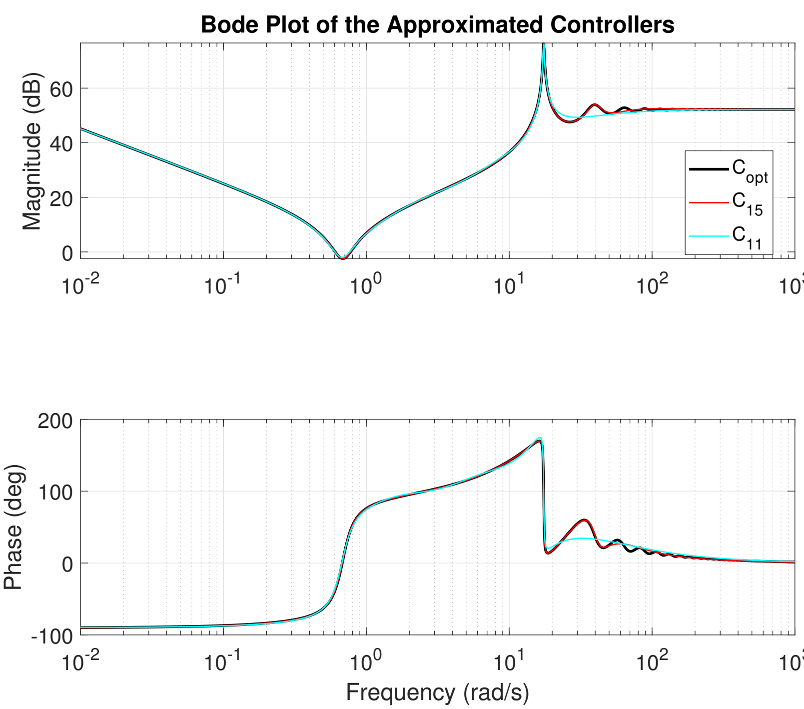

Figure 2.7: Bode plots of $F(s)$ and $F_a(s)$

Now that both the systems consists of finite dimensional controllers/filters, it is feasible to implement these structures into Simulink. To compare both tracking and robustness performances, the time delay of the system is introduced as a time-varying delay. In order to decrease the rate of variation of time-delay, the Laplace transform of the actual delay ($d(t)$) is represented by

$$D(s) := \frac{h_o}{s} + D_{add}(s) \left(\frac{1}{s/3+1} \right), \tag{2.60}$$

where $d_{add}(t) \sim U(-\kappa, \kappa)$ is the varying factor at each sampling period $T = 1$ second, such that $d(t) \in [h_o - \kappa,\ h_o + \kappa]$, in which κ represents the maximum deviation. The block diagram of the setup used to obtain time domain responses is shown in Fig. 2.8.

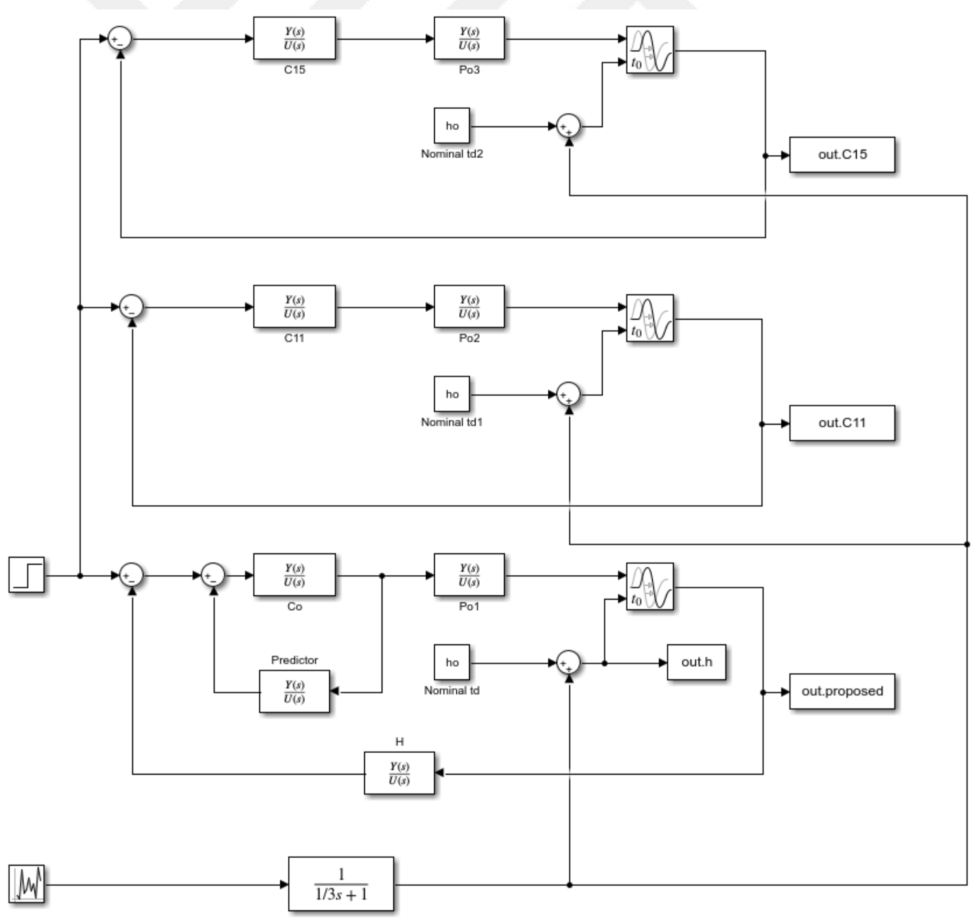

Figure 2.8: Block diagram of the configurations of sub-optimal $\mathscr{H}_\infty$ controllers and proposed structure

Two different cases had been worked on by using this setup:

- $\kappa = 0.05$. Fig. 2.9 illustrates the variation of time delay in 15 seconds. On the other hand, Fig. 2.10 shows the step responses of all aforementioned systems.

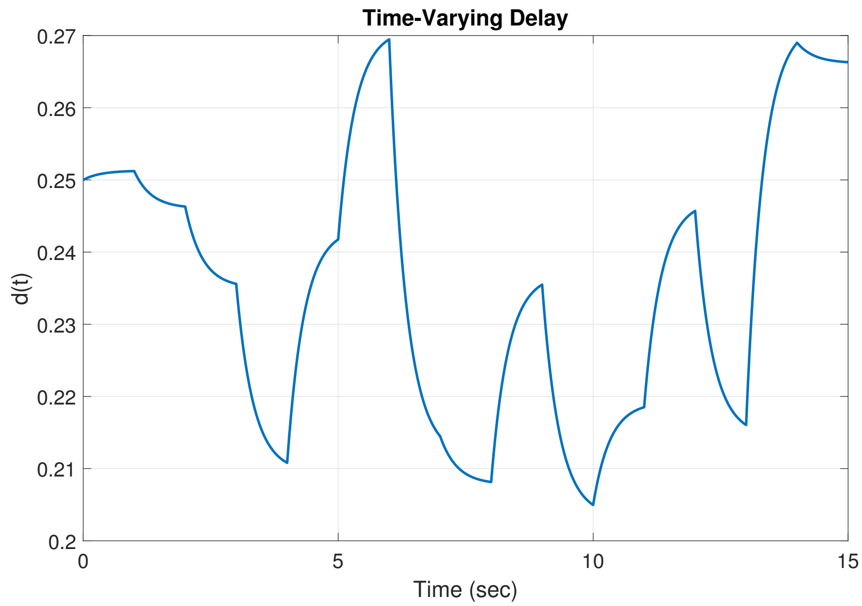

Figure 2.9: Simulated time-varying delay $d(t)$ for the case $\kappa = 0.05$

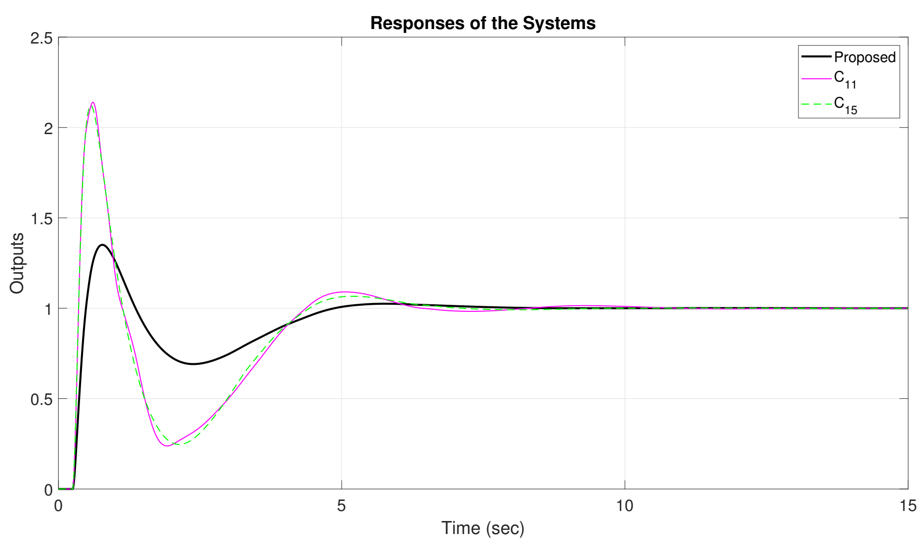

Figure 2.10: Step responses for the case $\kappa = 0.05$

- $\kappa = 0.1$. The time delay with respect to time in this case is illustrated in Fig. 2.11. Responses of the closed loop systems are also shown in Fig. 2.12.

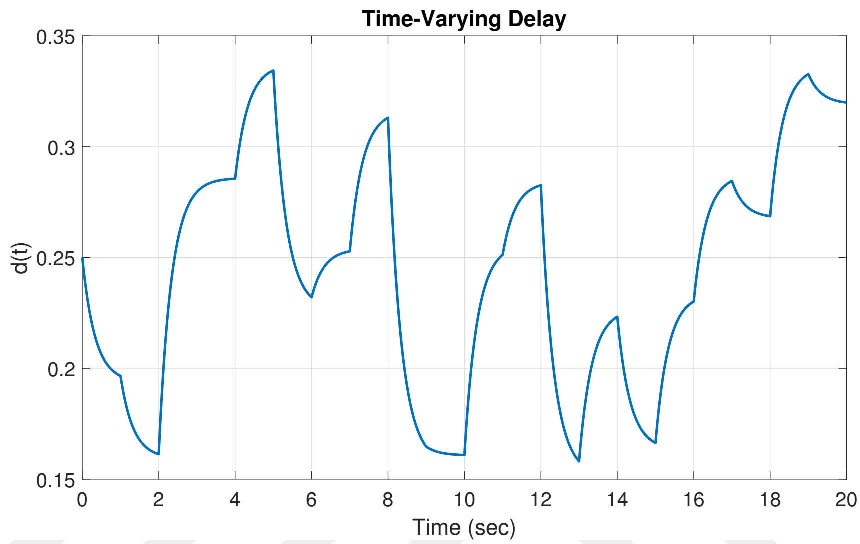

Figure 2.11: Simulated time-varying delay $d(t)$ for the case $\kappa = 0.1$

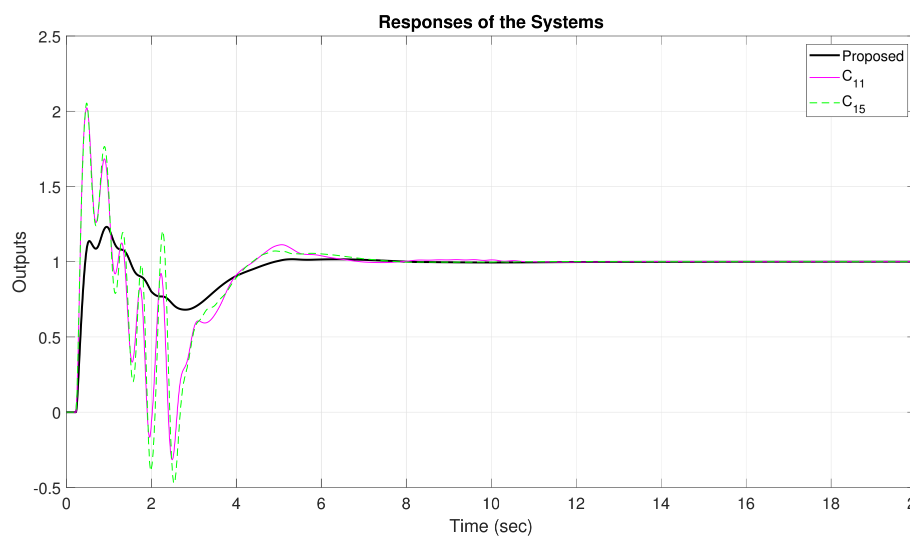

Figure 2.12: Step responses for the case $\kappa = 0.1$

Clearly, the proposed configurations in both cases have greater performance even though the order of controller structure is less than the dimensions of approximations of optimal $\mathscr{H}_\infty$ controller.

2.5.4 Trade-off Between Disturbance Rejection and Robustness

In most of the practical systems, disturbance signal has a significant impact on system response. Therefore, disturbance rejection is another crucial aspect to be considered during controller designs, in addition to robust stability. As mentioned in 1.2, many researchers focused on this capability of the closed loop system to improve the Smith-predictor based designs. In this section, the trade-off between disturbance rejection and robustness condition is discussed through an example in which the plant has only two unstable poles.

In case when the given system has only two poles in $\mathbb{C}_+$, a first order stable $H(s)$ can be used to find a stable $F(s)$, such that $H(s)$ stabilizes the closed loop system. Note that this H does not necessarily need to satisfy robust stability condition. $H(s)$ can be represented in the form

$$H(s) = K_0 \left(\frac{s+b_0}{s+a_0} \right). \tag{2.61}$$

When K_0 is fixed, the interpolation conditions for stability,

$$H(s) = K_0 \left(\frac{p_i+b_0}{p_i+a_0} \right) = e^{hp_i}, \tag{2.62}$$

where p_i are defined in (2.43), uniquely determine the coefficients a_0 and b_0. Hence, the only free parameter in such design is K_0, and through a single degree of freedom, it can be observed how disturbance rejection and robustness properties are affected. The following signal is chosen to compare the magnitude of disturbance rejection at low frequencies,

$$W_v = \frac{4}{2s+1}. \tag{2.63}$$

The plotted blue line in Figure 2.5.4 depicts the variation in the ratio of the $\mathscr{H}_\infty$-norm of the disturbance signal with respect to K_0. Conversely, the robustness deteriorates with an increment in K_0, as anticipated.

When $K_0 = 1.926$, first order H that guarantees the stability of the predictor, and hence the closed loop system is

$$H(s) = 1.926 \left(\frac{s+0.2216}{s+1.147} \right). \tag{2.64}$$

In this scenario, the robustness condition is fulfilled with an almost negligible robustness margin. However, the disturbance rejection performance of this design exceeds that of the system constructed with $H_{opt}(s)$ from (2.45) by a factor of four.

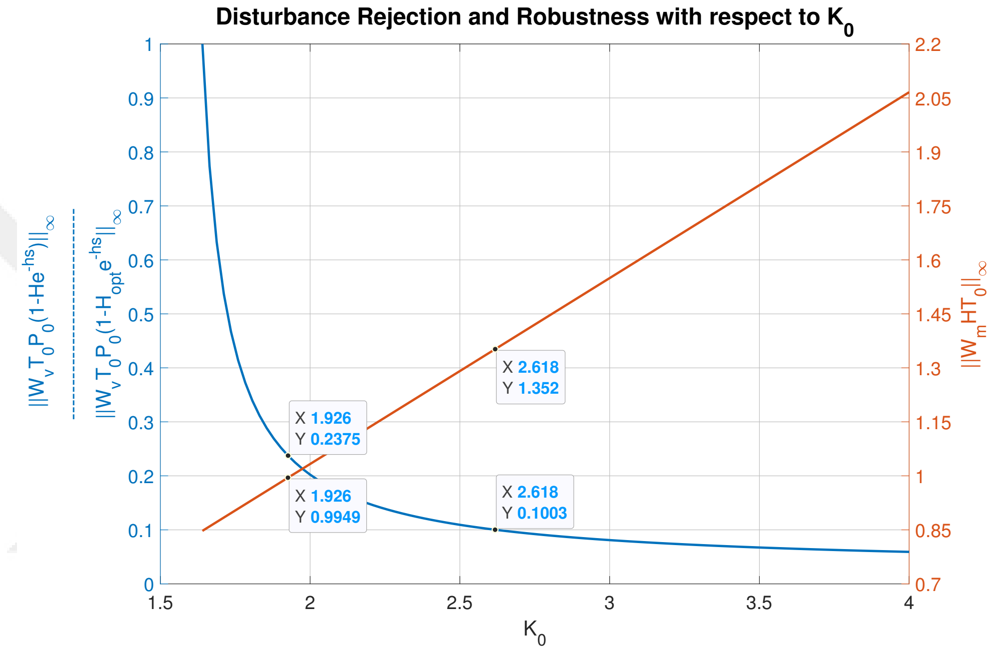

Figure 2.13: Trade-off between disturbance rejection and robustness

When $K_0 = 2.618$, first order H that fulfills the stability condition is

$$H(s) = 2.618\left(\frac{s+0.9339}{s+3.325}\right). \tag{2.65}$$

In this instance, the robustness condition is not met, necessitating a reduction in the magnitude of W_m. Nevertheless, the disturbance rejection capability of this design surpasses that of the system constructed with $H_{opt}(s)$ as specified in (2.45) by a factor of ten.

Chapter 3

Extension of Smith Predictor Based Controllers

3.1 Extension to a Class of Distributed Parameter Systems

In this section, LTI distributed parameter systems are considered, and finite-dimensional controllers are designed to stabilize the feedback system. Typically, this classical problem is addressed through two conventional approaches:

(i) approximate the plant and then design a finite dimensional controller,

(ii) approximate the infinite dimensional controller directly obtained from the original plant.

In both instances, it is imperative to keep track of the approximation errors, usually evaluated in the context of $\mathscr{H}_\infty$, to ensure the stability of the feedback system. This topic is extensively covered in the literature, as evidenced by the classical textbook [15] and a recent publication [41].

Here, a new method is proposed, which starts with a coprime and inner-outer factorization of the plant transfer function, as in [18]. The procedure is described in detail in the subsequent sections.

3.1.1 Plant Structure

Consider LTI plants that their transfer functions can be represented in the form

$$P_{\Delta}(s) = \frac{M(s)N_n(s)}{D(s)}\Big(1+\Delta_n(s)\Big), \tag{3.1}$$

where M and D are respectively an infinite dimensional inner function, and a stable bi-proper transfer function with finite order whose zeros are the unstable poles of the given plant. N_n represents a rational outer transfer function of the order $2(n+1)$, obtained as an approximation for the outer transfer function $N(s)$ possessing an infinite number of dimensions; the approximation error and uncertainty within the model are lumped into

$$\Delta_n(s) = W_n(s)\Delta(s) \tag{3.2}$$

with a finite order rational stable W_n that is assumed to be known. Moreover, W_n is designed judiciously such that the magnitude of the stable unknown function Δ is bounded as $\|\Delta\|_{\infty} < 1$. Furthermore, the covered systems are assumed to satisfy that the magnitude of the upper bound on the uncertainty decreases as the order of N_n increases, i.e.

$$|W_m(j\omega)| < |W_n(j\omega)|\,, \quad \forall\, \omega \in \mathbb{R}\,, \quad \forall\, m > n. \tag{3.3}$$

The system that has been worked on within this section is an Euler-Bernoulli beam having free ends with Kelvin-Voigt damping, [10, 47]. At this point, it is pertinent to note that the control of flexible beams has been extensively studied in the literature through the application of both state-space and frequency-domain methods. Some of those proposed techniques may be found in [5, 8, 10, 12, 13, 25, 26, 34, 51, 53]. For the sake of simplicity, all parameters except the damping constant $\varepsilon > 0$ are assumed to be normalized to unity. The deflection of the beam is $w(x,t)$, where t and x represent time and location along the elastic axis of the beam respectively. The SISO plant is supposed to have a transverse force as the input signal, denoted as $-u(x,t)$, is applied at the end of the normalized beam, implying that the force is exerted at $x = 1$. Fig. 3.1 visualizes the physical structure of such plant.

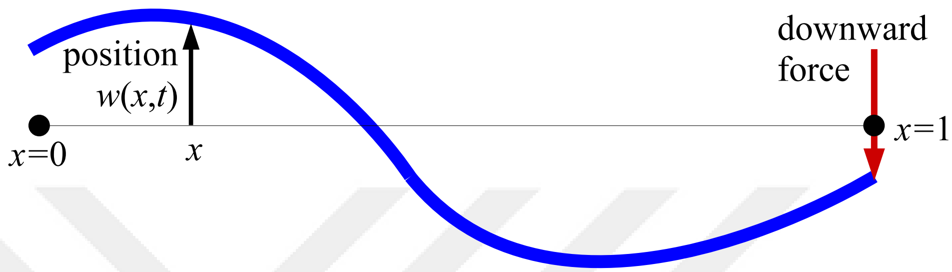

Figure 3.1: Flexible beam with free ends and normalized beam length

In [33], the mathematical model of this beam is represented by the following PDE

$$\frac{\partial^2 w}{\partial t^2} + \varepsilon \frac{\partial^5 w}{\partial x^4 \partial t} + \frac{\partial^4 w}{\partial x^4} = 0 \tag{3.4}$$

where the boundary conditions are

$$\frac{\partial^2 w}{\partial x^2}(0,t) + \varepsilon \frac{\partial^3 w}{\partial x^2 \partial t}(0,t) = 0,$$

$$\frac{\partial^2 w}{\partial x^2}(1,t) + \varepsilon \frac{\partial^3 w}{\partial x^2 \partial t}(1,t) = 0,$$

$$\frac{\partial^3 w}{\partial x^3}(0,t) + \varepsilon \frac{\partial^4 w}{\partial x^3 \partial t}(0,t) = 0,$$

$$\frac{\partial^3 w}{\partial x^3}(1,t) + \varepsilon \frac{\partial^4 w}{\partial x^3 \partial t}(1,t) = u(t).$$

The system response, $y(t)$, is assumed to be the position at $x = 0$, which is measured with a time delay of h seconds, i.e. $y(t) = w(0,t-h)$. Then, the transfer function of this system is

$$\frac{Y(s)}{U(s)} = P_\Delta(s) = \frac{e^{-hs}\,(\sinh\beta - \sin\beta)}{\beta^3(1+\varepsilon s)(\cos\beta\cosh\beta - 1)}, \tag{3.5}$$

where $\beta^4 = \frac{-s^2}{(1+\varepsilon s)}$, as stated in [33]. Similar beam transfer functions and further examples on such systems can be found in [14, 32]. It is also worth noting that there is a considerable body of literature addressing the consideration of time delays in systems represented by PDEs. This is exemplified by recent publications such as [29, 35] and their respective references.

It can be demonstrated that, the representation of $P_\Delta(s)$ with trigonometric equations in (3.5) $P_\Delta(s)$ can also be expressed as an infinite product of second order terms. This representation simplifies inner/outer factorizations of the general form (2.15), which are essential for our controller design scheme.

$$P_\Delta(s) = \frac{2e^{-hs}}{s^2}\prod_{i=1}^{\infty} g_i(s)\ ,\ \ g_i(s) = \frac{\left(1+\varepsilon s - \frac{s^2}{4\alpha_i^4}\right)}{\left(1+\varepsilon s + \frac{s^2}{\phi_i^4}\right)} \tag{3.6}$$

where $\cos(\alpha_i)\sinh(\alpha_i) = \sin(\alpha_i)\cosh(\alpha_i)$, for $\alpha_i > 0$ and $\cos(\phi_i)\cosh(\phi_i) = 1$, for $\phi_i > 0$.

In [32], it is shown that the infinite product in (3.6) converges everywhere in the $\mathbb{C}_+$. Hence, the coprime factorization of the transfer function of this flexible beam, $P_\Delta = (M\,N)\,D^{-1}$, can be derived, where $D^{-1}(s) = s^2/(s+1)^2$,

$$M(s) = e^{-hs}B(s). \tag{3.7}$$

$$B(s) = \prod_{i=1}^{\infty}\left(\frac{2\alpha_i^4\left(\varepsilon+\sqrt{\varepsilon^2+\frac{1}{\alpha_i^4}}\right)-s}{2\alpha_i^4\left(\varepsilon+\sqrt{\varepsilon^2+\frac{1}{\alpha_i^4}}\right)+s}\right), \tag{3.8}$$

$$N(s) = \frac{2}{(s+1)^2}\prod_{i=1}^{\infty}\left(\frac{1+s\sqrt{\varepsilon^2+\frac{1}{\alpha_i^4}}+\frac{s^2}{4\alpha_i^4}}{1+\varepsilon s+\frac{s^2}{\phi_i^4}}\right). \tag{3.9}$$

It is shown within [33], that both N and B are stable functions, where N is outer; and B is inner, so that M is an infinite dimensional inner function. Note that all poles of P_Δ resides in the open left half-plane, except for the double pole at $s = 0$. Furthermore, due to the structure of $B(s)$, as displayed in (3.8), and time delay, it has infinitely many zeros in $\mathbb{C}_+$. Detailed discussion on the pole-zero locations of this plant can be found in [32].

By defining

$$N_n(s) = \frac{2}{(s+1)^2}\prod_{i=1}^{n}\left(\frac{1+s\sqrt{\varepsilon^2+\frac{1}{\alpha_i^4}}+\frac{s^2}{4\alpha_i^4}}{1+\varepsilon s+\frac{s^2}{\phi_i^4}}\right). \tag{3.10}$$

the plant can be rewritten in the form of (3.1), with $\Delta_n = (N - N_n)/N_n$. Then, by applying proper linear algebra,

$$\Delta_n = -1 + \prod_{i=n+1}^{\infty} \left(\frac{1 + s\sqrt{\varepsilon^2 + \frac{1}{\alpha_i^4}} + \frac{s^2}{4\alpha_i^4}}{1 + \varepsilon s + \frac{s^2}{\phi_i^4}} \right). \tag{3.11}$$

3.1.2 Outline of the Proposed Approach for Such Systems

The extension of the proposed design within this thesis for such systems has three steps:

1. According to various specifications regarding the performance and robustness of the closed loop system, a stabilizing controller K_n for

   $$P_{on} = \frac{N_n}{D} \ . \tag{3.12}$$

   needs to be designed. Note that P_{on} is a finite order transfer function in case the plant has a finite amount of unstable poles, which is mandatory for the limited number of interpolation conditions, therefore the proposed technique.

2. A “predictor-like” feedback around K_n needs to be constructed, such that the closed loop system is stable. The aim of this procedure is foretold in section 2.2; however, this technique needs to be slightly modified due to the Blaschke product $B(s)$.

3. In order to implement the local predictor F in (2.14), that is an infinite dimensional transfer function, due to the FIR structure within; a rational $\mathscr{H}_\infty$-approximation of F needs to be applied, which results in a finite dimensional filter. The reason behind the application of $\mathscr{H}_\infty$-approximation method is that the robust stability of the system should be preserved, with least effect on the robustness margin of the closed loop system.

The main idea behind this approach is to offer a comparatively straightforward low-order controller design for P_{on} where N_n and D are outer function. The inner factor,

M, of the plant can be conceptualized as a 'time delay,' thereby justifying the predictor structure.

Utilizing the aforementioned notation and methodology, the feedback controller depicted in Fig.**??** is implemented as illustrated in Fig.3.2, where the design of the low-order filter $H(s)$ adheres to stability conditions derived in the following subsection.

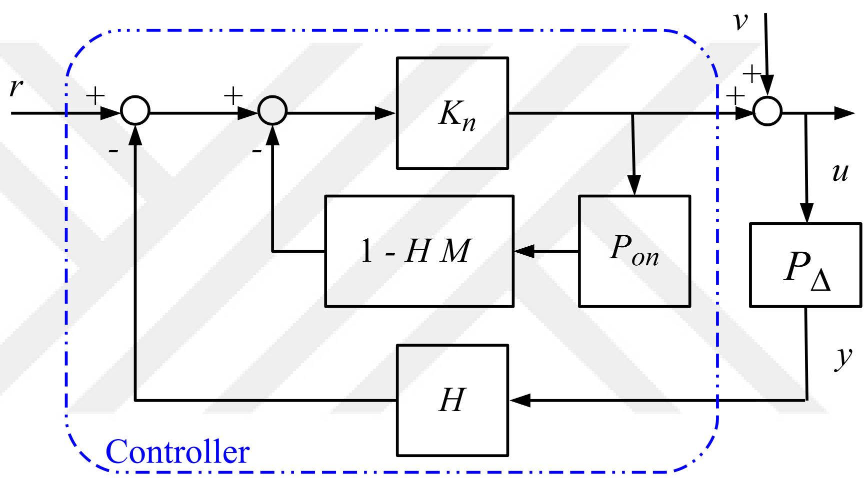

Figure 3.2: Feedback system with two degree of freedom controller

3.1.3 Stability Analysis

Due to the structure of M, and double non-distinct poles at $s = 0$, conditions on the design of $H(s)$ to stabilize the feedback system in Fig. 3.2 varies from the interpolation conditions given within the previous chapter. Moreover, the effect of the approximation N_n and the uncertainty Δ_n on stability is analyzed. In this subsection, the process of controller design to stabilize the closed loop system is revised.

Suppose that the initial step is satisfied, i.e. a controller K_n is designed to stabilize the finite order transfer function P_{on}, so that

- $S_n := (1+P_{on}K_n)^{-1}$
- K_nS_n

- $P_{on}S_n$
- $T_n := 1 - S_n$

are stable.

After a simple algebra, it can be shown that the closed loop transfer functions from internal signals (r, v) to external signals (u, y) are in the following forms (see also [59]):

$$\begin{aligned} T_{ry} &= M\, T_n \, \frac{1+\Delta_n}{1+\Delta_n M T_n H} \\ T_{ru} &= K_n S_n \, \frac{1}{1+\Delta_n M T_n H} \\ T_{vy} &= \big(P_{on}S_n + T_n(1-HM)P_{on}\big)\left(\frac{M(1+\Delta_n)}{1+\Delta_n M T_n H}\right) \\ T_{vu} &= \big(S_n + T_n(1-HM)\big)\left(\frac{1}{1+\Delta_n M T_n H}\right) \end{aligned}$$

Using the facts that K_n stabilizes $P_{on} = N_n/D$, M is an inner function, and $\Delta_n = W_n\Delta$ is stable, it can be deduced that the feedback system is stable when the following conditions are met:

$$H \text{ is stable,} \tag{3.13}$$

$$F(s) := \left(\frac{1 - H(s)M(s)}{D(s)}\right) N_n \text{ is stable,} \tag{3.14}$$

$$\|W_n\, T_n\, H\|_\infty < 1. \tag{3.15}$$

In [59], it is shown how $H(s)$ can be designed by using Nevanlinna-Pick interpolation to robustly stabilize the finite dimensional unstable systems with time delay. The proposed technique extends the method described within [59] to a larger class of distributed parameter systems.

3.1.4 Example on Normalized Flexible Beam

In case the plant is defined as in (3.6), where D is a second order inner function, a first order $H(s)$ that meets the conditions represented in (3.13), (3.14) and (3.15) can be designed by following the steps below.

Firstly, let $n = 2$ in (3.10). Then, $N_n(s)$ is obtained as a 6^{th} order outer function,

$$N_n(s) = \frac{0.4(s+105)(s+95)(s+31.3)(s+30.4)}{(s+1)^2(s^2+0.5s+501)(s^2+3.8s+3804)}.$$

As a result, the approximation of the non-delayed component of the plant defined in (3.12) is

$$P_{on}(s) = \frac{0.4(s+105)(s+95)(s+31.3)(s+30.4)}{s^2(s^2+0.5s+501)(s^2+3.8s+3804)}.$$

Also, when $n = 2$, Δ_n defined in (3.11) can be bounded by

$$W_n = \frac{27.6s(s+12)}{s^2+90s+14400} \tag{3.16}$$

as shown in Fig. 3.3. Note that as $m \to \infty$ the approximation error is close to $\Delta_{m,n}$ for $m = 10^4$.

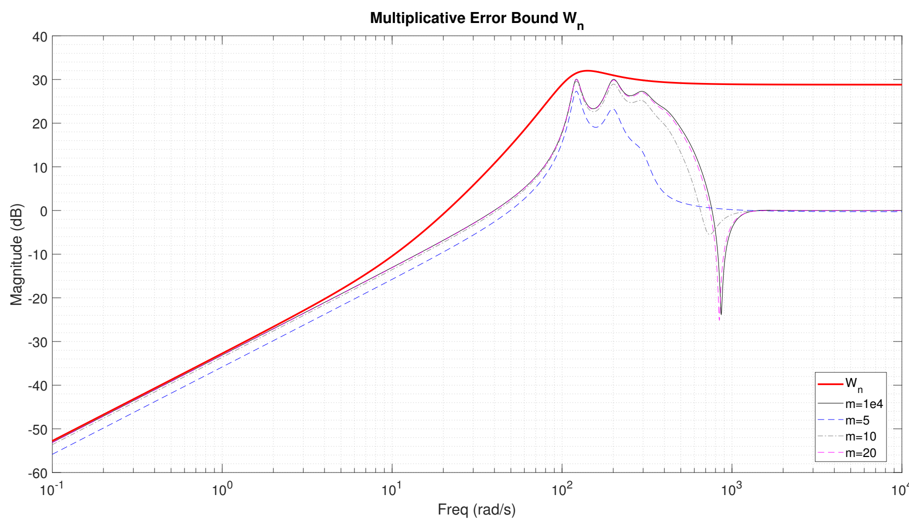

Figure 3.3: $\Delta_{m,n}$ and the corresponding bound W_n

Now that the clear representation of approximated system and the upper bound on approximation error are derived, the initial step described within the outline in 3.1.2 can be applied. In order to simplify the design process of $K_n(s)$, another representation of $P_{on}(s)$ can be used, which is

$$P_{on}(s) = \frac{0.4}{s^2} \times R_{on}(s),$$

where R_{on} is a bi-proper outer function. Then, a stabilizing controller can be found which contains $1/R_{on}(s)$. In this example, the closed loop system poles are placed such that they have low damping. The designed $K_n(s)$ is

$$K_n(s) = \frac{250(s+0.8)}{(s+8)(s+10)} \times \frac{1}{R_{on}(s)}, \tag{3.17}$$

which is a 6^{th} order controller.

To fulfill the stability condition represented in (3.14), the zeros of $D(s)$ must be canceled by the zeros of $(1-H(s)M(s))$. Since $D(s)$ has only two zeros, which are located at $s=0$, the following interpolation conditions needs to be satisfied:

$$\begin{aligned} 1-H(0)M(0) &= 0 & (3.18)\\ H(0)M'(0)+H'(0)M(0) &= 0 & (3.19) \end{aligned}$$

Even though $M(s)$ is an infinite dimensional inner function, $M(0)$ and $M'(0)$ can be easily derived by using (3.7) and (3.8):

$$\begin{aligned} M(0) &= 1 & (3.20)\\ \left.\frac{dM}{ds}\right|_{s=0} &= -h-\sum_{i=1}^{\infty}\frac{1}{\alpha_i^4\left(\varepsilon+\sqrt{\varepsilon^2+\frac{1}{\alpha_i^4}}\right)} & (3.21) \end{aligned}$$

Note that the term with infinite sum converges due to definition of α in (3.6) for all $\varepsilon > 0$. For the sake of simplicity, let this term be represented by

$$h_B := \sum_{i=1}^{\infty}\frac{1}{\alpha_i^4\left(\varepsilon+\sqrt{\varepsilon^2+\frac{1}{\alpha_i^4}}\right)}, \tag{3.22}$$

which leads to an easier representation of $M'(s)$ at $s=0$, $M'(0) = -h-h_B$.

As in [33], the damping coefficient ε is selected as $\varepsilon = 0.001$. Hence, the infinite sum h_B is approximately equal to 0.105. Then, a stable first order $H(s)$ which satisfies the interpolation conditions

$$\begin{aligned} H(0) &= 1, & (3.23)\\ H'(0) &= -M'(0) = h+h_B, & (3.24) \end{aligned}$$

is able to meet the requirements for stability shown in (3.13) and (3.14). For further calculations, let $H(s)$ be represented in the form

$$H(s) = \frac{(\alpha+\beta)s+1}{\beta s+1}. \tag{3.25}$$

In this case, derivative of $H(s)$ with respect to s is at $s = 0$ is

$$\left.\frac{dH(s)}{ds}\right|_{s=0} = \frac{\alpha+\beta}{1} - \beta = \alpha \tag{3.26}$$

which implies that $\alpha = h + h_B$ due to (3.24). Then, β is a positive real free parameter which satisfies (3.15).

In this example, the time delay of the system is given as $h = 0.1$ seconds. Hence,

$$\alpha = h + h_B = 0.205 \ . \tag{3.27}$$

Moreover, due to the design of controller K_n and the upper bound W_n, (3.15) is satisfied for all $\beta > 0$. Even when $\beta = 0$,

$$\|W_n \; T_n \; H\|_\infty = 0.1502 < 1 \ . \tag{3.28}$$

Therefore, during designs of the haptic feedback $H(s)$ and the predictor filter $F(s)$, β is chosen as $\beta = 0.01$. Hence,

$$H(s) = \frac{0.215s+1}{0.01s+1}, \;\; H \in \mathscr{H}_\infty \ , \tag{3.29}$$

$$F(s) = \left(1 - \left(\frac{0.215s+1}{0.01s+1}\right) M(s)\right) P_{on}(s), \;\; F \in \mathscr{H}_\infty \ , \tag{3.30}$$

due to cancellation of unstable poles of $P_{on}(s)$.

3.1.5 Conditions on the Approximation

Although the controller structure in Fig. 3.2 is constructed, $F(s)$ is infinite dimensional, and needs to be approximated by a stable finite order transfer function, denoted as F_a. The condition derived in section 2.4 is used for $M(s) = e^{-hs}$, therefore it is essential to reevaluate the stability conditions for (3.7). With this approximation, the main controller block can be defined as

$$C_a(s) := \frac{K_n(s)}{1 + K_n(s)F_a(s)}. \tag{3.31}$$

Initially, opt for a stable transfer function M_a, which is not necessarily finite-dimensional, to serve as an approximation of M. The approximation error between M and M_a is defined as

$$\Delta_M = M - M_a. \tag{3.32}$$

Subsequently, through straightforward algebraic manipulations, it can be demonstrated that the sensitivity function $S_v := 1/(1 + C_a H P_\Delta)$ can be expressed as

$$S_v = \frac{S_a}{1+X} \ , \ \text{ with } \ S_a := \frac{1}{1 + C_a H P_{on} M_a} \ . \tag{3.33}$$

In order to simplify notation, let X be defined as

$$X = \frac{C_a H P_{on}}{1 + C_a H P_{on} M_a} \left(M\Delta_n + \Delta_M\right) . \tag{3.34}$$

Then, for the stability of the closed loop system, the following two conditions must be fulfilled:

- $(C_a H)$ stabilizes $(P_{on} M_a)$,
- $\|X\|_\infty < 1$.

Consider a stable upper bound W_M satisfying

$$|W_M(j\omega)| > |\Delta_M(j\omega)|, \ \ \forall \omega \in \mathbb{R}. \tag{3.35}$$

Then the condition $\|X\|_\infty < 1$ reduces to

$$\Psi(\omega) \leq 1 \tag{3.36}$$

for all $\omega \in \mathbb{R}$, where

$$\Psi(\omega) = \left| \frac{C_a(j\omega) H(j\omega) P_{on}(j\omega) \ \left(|W_n(j\omega)| + |W_M(j\omega)|\right)}{1 + C_a(j\omega) H(j\omega) P_{on}(j\omega) M_a(j\omega)} \right| . \tag{3.37}$$

Note that the approximation M_a is exclusively utilized for stability analysis of S_a and verification of the small gain condition (3.36); therefore, in case F_a is directly formulated without reliance on it, the transfer function M_a does not play a role in the construction of the finite-dimensional controller. The subsequent subsection illustrates the application of this approach using the beam example.

3.1.6 Example Continued

A 7^{th} order stable transfer function that has the same relative degree as the predictor obtained in (3.30), two, is used to approximate $F(s)$. This approximation is denoted as $F_{a,7}(s)$, and calculated as

$$\begin{aligned} F_{a,7}(s) = & \frac{-8.4691(s-360)(s^2-24s+1600)}{(s+220)(s^2+0.492s+500)} \\ & \times \frac{(s^2-108s+8100)}{(s^2+45s+2025)(s^2+3.72s+3844)}. \end{aligned} \tag{3.38}$$

The Bode plots of both the original predictor $F(s)$ and its 7 order stable approximation $F_{a,7}$ are given in Fig. 3.4. It is worth to note that in this example, $F(s)$ is manually approximated. The next chapter shows some of the methods that can be applied to find an $\mathscr{H}_\infty$ approximation of $F(s)$.

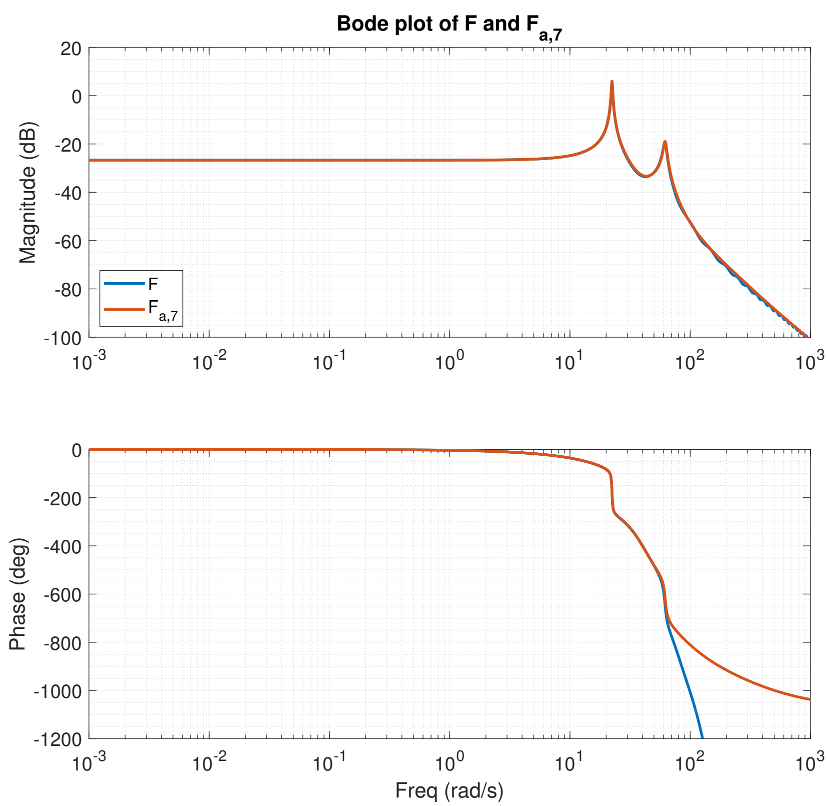

Figure 3.4: Bode plots of the predictor F and its 7 order approximation $F_{a,7}$

By replacing the term F_a with $F_{a,7}$ in (3.31), the finite dimensional main controller C_a can be obtained. The cancellation of internal pole zero pairs, this transfer function becomes 8^{th} order.

In order to check the stability conditions defined in section 3.1.5, let $M_a(s)$ be defined as

$$M_a(s) = e^{-hs} \prod_{i=1}^{20} \left(\frac{2\alpha_i^4 \left(\varepsilon + \sqrt{\varepsilon^2 + \frac{1}{\alpha_i^4}} \right) - s}{2\alpha_i^4 \left(\varepsilon + \sqrt{\varepsilon^2 + \frac{1}{\alpha_i^4}} \right) + s} \right), \tag{3.39}$$

which still is an infinite dimensional approximation of $M(s)$ due to time delay, and contains the first 20 factors of the Blaschke product $B(s)$.

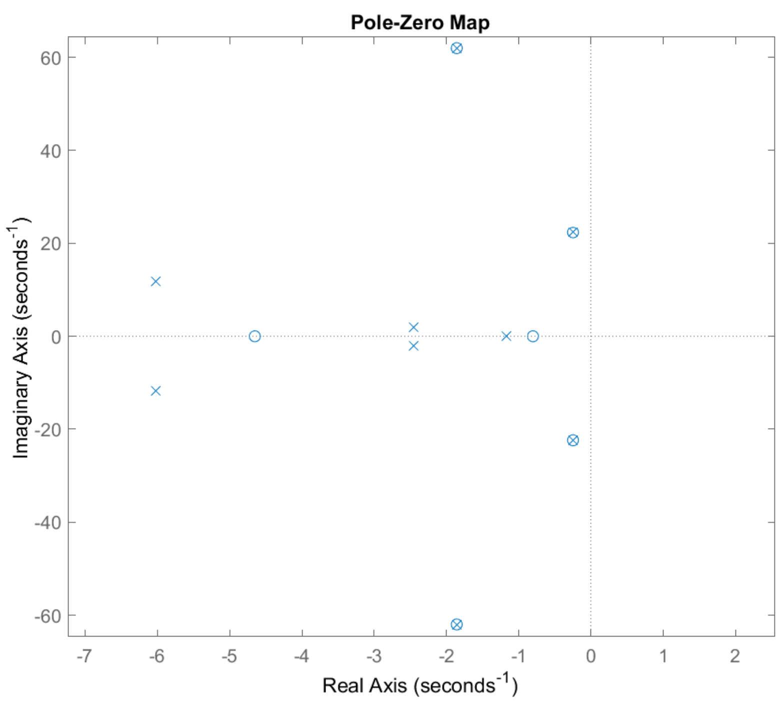

Figure 3.5: The rightmost poles of $T(s)$

Now that both $C_a(s)$ an $M_a(s)$ are known, it can be ascertained whether the stability conditions are met or not. The first of two conditions is to verify that (C_aH) stabilizes $(P_{on}M_a)$. The stability of this system can be checked by observing the pole locations of the closed loop transfer function

$$T(s) = \frac{C_a(s)H(s)P_{on}(s)M_a(s)}{1+C_a(s)H(s)P_{on}(s)M_a(s)}. \tag{3.40}$$

The poles that has the largest real parts are shown in Fig. 3.5 by 'x' marks. Hence, as it can be seen, all the poles of $T(s)$ resides in $\mathbb{C}_-$. Therefore, (C_aH) stabilizes $(P_{on}M_a)$.

Then, the only condition left to verify is given in (3.36). In order to obtain $\Psi(\omega)$ in (3.37), firstly, a stable function W_M that bounds the error Δ_M must be derived. For this purpose, a first order W_M, which satisfies (3.35), is found as illustrated in Fig. 3.6:

$$W_M(s) = \frac{2.76s}{s+12000}. \tag{3.41}$$

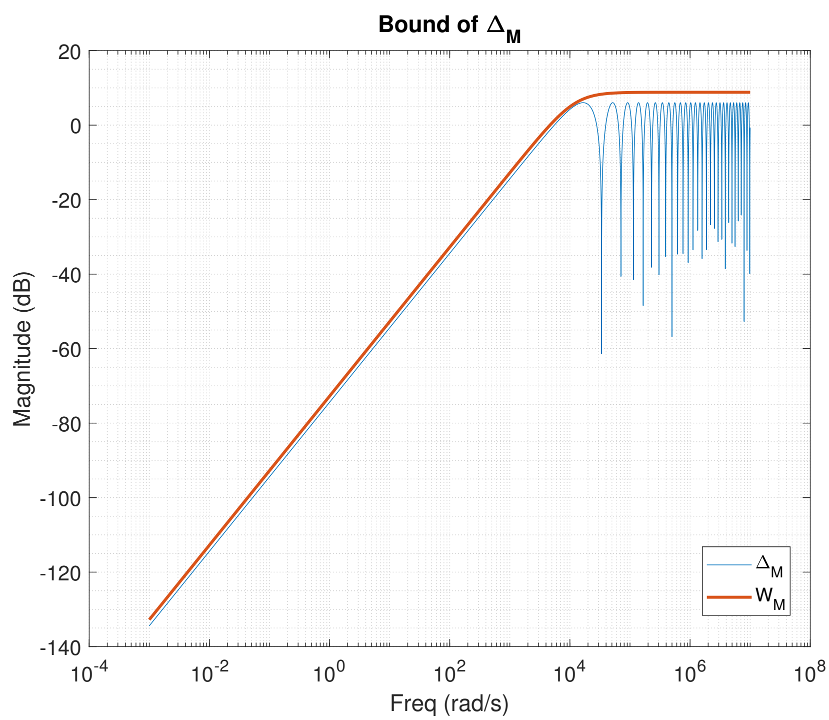

Figure 3.6: Magnitude plot of W_M and Δ_M

Then, the condition (3.36) holds as shown by Fig. 3.7.

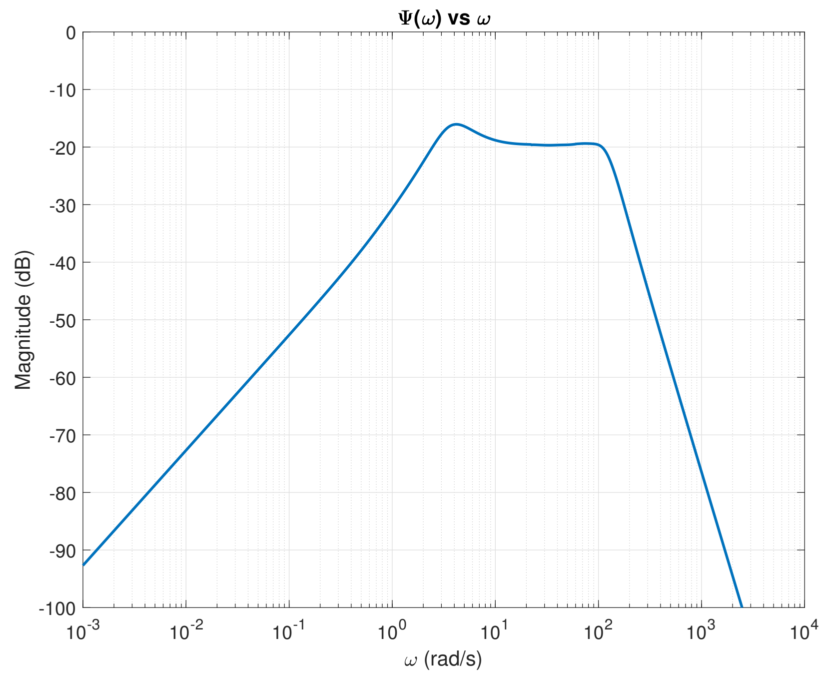

Figure 3.7: $\Psi(\omega)$ vs ω

3.2 Extension to MIMO Systems

The proposed method can also be used on MIMO systems. In this case, instead of conventional Nevanlinna-pick interpolation, tangential Nevanlinna-pick interpolation must be used to derive the proper haptic filter $H(s)$. The first subsection describes how the suggested design process is modified for MIMO system. Lastly, the altered method is applied on a single example.

3.2.1 Suggested Method for MIMO Case

The nominal representation of the non-delayed components of the set of plants considered within this section is $P_o(s) \in \mathbb{C}^{M \times M}$, which means the amount of the inputs and outputs are the same and equal to M. Hence, apart from the previously described structure, all the filters and controllers within the configuration are transfer matrices with the dimension of $(M \times M)$. For the sake of simplicity, the following assumptions have been established. Let $P_o(s) = D_l^{-1}N_l$ be a left coprime factorization.

Assumption 1 *D_l has distinct zeros in $\mathbb{C}_+$.*

Assumption 2 *The following transfer matrices commute: $H(s)$ and the time delay matrix $\Lambda(s)$, and $H(s)$ and $D_l(s)$.*

To meet the condition of commutativity, only systems with diagonal time-delay matrices are taken into account. Under these assumptions, the revised objectives of the proposed method can be summarized as

1. $H \in \mathscr{H}_\infty$, and satisfies the commutativity assumptions,
2. $F(s) := [(I - H(s)\Lambda(s))P_o(s)] \in \mathscr{H}_\infty$,
3. $||H||_\infty \leq \gamma$ for some pre-specified robustness level γ.

Multiplying both sides of the second objective with D_l leads to the following equations:

$$D_l F = D_l(I - H\Lambda)P_o \tag{3.42}$$

$$D_l F = D_l(I - H\Lambda)D_l^{-1}N_l \tag{3.43}$$

$$D_l F = (D_l - D_l H\Lambda)D_l^{-1}N_l \tag{3.44}$$

Due to the commutativity assumptions defined in assumption 2, and the fact that $\Lambda(s)$ is a diagonal matrix,

$$D_l F = (I - \Lambda H)N_l. \tag{3.45}$$

Since N_l is obtained through coprime factorization, this transfer matrix is stable. Then, (3.45) implies that satisfying the following interpolation conditions guarantees the stability of the predictor filter $F(s)$:

$$x_i(I - \Lambda(z_i)H(z_i)) = 0 \tag{3.46}$$

where z_i are the zeros of D_l, and x_i are the corresponding non-zero vectors such that

$$x_i D_l(z_i) = 0. \tag{3.47}$$

Note that when assumption 1 holds, z_i are distinct and reside in $\mathbb{C}_+$. As a result, given that D_l has n zeros at the open right half plane, the objectives can be rewritten as follows:

1. H is a stable transfer matrix, and it fulfills the commutativity assumptions,
2. $y_i := x_i H(z_i) = x_i \Lambda^{-1}(z_i)$ for $i = \{1,\ 2,\ \ldots,\ n\}$,
3. $||H||_\infty \leq \gamma$ for the smallest possible γ to maximize the robustness level.

The problem above can be solved by applying the tangential Nevanlinna-Pick interpolation, which is the solution of Nevanlinna-Pick problem for MIMO systems. This method guarantees that $(I - H\Lambda)$ has zeros at the unstable poles of P_o, which satisfies the Smith Predictor principle in designing the stable filter $F(s)$. This extended method is applied on a plant with 2 inputs and 2 outputs with a diagonal time-delay matrix, as illustrated in the next section.

3.2.2 Example with a MIMO System

Let the MIMO system $P(s) = P_o(s)\Lambda(s)$ be given as

$$P_o(s) = \begin{bmatrix} \frac{s+1}{(s+2)(s-1)} & \frac{s-3}{(s+2)(s-1)} \\ \frac{s+2}{(s-2)(s+1)} & \frac{(s+2)(s-3)}{(s-2)(s+3)} \end{bmatrix}, \quad \Lambda(s) = \begin{bmatrix} e^{-0.5s} & 0 \\ 0 & e^{-0.4s} \end{bmatrix}. \tag{3.48}$$

Then, the coprime factorization of the non-delayed nominal plant yields

$$D_l(s) = \begin{bmatrix} \frac{s-1}{s+1} & 0 \\ 0 & \frac{s-2}{s+2} \end{bmatrix}, \quad N_l(s) = \begin{bmatrix} \frac{1}{s+2} & \frac{s-3}{(s+1)(s+2)} \\ \frac{1}{s+1} & \frac{s-3}{s+3} \end{bmatrix}. \tag{3.49}$$

Note that, since both $\Lambda(s)$ and $D_l(s)$ are diagonal, assumption 2 holds for any design of $H(s)$ that is also diagonal. From (3.49), clearly, there exists two distinct zeros of D_l at the right half-plane: $z_1 = 1,\ z_2 = 2$. As D_l is diagonal, it is trivial that (3.47) leads to $x_1 = [1\ 0]^T,\ x_2 = [0\ 1]^T$. Then, by applying tangential Nevanlinna-pick interpolation, the haptic filter is designed as

$$H(s) = \begin{bmatrix} \frac{7.305}{s+3.431} & 0 \\ 0 & \frac{21590}{s+9697} \end{bmatrix} \in \mathscr{H}_\infty \text{ such that } ||H||_\infty \leq \gamma_{opt} = 2.226 \tag{3.50}$$

Now that the first and third objectives are fulfilled, the second objective, which is to design a stable $F(s)$, needs to be proved. This verification can be done by checking the transfer matrix $F(s) = [(I - H(s)\Lambda(s))P_o(s)]$ at the zeros of $D_l(s)$:

$$(I - \Lambda(1)H(1))\,P_o(1) = \begin{bmatrix} 0.1505 & -0.1505 \\ 0.7380 & -0.7380 \end{bmatrix} \tag{3.51}$$

$$(I - \Lambda(2)H(2))\,P_o(2) = \begin{bmatrix} 0.3789 & -0.1263 \\ 0.0001 & -0.0001 \end{bmatrix} \tag{3.52}$$

As a result, $F(s) \in \mathscr{H}_\infty$, and all objectives are met.

Chapter 4

Approximation of Infinite Dimensional Stable Systems in $\mathscr{H}_\infty$

Due to the occurrence of time delay in practical systems, many of the observer-predictor-based controllers have an infinite dimensional structure. When the system has high delay, Smith predictor based design is one of the most applied methods, in which the controller structure contains an FIR filter and presumably an additive stable function to compensate the delay. In order to implement this block on physical plants, one needs to use an approximation method to obtain a finite order transfer function. Nevertheless, utmost consideration must be given to stability condition throughout the approximation and its effect on robustness. Therefore, this thesis focuses on model order reduction methods that aim to minimize the $\mathscr{H}_\infty$-norm.

In this chapter, firstly, the proposed approach to approximate the predictor filter is described. The second section presents a new method that is proposed for finding sub-optimal $\mathscr{H}_\infty$ reduced-order model. The third section discusses similarities between the proposed method and optimal Hankel norm approximation. Lastly, several methods in the literature are compared with our method by using two examples.

4.1 Outline of the Proposed Approach

The predictor filters in the designs that are originated from the Smith predictor contains FIR structure, which are stable infinite dimensional functions. In order to implement such designs into practical systems, the order must be reduced to a desired level by using a proper approximation method. This operation must also preserve the robust stability of the closed loop system. Therefore, the error of the approximation should be minimized to maintain the robustness margin at highest possible level. Hence, the following approach is proposed to find a suboptimal $\mathscr{H}_\infty$ model with finite order.

Let $P_\infty(s, e^{-hs})$ be a stable transfer function that consists of an FIR structure and an additive stable rational function. The aim is to find an r^{th} order stable $P_r(s)$ such that

$$||P_\infty - P_r||_\infty \leq \gamma \tag{4.1}$$

for the smallest possible $\gamma > 0$. The inequality defined in (4.1) is actually a challenging unsolved problem that is being researched on during the last four decades. Most popular techniques used for such model order reductions within the literature are balanced truncation and Hankel norm approximation. An alternative approach to those methods can be described as follows:

1. First, reduce the infinite order $P_\infty(s, e^{-hs})$ to a finite order rational transfer function, $P(s, Pade(h, N_p))$, by using a high order (N_p) Pade approximation on the delay term such that the error is lower than a prespecified level, ε:

   $$P_\infty(s, e^{-hs}) \;\rightarrow\; P(s, Pade(h, N_p)) \quad s.t. \quad ||P_\infty - P||_{\mathscr{L}_\infty} \leq \varepsilon \tag{4.2}$$

   To find the appropriate N_p according to given ε, the following theorem is applied.

   Theorem 1 *[30] The magnitude of the error between time delay and its N_p order Pade approximation, $P_d(j\omega, N_p)$ is bounded by*

   $$|e^{-j\omega h} - P_d(j\omega, N_p)| \leq \begin{cases} 2\left(\frac{eh\omega}{4N_p}\right)^{2N_p+1}, & if \;\; \omega \leq \frac{4N_p}{eh} \\ 2, & if \;\; \omega \geq \frac{4N_p}{eh} \end{cases} .$$

After this operation, P may be unstable with "close" poles-zeros in $\mathbb{C}_+$. By using partial fraction expansion, the terms with unstable poles may be canceled, which yields to an N^{th} order stable approximation, denoted as $P_a(s)$, which is also represented by $P_N(s)$.

2. The suggested procedure continues with finding and $(N-1)$ order approximation of P_N, P_{N-1}, such that

$$||P_N - P_{N-1}||_\infty = \gamma_{opt} \tag{4.3}$$

where γ_{opt} is the minimum error. The key step in finding this optimal approximation is explained in the following theorem.

Theorem 2 *[55] Let $H(s)$ be a stable transfer function. Then, the r^{th} order optimal $\mathscr{H}_\infty$ approximation of $H(s)$, denoted as $H_r^{opt}(s)$, needs to satisfy*

$$\min_{\omega\in\mathbb{R}} |H(j\omega) - H_r(j\omega)| \leq ||H - H_r^{opt}||_{\mathscr{H}_\infty} \leq ||H - H_r||_{\mathscr{H}_\infty}.$$

In this context, H_r represents any r^{th} order stable approximation of $H(s)$ that interpolates $H(s)$ at $2r+1$ points within the open right half-plane. Especially, when $|H(j\omega) - H_r(j\omega)| = k\ \forall\omega$, where k is a constant, then H_r itself is an optimal $\mathscr{H}_\infty$ approximation of $H(s)$.

3. One way to find an r^{th} reduced order model of P_N is to sequentially find optimal $\mathscr{H}_\infty$ approximation of P_{N-1} as P_{N-2}, P_{N_2} as P_{N_3}, and so on, until the estimation of P_r. As illustrated in the next chapter, this technique is improved either by using nonlinear minimization algorithms or using additional terms within the linear equations.

4.2 Proposed Methods on $\mathscr{H}_\infty$ Model Order Reduction

Several methods based on interpolation conditions found by the following linear equations derived, are proposed within the subsequent subsections. Firstly, the optimal $\mathscr{H}_\infty$ approximation of N order stable transfer function with $m = N-1$ order is obtained by using linear equations. Later, some extensions of these set of equations are investigated throughout this section.

4.2.1 Optimal $\mathscr{H}_\infty$ Approximation Through Linear Equations

Theorem 2 is a crucial baseline on finding the optimal $\mathscr{H}_\infty$ approximation of P_N. According to the last sentence of this theorem, the following equality can be constructed for the error between P_N and its $(N-1)^{th}$ order optimal $\mathscr{H}_\infty$ approximation that satisfies (4.3).

$$E = P_N - P_{N-1} = \frac{nP_N}{dP_n} - \frac{nP_{N-1}}{dP_{N-1}} = \gamma_{opt}\frac{dP_N^*\, dP_{N-1}^*}{dP_N\, dP_{N-1}} \tag{4.4}$$

where nP_N and dP_N represent the numerator and the denominator of P_N respectively, and dP_N^* notates the conjugate of the polynomial $dP_N(s)$.

By applying proper linear algebra, one can show that the optimal solution can be found by using the following interpolation points

$$nP_N(p_k)\, dP_{N-1}(p_k) - \gamma\, dP_N^*(p_k)\, dP_{N-1}^*(p_k) = 0, \;\; k = \{1, 2, \ldots, N\} \tag{4.5}$$

where p_k are the poles of P_N. The interpolation conditions yields N equations with $N+1$ unknowns. N parameters are the coefficients of dP_{N-1}, which is defined as

$$dP_{N-1}(s) = a_{N-1}s^{N-1} + a_{N-2}s^{N-2} + \ldots + a_0. \tag{4.6}$$

Then, the interpolation conditions are satisfied with the following linear equation:

$$\frac{1}{\gamma}Vx - \Lambda VJx = 0, \text{ where } x = [a_0\; a_1\; \cdots\; a_{(N-1)}]^T, \tag{4.7}$$

where $N \times N$ matrices V, which is a Vandermonde matrix, Λ and J, that are diagonal matrices, and $N \times 1$ vector x, are constructed as shown below,

$$V = \begin{bmatrix} 1 & p_1 & \cdots & p_1^{N-1} \\ 1 & p_2 & \cdots & p_2^{N-1} \\ \vdots & \vdots & \ddots & \vdots \\ 1 & p_N & \cdots & p_N^{N-1} \end{bmatrix}, \; J = \begin{bmatrix} 1 & 0 & \cdots & 0 \\ 0 & -1 & \cdots & 0 \\ \vdots & \vdots & \ddots & \vdots \\ 0 & 0 & \cdots & (-1)^{N-1} \end{bmatrix},$$

$$\Lambda = \begin{bmatrix} \frac{dP_N^*(-p_1)}{nP_N(p_1)} & 0 & \cdots & 0 \\ 0 & \frac{dP_N^*(-p_2)}{nP_N(p_2)} & \cdots & 0 \\ \vdots & \vdots & \ddots & \vdots \\ 0 & 0 & \cdots & \frac{dP_N^*(-p_N)}{nP_N(p_N)} \end{bmatrix}, \; x = \begin{bmatrix} a_0 \\ a_1 \\ \vdots \\ a_{N-1} \end{bmatrix}$$

Hence, the optimal γ is the reciprocal of the eigenvalue of $V^{-1}\Lambda VJ$ with the largest magnitude, where all the roots of corresponding eigenvector $dP_{N-1}(s)$ reside in the open left half-plane, due to the following equation:

$$\left(\frac{1}{\gamma}I - V^{-1}\Lambda VJ\right)x = 0. \tag{4.8}$$

Clearly, the numerator of $P_{N-1}(s)$, $nP_{N-1}(s)$, can then be calculated by applying simple algebra on (4.4). An example based on the proposed design is given to illustrate how the approximation error in (4.4) abides the Theorem 2.

According to the suggested method, for the plant

$$P(s) = P_0(s)e^{-hs}, \; P_0(s) = \frac{1}{(s^2-2s+2)}, \; h = 0.5 \tag{4.9}$$

the predictor filter $F(s)$ is designed as

$$F(s) = \left(1 - 2.62\frac{(s-0.483)}{(s+0.483)}e^{-0.5s}\right)\frac{1}{(s^2-2s+2)}.$$

As described within section 4.1, initially, a Pade approximation of the time delay needs to be found. The order of this approximation is determined based on Theorem 1. The resulting filter is denoted by

$$F_a(s) = \left(1 - 2.62\frac{(s-0.483)}{(s+0.483)}Pade(h,N_p)\right)\frac{1}{(s^2-2s+2)},$$

where N_p is defined in (4.2). Let the boundary on the error of this technique be specified as $\varepsilon = 0.01$. Then, the aim is to find the minimum N_p such that the following condition is satisfied:

$$|F(j\omega) - F_a(j\omega)| = \left|2.62\left(P_d(j\omega, N_p) - e^{-0.5s}\right) P_0(j\omega)\right| \leq \varepsilon \tag{4.10}$$

By using Theorem 1, firstly, (ω_0) must be calculated such that

$$2.62\left|\frac{1}{-\omega^2 - 2j\omega + 2}\right| \leq \frac{\varepsilon}{2} = 0.005 \;\; \forall\; \omega \geq \omega_0 \;. \tag{4.11}$$

Since $P_0(s)$ is a strictly proper transfer function, there obviously exists an ω_0. As shown in Fig. 4.2.1, $\omega_0 = 22.9$ rad/s satisfies this condition.

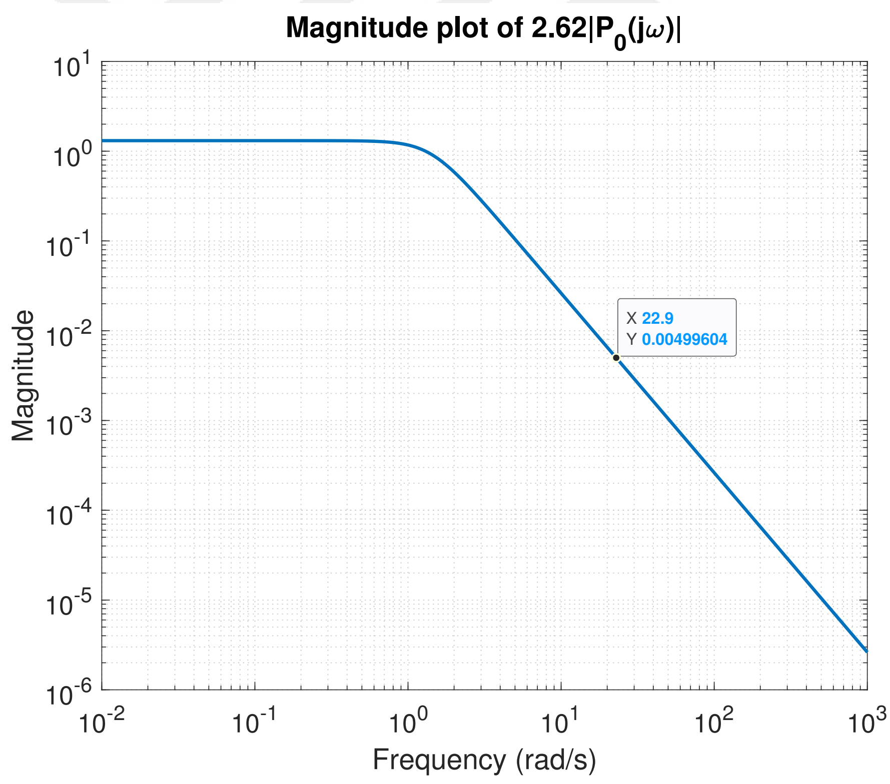

Figure 4.1: Magnitude of the left hand side of (4.11)

Then, fulfilling the following condition is sufficient to satisfy $\|F - F_a\|_\infty \leq \varepsilon$:

$$N_p \geq \frac{e\, h\, \omega_0}{4} = 0.6796\, h\, \omega_0 = 7.781,\; N_p \in \mathbb{Z}^+ \tag{4.12}$$

Therefore, $N_p = 8$ meets the specified criterion in (4.10). The magnitude of the approximation error is illustrated in Fig. 4.2.1

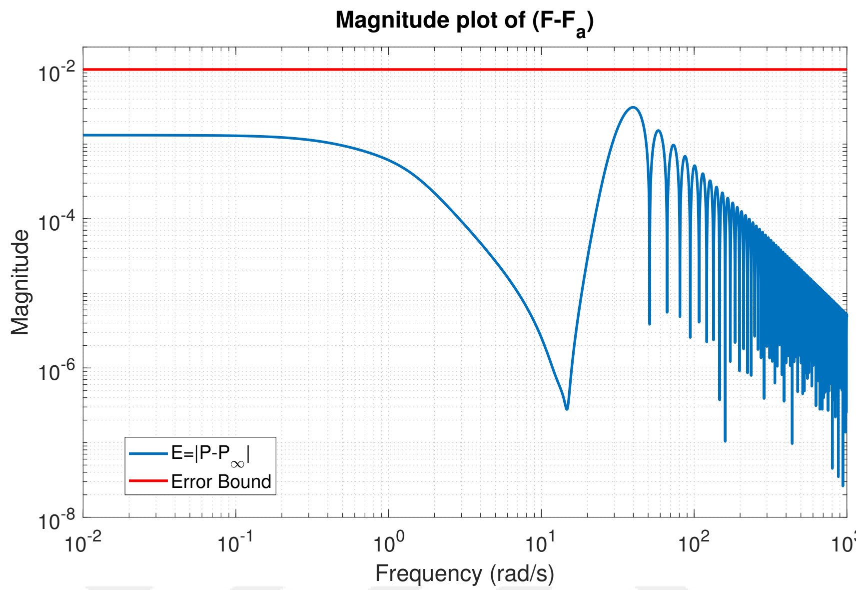

Figure 4.2: Magnitude of the Pade approximation error and specified bound ε

By using 8^{th} order pade approximation of the time delay term, $e^{-0.5s}$, a finite order model of F_a can be obtained. Cancellation of unstable poles with zeros approximately located in the vicinity results in

$$\begin{aligned} F_a &= \frac{1.8\left(1-\frac{s}{300}\right)\left(1-0.3\frac{s}{12.9}+\left(\frac{s}{12.9}\right)^2\right)\left(1-0.16\frac{s}{25.4}+\left(\frac{s}{25.4}\right)^2\right)}{\left(1+\frac{s}{0.483}\right)\left(1+2\frac{s}{22.6}+\left(\frac{s}{22.6}\right)^2\right)\left(1+1.8\frac{s}{23.3}+\left(\frac{s}{23.3}\right)^2\right)} \\ &\times \frac{\left(1-0.28\frac{s}{47.3}+\left(\frac{s}{47.3}\right)^2\right)}{\left(1+1.4\frac{s}{24.8}+\left(\frac{s}{24.8}\right)^2\right)\left(1+0.8\frac{s}{27.8}+\left(\frac{s}{27.8}\right)^2\right)}, \end{aligned} \tag{4.13}$$

which is a stable 9^{th} order proper transfer function with distinct poles. As illustrated in Fig. 4.2.1 , the optimal $\mathscr{H}_\infty$ approximation of F_a with 8^{th} order, denoted as $F_{a,8}$, returns a flat approximation error through $\omega \in \mathbb{R}$.

Note that the magnitude of the approximation error is equal to 1.0833×10^{-4}, which is the least Hankel singular value (hsv) of F_a, meaning that it is the least achievable error on $\mathscr{H}_\infty$ approximation [50].

As mentioned in the previous section, an approximation can be found by recursively reducing the order by one. This method is illustrated through the second order

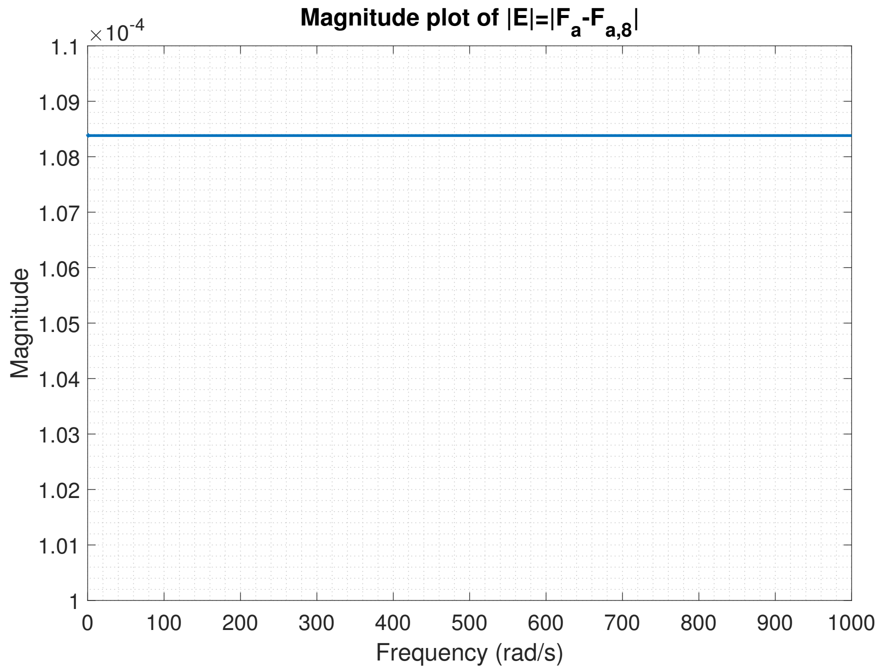

Figure 4.3: Magnitude of the approximation error

approximation of F_a. The resulting transfer function is

$$F_{a,2}(s) \quad = \quad 1.789\frac{1-1.372\left(\frac{s}{14.15}\right)+\left(\frac{s}{14.15}\right)^2}{(1+\frac{s}{4.24})(1+\frac{s}{0.5116})}.$$

The magnitude of the error function is given in Fig. 4.4. The following theorem constitutes the foundation of further derivations and analyses.

Theorem 3 *[21] Let m order complex rational function $F_{opt,m}(s)$ denote the optimal $\mathscr{H}_\infty$ approximation of n order transfer function $F(s)$. Then, the approximation error function $E_{opt} := F - F_{opt,m}$ must satisfy*

$$|E_{opt}(j\omega_i)| = \|E_{opt}\|_\infty = \gamma_{opt}, \textit{ for some } \omega_i,\ i = 1,2,\ldots,2m+2, \tag{4.14}$$

where γ_{opt} is the minimum achievable $\mathscr{H}_\infty$ error. This implies that at only $(2m+2)$ frequency points the magnitude of $E_{opt}(j\omega)$ should be equal to γ_{opt}. At the remaining points, the magnitude of the error must be less than this value.

The main problem in applying the above theorem is that for the optimal solution the locations of ω_i are unknown; they have to be estimated somehow. See further discussion below.

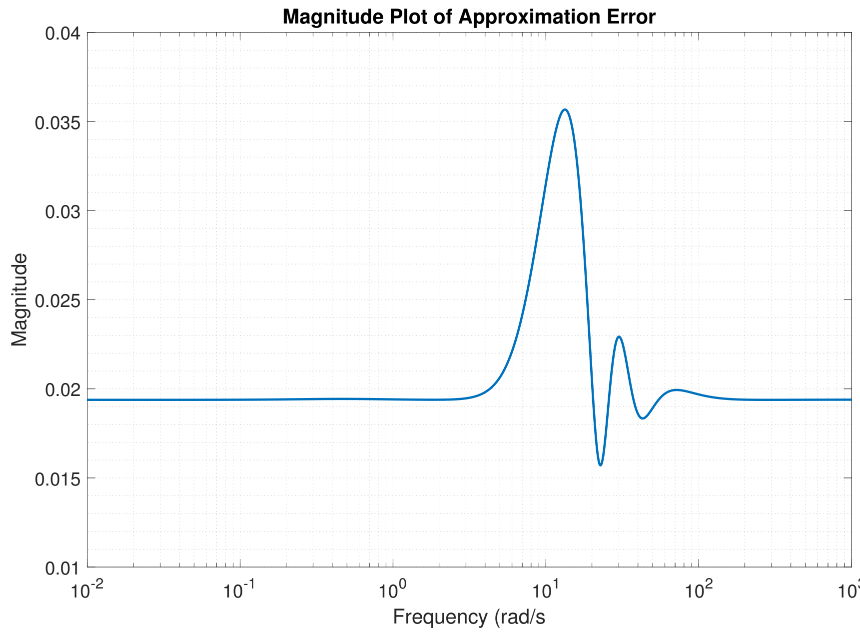

Figure 4.4: Example (4.13): Magnitude of $E = F_a - F_{a,2}$

Due to the fact that $|F_a(j\omega) - F_{a,2}(j\omega)| = \|F_a - F_{a,2}\|_\infty = 0.037$ is satisfied at only two frequencies (one is shown in the figure, the other peak is located at $\omega = -13.33$), instead of 6, clearly it is not a desired solution according to Theorem 3. Therefore, the subsequent sections propose several extensions of these linear equations combined with nonlinear minimization techniques in order to find sub-optimal $\mathscr{H}_\infty$ approximants.

The linear equations are firstly extended to derive the optimal $\mathscr{H}_\infty$ approximation, which is a challenging problem that still could not be solved. Although the set of equations lead to an insolvable structure currently, we believe that it provides a new perspective against model order reduction in $\mathscr{H}_\infty$-norm. Furthermore, several methods are developed to derive sub-optimal results.

Let $P \in \mathscr{H}_\infty$ be a finite dimensional proper SISO system with an order of n. Let us denote $Q \in \mathscr{H}_\infty$, as an approximant of P with respect to $\mathscr{H}_\infty$-norm with an order of $m < n$. Then, by Theorem 3, the error between Q and P can further be extended as

$$E := P - Q = \frac{nP}{dP} - \frac{nQ}{dQ} = \frac{nP\,dQ - nQ\,dP}{dP\,dQ} \tag{4.15}$$

$$= \gamma\left(\frac{T^*\,dP^*\,dQ^* - M\,F}{T\,dP\,dQ}\right), \tag{4.16}$$

where the degrees of polynomials T, M and F are $(n-m-1)$, $(2m+2)$, and $(2n-2m-3)$ respectively. Note that (nX) stands for the numerator of rational function X, and (dX) represents the denominator. Due to Theorem 3, the polynomial M is selected to have roots on imaginary axis, i.e.

$$M := \prod_{k=1}^{m+1}(s^2+a_k^2), \quad a_k \in \mathbb{R} \text{ are distinct.} \tag{4.17}$$

This definition ensures that the magnitude of the error function is equal to γ at $(2m+2)$ points on imaginary axis. The main difficulty here is that the frequency points a_k are not known a priori. Then, the square of magnitude of E defined in (4.16) is represented by

$$\begin{aligned} |E|^2 &= \gamma^2\left(\frac{T^*\,dP^*\,dQ^*-M\,F}{T\,dP\,dQ}\right)\left(\frac{T\,dP\,dQ-M\,F^*}{T^*\,dP^*\,dQ^*}\right) && (4.18)\\ &= \gamma^2\left[1-\left(\frac{M(T\,F\,dP\,dQ+T^*\,F^*\,dP^*\,dQ^*)-M^2\,F\,F^*}{T\,dP\,dQ\,T^*\,dP^*\,dQ^*}\right)\right] && (4.19)\end{aligned}$$

For the sake of simplification in the notation, let the rational complex functions X_1 and X_2 denote

$$X_1(s) := \frac{M(s)\,[T(s)\,F(s)\,dP(s)\,dQ(s)+T^*(s)\,F^*(s)\,dP^*(s)\,dQ^*(s)]}{T(s)\,dP(s)\,dQ(s)\,T^*(s)\,dP^*(s)\,dQ^*(s)} \tag{4.20}$$

$$X_2(s) := \frac{(M^2(s)\,F(s)\,F^*(s))}{T(s)\,dP(s)\,dQ(s)\,T^*(s)\,dP^*(s)\,dQ^*(s)}\,. \tag{4.21}$$

Again, by Theorem 3, the derivative of magnitude of the error function E with respect to s must be equal to zero at the roots of the polynomial M, defined in (4.17). Note that the derivative $(\partial|E|/\partial s)$ can be derived from $(\partial|E|^2/\partial s)$ at points $s=\mp ja_k$ as

$$\left.\frac{\partial|E|}{\partial s}\right|_{s=\mp ja_k} = \left.\frac{\frac{\partial|E|^2}{\partial s}}{2|E|}\right|_{s=\mp ja_k}. \tag{4.22}$$

Note that at the zeros of M, E defined in (4.16) becomes

$$E|_{s=\mp ja_k} = \gamma\frac{T^*\,dP^*\,dQ^*}{T\,dP\,dQ}, \tag{4.23}$$

which implies that

$$|E|\Big|_{s=\mp ja_k} = \gamma\,. \tag{4.24}$$

Hence,

$$\left.\frac{\partial |E|}{\partial s}\right|_{s=\mp ja_k} = \left.\frac{\frac{\partial |E|^2}{\partial s}}{2\gamma}\right|_{s=\mp ja_k} = \left.\frac{\partial |E|^2}{\partial s}\right|_{s=\mp ja_k} = 0. \tag{4.25}$$

Then, by using (4.19), (4.20) and (4.21)

$$\left.\frac{\partial |E|^2}{\partial s}\right|_{s=\mp ja_k} = 0 - \gamma^2 \left.\frac{\partial \left(X_1(s)\right)}{\partial s}\right|_{s=\mp ja_k} + \gamma^2 \left.\frac{\partial \left(X_2(s)\right)}{\partial s}\right|_{s=\mp ja_k}. \tag{4.26}$$

Since the numerator of $X_2(s)$, $nX_2(s)$, contains the term $M^2(s)$ as a multiplying factor,

$$\left.\frac{\partial \left(X_2(s)\right)}{\partial s}\right|_{s=\mp ja_k} = \left.\frac{\partial \left(\frac{(M^2(s)\ F(s)\ F^*(s))}{T(s)\ dP(s)\ dQ(s)\ T^*(s)\ dP^*(s)\ dQ^*(s)}\right)}{\partial s}\right|_{s=\mp ja_k} = 0. \tag{4.27}$$

Furthermore, $nX_1(s)$ includes the term $M(s)$ as a multiplier, which leads to

$$\left.\frac{\partial \left(X_1\right)}{\partial s}\right|_{s=\mp ja_k} = \frac{\partial M}{\partial s}\left.\left(\frac{T\ F\ dP\ dQ + T^*\ F^*\ dP^*\ dQ^*}{T\ dP\ dQ\ T^*\ dP^*\ dQ^*}\right)\right|_{s=\mp ja_k}. \tag{4.28}$$

Therefore, at the roots of M, (4.26) becomes

$$\left.\frac{\partial |E|^2}{\partial s}\right|_{s=\mp ja_k} = -\gamma^2 \left(\frac{\partial M}{\partial s}\right)\left.\left(\frac{T\ F\ dP\ dQ + T^*\ F^*\ dP^*\ dQ^*}{T\ dP\ dQ\ T^*\ dP^*\ dQ^*}\right)\right|_{s=\mp ja_k} = 0. \tag{4.29}$$

Due to definition of M, a_k are distinct values, hence $\partial M/\partial s$ is not equal to zero at the roots of M. Consequently, (4.29) leads to the following interpolation conditions

$$T(r)F(r)dP(r)dQ(r) + T(-r)F(-r)dP(-r)dQ(-r) = 0 \tag{4.30}$$

where $r = \mp ja_k$ are the roots of M, as defined in (4.17).

Therefore,

$$T\ F\ dP\ dQ + T^*\ F^*\ dP^*\ dQ^* = M\ Z \tag{4.31}$$

where Z is a polynomial with a degree of $2(4n-4m-6)$.

The equations that lead to optimal $\mathscr{H}_\infty$ norm is concluded with the condition $||E||_\infty = \gamma$, which leads to

$$\left|\frac{T^*(j\omega)dP^*(j\omega)dQ^*(j\omega) - M(j\omega)F(j\omega)}{T(j\omega)dP(j\omega)dQ(j\omega)}\right| \leq 1 \ \ \forall\ \omega. \tag{4.32}$$

By using the interpolation and boundary conditions derived above, four different techniques are suggested to estimate sub-optimal $\mathscr{H}_\infty$ approximations. Firstly, the linear equations are constructed in such a way that the result is the same as the reduced order model obtained through optimal HNA. The number of unknown coefficients of F is reduced under an assumption as a second method, which is proven to be wrong by using a counter example. The third procedure uses $m+1$ order HNA approximation and introduces another assumption to derive the approximant with order m by applying minimax algorithms. Finally, as described within step-3 of the outline, an iterative process can be used with nonlinear minimization techniques.

4.2.2 Relations with Hankel Norm Approximation

In case the error function given in (4.16) is represented in the form

$$E = P - Q = \gamma \left(\frac{T^*\ dP^*\ dQ^* - dP\ Y}{T\ dP\ dQ} \right) \tag{4.33}$$

where T is again a polynomial with order $n-m-1$ it is observed that the resulting approximation leads to the same result as HNA. In this representation, Y is a polynomial with $n-m-2$ order such that the denominator of the error function E only contains the poles of P and Q, which necessitates the interpolation conditions

$$dP^*(p_T)dQ^*(p_T) - dP(p_T)Y(p_T) = 0 \tag{4.34}$$

where p_T are the roots of the polynomial T. When $E(s)$ is in this form, at the poles of P, the interpolation conditions given in 4.5 are obtained as

$$nP_N(p_k)T(p_k)dQ(p_k) - \gamma\, dP_N^*(p_k)T^*(p_k)dQ^*(p_k) = 0,\ \ k = \{1, 2, \ldots, N\}. \tag{4.35}$$

Since there exist n poles and the order of $(T\ dQ)$ is $n-1$, the same procedure to obtain $(n-1)$ order approximation described in section 4.2.1 may be applied. However, in this scenario, the resulting eigenvector must have m roots in $\mathbb{C}_-$, and $(n-m-1)$ roots in $\mathbb{C}_+$. Consequently, (4.8) can be used to obtain the γ value and the polynomial dQ and T. Both this method and HNA are applied to obtain the γ values for $m < n$ on the example given in (4.13). The resulting reciprocal of eigenvalues through the

Order (m)	**Hankel Singular Values** $(\sigma_{HSV,m})$	**Reciprocal of Eigenvalues** (γ_m)
0	1.005326658195529	1.005326658197479
1	0.120599944476631	0.120599944476635
2	0.026181350029550	0.026181350029553
3	0.010129364437567	0.010129364437545
4	0.005268791248765	0.005268791248783
5	0.003084112913546	0.003084112913360
6	0.001690297735253	0.001690297735299
7	0.000650313941818	0.000650313941811
8	0.000108334388528	0.000108334388528

Table 4.1: Example (4.13): Comparison of HSV and reciprocal of eigenvalues, γ

described technique and Hankel singular values (HSV) are illustrated in Table 4.1 with a precision of 16 digits.

Note that, according to our observations,

$$\left|\frac{dP(j\omega)\,Y(j\omega)}{dP(j\omega)\,dQ(j\omega)}\right| < 0.25\sigma_{HSV,m} \;\; \forall\omega,\; m = 0, 1, \ldots, 8.$$

Therefore, HNA returns a good estimation of the optimal $\mathscr{H}_\infty$ approximation. However, since $(M \times F)$ denoted in (4.16) is a polynomial with a small DC gain, the assumption of (4.33) returns worse estimation of frequencies of peak gain as frequency increases. Also, the error on frequencies of peak errors becomes significantly larger as $(n-m)$ increases.

4.2.3 Sub-optimal $\mathscr{H}_\infty$ Approximation for $m = n-2$

Under the assumption of $(F = T^*\,R)$, where R is a polynomial with $n-m-2$ order, the error function defined in (4.16) becomes

$$E = P - Q = \gamma\left(\frac{T^*\;(dP^*\,dQ^* - M\,R)}{T\;dP\,dQ}\right). \tag{4.36}$$

Then, this assumption leads (4.29) to be simplified as

$$\left.\frac{\partial |E|^2}{\partial s}\right|_{s=\mp ja_k} = -\gamma^2 \left(\frac{\partial M}{\partial s}\right) \left.\left(\frac{R\, dP\, dQ + R^*\, dP^*\, dQ^*}{dP\, dQ\, dP^*\, dQ^*}\right)\right|_{s=\mp ja_k} = 0. \tag{4.37}$$

Since $\partial M/\partial s$ can not be equal to zero at the roots of M by definition, (4.37) implies that the interpolation conditions

$$R(r)dP(r)dQ(r) + R(-r)dP(-r)dQ(-r) = 0 \tag{4.38}$$

where $r = \mp ja_k$ are the roots of M, must be satisfied. Hence,

$$R\, dP\, dQ + R^*\, dP^*\, dQ^* = M\, Z \tag{4.39}$$

where Z is a polynomial with a degree of $2n-2m-4$. Furthermore, when $(F = T^*\, R)$, (4.32) becomes

$$\left|\frac{T^*\,(dP^*\, dQ^* - M\, R)}{T\, dP\, dQ}\right| = \left|\frac{(dP^*\, dQ^* - M\, R)}{dP\, dQ}\right| \leq 1. \tag{4.40}$$

Then,

$$E\, E^* = 1 - \left(\frac{M(R\, dP\, dQ + R^*\, dP^*\, dQ^*) - M^2\, R\, R^*}{dP\, dQ\, dP^*\, dQ^*}\right) \leq 1 \tag{4.41}$$

Hence,

$$\left(\frac{M^2(Z - R\, R^*)}{dP\, dQ\, dP^*\, dQ^*}\right) = \frac{M^2}{dP\, dQ\, dP^*\, dQ^*}(Z - R\, R^*) \geq 0. \tag{4.42}$$

Because that $|E| = \gamma$ only if $s = \pm ja_k$, (4.42) implies that $(Z > R\, R^*)$ $\forall\omega$. Therefore, Z is a positive-definite polynomial and can be represented as

$$Z = A\, A^* \tag{4.43}$$

where the order of A is $n-m-2$. Then, (4.39) becomes

$$R\, dP\, dQ + R^*\, dP^*\, dQ^* = M\, A\, A^*. \tag{4.44}$$

Remark 5 *Since both P and Q are in $\mathscr{H}_\infty$, and A does not have any roots on imaginary axis, the roots of R must be in the Right Half Plane (RHP) in order to satisfy* (4.44).

In the case of $(m = n-2)$, the order of R and A are equal to 0, which implies that they are constants. Moreover, T is a first order polynomial, and the order of M is $2n-2$. Let $R = c$, where $c \in \mathbb{R}$, so (4.44) becomes

$$c(dP\, dQ + dP^*\, dQ^*) = MAA^*. \tag{4.45}$$

Since the order of $(dP\ dQ)$ is $2n-2$, which is equal to the order of M, M and A can be selected as

$$M = dP\ dQ + dP^*\ dQ^*, \quad A = \sqrt{c} \tag{4.46}$$

which implies that $c \in \mathscr{R}^+$. Then, by replacing the terms M, A and R in (4.36) with (4.46) and c respectively, we obtain

$$E = \gamma \frac{T^*(dP\ dQ - c(dP\ dQ + dP^*\ dQ^*)}{T\ dP\ dQ} = \gamma \frac{T^*[(1-c)\ dP^*\ dQ^* - c\ dP\ dQ]}{T\ dP\ dQ} \tag{4.47}$$

Then, the following interpolation conditions need to be satisfied:

$$nP(p_k)dQ(p_k)T(p_k) = \gamma(1-c)T^*(p_k)dP^*(p_k)dQ^*(p_k) \tag{4.48}$$

where p_k are the roots of (dP) and the root of T lies in $\mathbb{C}_+$ due to remark 5 and (4.34).

Then, returning back to the 9th order system (4.13), by solving the aforementioned linear equations, the sub-optimal 7^{th} order $\mathscr{H}_\infty$ approximation, denoted as $F_{a,7}$, is found as

$$\begin{aligned}
F_{a,7} &= Q_{7,1}\ Q_{7,2} \\
Q_{7,1} &= 1.8088 \frac{(1-s/83.78)(1-0.2985(s/12.87)+(s/12.87)^2)}{(1+s/0.482)(1+1.705(s/9.06)+(s/9.06)^2)} \\
Q_{7,2} &= \frac{(1-0.163(s/25.5)+(s/25.5)^2)(1-0.2384(s/51.8)+(s/51.8)^2)}{(1+0.693(s/16.3)+(s/16.3)^2)(1+0.285(s/28)+(s/28)^2)}
\end{aligned}$$

where the $\mathscr{H}_\infty$-norm error is found as $\gamma_7 = 6.833606313555466 \times 10^{-4}$.

The magnitude of the error functions obtained by proposed approach and HNA are shown in Fig. 4.5. Additionally, the $\mathscr{H}_\infty$-norm error of the proposed technique and HSV for $m = 7$ are illustrated in the same figure. Although the resulting $\mathscr{H}_\infty$-norm error $\gamma < 1.051\sigma_{HSV,7}$, this method does not return the optimal result. By using `systune` command in MATLAB, which uses nonsmooth optimization algorithms described in [4], a better $\mathscr{H}_\infty$ approximation can be found as given in Fig. 4.6, where the $\mathscr{H}_\infty$-norm error is found as $6.705736767685825 \times 10^{-4}$. Within this figure, the approximation error obtained by `systune` is represented by E_{ST}. Therefore, the assumption of $(F = T^*\ R)$ fails.

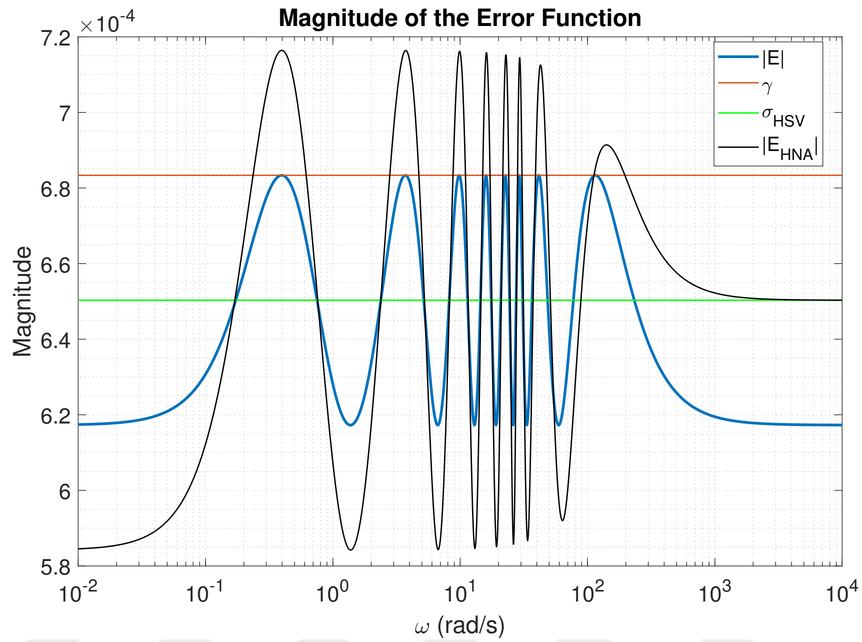

Figure 4.5: Example (4.13): Absolute error between F_a and $F_{a,7}$

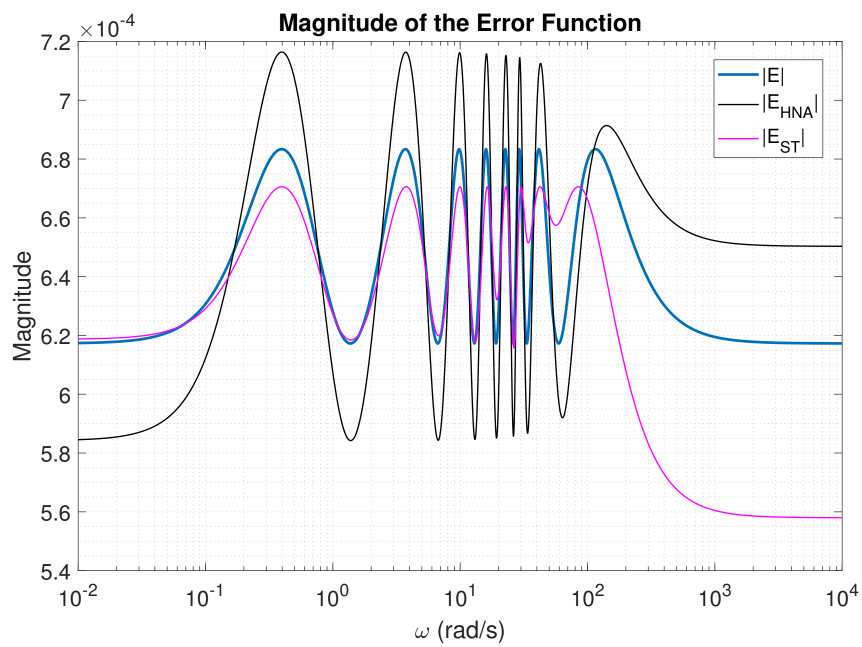

Figure 4.6: Example (4.13): Absolute approximation errors of proposed technique and `systune` for 7 order approximations

4.2.4 An Extension of the Proposed Method

Let U_{m+1} denote the $m+1$ order HNA of P, the stable transfer function that is to be approximated. Also, let Q_m represent the m order sub-optimal $\mathscr{H}_\infty$ approximation of this function. Then, the error function E can be written as

$$\begin{aligned} E &= P - Q = (P - U_{m+1}) + (U_{m+1} - Q_m) && (4.49) \\ &= \gamma_{m+1}\left(\frac{T^*\, dP^*\, dU^*_{m+1} - dP\, Y}{T\, dP\, dU_{m+1}}\right) + \frac{nU_{m+1}\, dQ_m - nQ_m\, dU_{m+1}}{dU_{m+1}\, dQ_m} && (4.50) \end{aligned}$$

It has been observed that, representing E in the form

$$E = \gamma_{m+1}\left(\frac{T^*\, dP^*\, dU^*_{m+1} - dP\, Y}{T\, dP\, dU_{m+1}}\right) + k_1\left(\frac{dU^*_{m+1} dQ^*_m}{dU_{m+1}\, dQ_m}\right) + k_2\frac{dU^*_{m+1}}{dU_{m+1}} \tag{4.51}$$

results with good estimation on Q_m, where $k_1 \in \mathbb{R}$ and $k_2 \in \mathbb{R}$. To simplify the notation, let

$$E_{m+1} = P - U_{m+1} = \gamma_{m+1}\left(\frac{T^*\, dP^*\, dU^*_{m+1} - dP\, Y}{T\, dP\, dU_{m+1}}\right). \tag{4.52}$$

Since the denominator of E should only contain poles of P and Q_{m+1}, the following interpolation conditions must be fulfilled:

$$\frac{nE_{m+1}(p_u) dQ_m(p_u)}{T(p_u)} + dP(p_u) dU^*_{m+1}(p_u)[k_1 dQ^*_m(p_u) + k_2 dQ_m(p_u)] = 0 \tag{4.53}$$

where p_u are the poles of U_{m+1}. Because that there exist two unknowns, k_1 and k_2, in addition to the unknown coefficients of dQ_m, the eigenvalue problem defined in (4.8) can be solved by selecting k_2 as linearly separated samples within the range $-2\gamma_{m+1} < k_2 < 2\gamma_{m+1}$. Then, within these samples, $\mathscr{H}_\infty$-norm of $E(s)$ is checked and the variables that correspond to minimum $\mathscr{H}_\infty$ error are returned as the solution. Then, by using the estimated dQ_m and (4.51), corresponding nQ_m is calculated. In order to minimize the approximation error, the numerator of Q_m can be optimized by using minimax algorithms.

The aforementioned method is applied on F_a given in (4.13) in order to obtain Q_2. In Fig. 4.7, approximation errors of the proposed technique and various other methods are illustrated. Table 4.2.4 shows the $\mathscr{H}_\infty$-norm of the resulting errors. Note that none of these procedures are able to return optimal $\mathscr{H}_\infty$ solution.

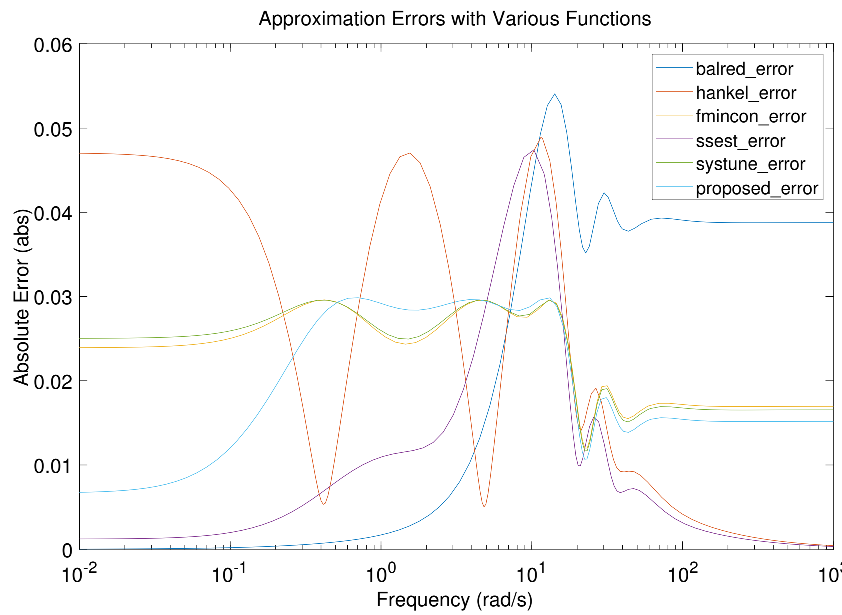

Figure 4.7: Example (4.13): Approximation errors of proposed technique and various methods

Method	**$\mathscr{H}_\infty$-norm of approximation errors**
Balanced Truncation	0.054068009431852
Hankel Norm Approximation	0.048916032296836
`ssest` Command	0.047490294465929
Proposed Method	0.029914907532992
`fmincon` Command	0.029603930130908
`systune` Command	0.029597228065033

Table 4.2: $\mathscr{H}_\infty$-norm of approximation errors for Example (4.13)

4.3 Comparison of Several Model Order Reduction Methods in $\mathscr{H}_\infty$

The approximation of the predictor filter $F(s)$ designed for the example given in section 3.1 is taken into consideration to compare several model order reductions in the literature with the proposed procedure described in section 4.2.4.

Initially, considering the infinite-dimensional nature of $F(s)$, a finite high-order approximation, denoted as $F_h(s)$, is obtained by utilizing the following finite-dimensional structures and canceling the poles in $\mathbb{C}_+$ with the approximate zeros.

$$
\begin{aligned}
N_{10}(s) &= \frac{2}{(s+1)^2}\prod_{i=1}^{10}\left(\frac{1+s\sqrt{\varepsilon^2+\frac{1}{\alpha_i^4}}+\frac{s^2}{4\alpha_i^4}}{1+\varepsilon s+\frac{s^2}{\phi_i^4}}\right), && (4.54)\\
B_{10}(s) &= \prod_{i=1}^{10}\left(\frac{2\alpha_i^4\left(\varepsilon+\sqrt{\varepsilon^2+\frac{1}{\alpha_i^4}}\right)-s}{2\alpha_i^4\left(\varepsilon+\sqrt{\varepsilon^2+\frac{1}{\alpha_i^4}}\right)+s}\right), && (4.55)\\
M_a(s) &= P_d(j\omega,5)\,B_{10}(s), && (4.56)\\
F_h(s) &= (1-H(s)M_a(s))\left(\frac{N_{10}(s)}{D(s)}\right) && (4.57)
\end{aligned}
$$

where $P_d(j\omega,5)$ represents the 5^{th} order Pade approximation of the time delay, $h_o = 0.1$. The resulting $F_h(s)$ is a 26^{th} order stable transfer function. Then, the aim is to construct a third order stable $F_{a,3}(s)$ with the least $\mathscr{H}_\infty$-norm error. 7 different approximation methods are used in order to find $F_{a,3}$:

- Balanced reduction [22]
- HNA [20]
- `systune`: The optimization techniques used in this method are given in [4].
- `fitfrd`: Details of this command can be found in [11].
- `ssest`: Detailed information can be seen in [49].

- Interpolatory $\mathscr{H}_\infty$ approximation [3]: This method basically uses IRKA to find $\mathscr{H}_2$-optimal reduced model $F_r^0(s)$ with order r, and estimates the proper constant $d_r \in \mathbb{R}$ that minimizes the $\mathscr{H}_\infty$-norm of the approximation error.

- Proposed method in section 4.2.4.

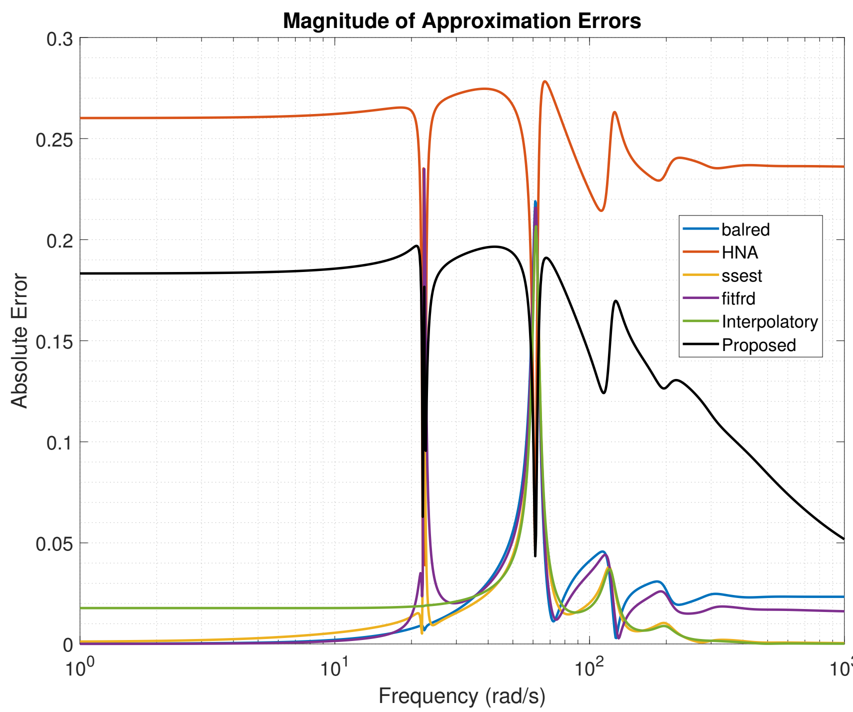

Figure 4.8: Example (4.57): Absolute approximation errors of various methods

Approximation Method	**$\mathscr{H}_\infty$-Norm of Approximation Error**
`systune`	1.421585160252459
Hankel Norm Approximation	0.278354888611445
Balanced Reduction	0.260263755367770
`fitfrd`	0.235245602705347
`ssest`	0.210723689326036
Interpolatory	0.206749701877522
Proposed	0.196935904427445

Table 4.3: Example (4.57): $\mathscr{H}_\infty$-norm of Approximation Errors of Various Methods

The third order transfer functions obtained through these methods are then optimized by applying the interior-point approach constrained minimization, which can be done by using `fmincon` command in MATLAB.

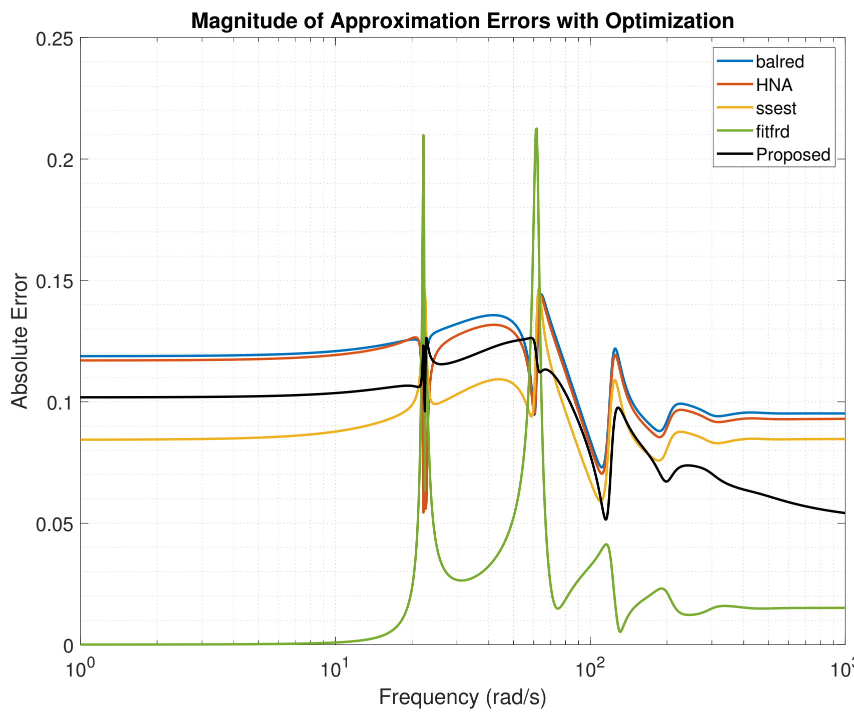

Figure 4.9: Example (4.57): Absolute approximation errors of various methods after optimization

Approximation Method	$\mathscr{H}_\infty$-Norm of Approximation Error
`systune`	1.040009603373669
`fitfrd`	0.213680480847876
Hankel Norm Approximation	0.143801635530831
Balanced Reduction	0.144247986346730
`ssest`	0.146807020029274
Proposed	0.126315419127930

Table 4.4: Example (4.57): $\mathscr{H}_\infty$-norm of Approximation Errors of Various Methods with Optimization

Note that because of its high error compared to other methods, the approximation error obtained by `systune` command is illustrated on neither Fig. 4.8 nor Fig. 4.9. Also, due to an unknown error, the result obtained by interpolatory $\mathscr{H}_\infty$ approximation method could not be optimized by the function `fmincon`. The results above show that the proposed method returns a better approximation in terms of $\mathscr{H}_\infty$-norm, especially when the order of approximation is low as chosen within this example.

Finally, the resulting third order filter obtained by the proposed procedure whose approximation error is illustrated in Fig. 4.9 is

$$F_{a,3}(s) = \frac{-0.05626\left(1-\frac{s}{479.2}\right)\left(1+0.4382\left(\frac{s}{18.3}\right)+\left(\frac{s}{18.3}\right)^2\right)}{\left(1+\frac{s}{290.8}\right)\left(1+0.01914\left(\frac{s}{22.34}\right)+\left(\frac{s}{22.34}\right)^2\right)},$$

and the properly scaled magnitude plot of $|F_h(j\omega) - F_{a,3}(j\omega)|$, where F_h is 26^{th} order as defined in (4.57), is shown in Fig. 4.10.

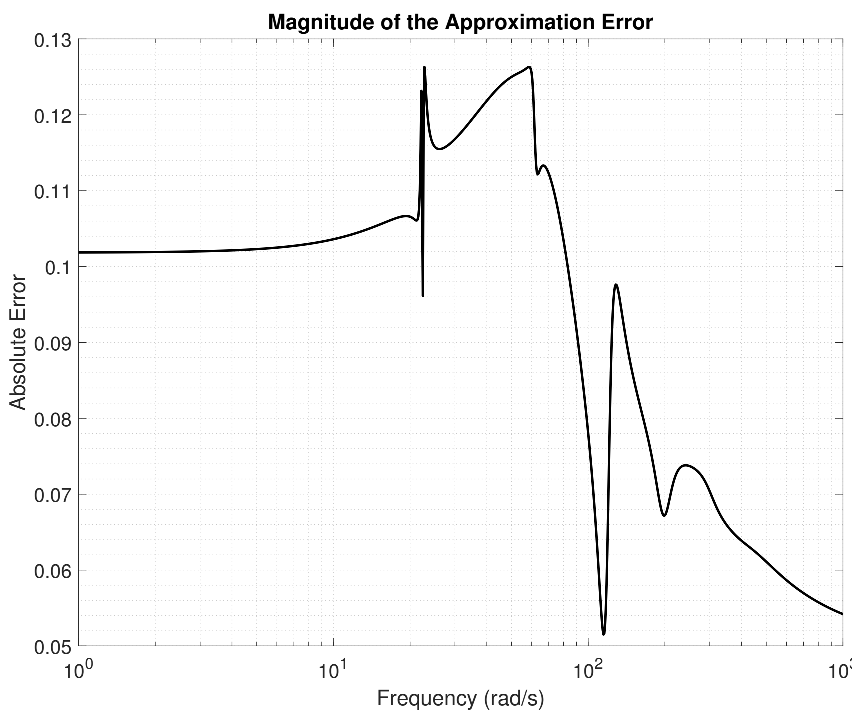

Figure 4.10: $|F_h(j\omega) - F_{a,3}(j\omega)|$, F_h is 26^{th} order as defined in (4.57)

Chapter 5

Conclusion and Future Works

Smith predictor and its modifications are a significant area of controller design due to its ability to remove the effect of dead time delay in the feedback loop from the reference signal to the plant output. However, due to the necessity of an accurate model, and low robustness against parametric uncertainty, especially in time delay, robust stability condition is a crucial aspect of such designs. In order to simplify both the controller design and robustness analysis, a new structure is proposed based on Smith principle, which is applicable on LTI SISO systems with finite order and distinct unstable poles. The haptic feedback and predictor filter provide the inner controller to be designed solely for the non-delayed nominal plant according to pre-specified performance and robustness criteria. The proposed technique uses Nevanlinna-Pick interpolation during the design of the haptic feedback $H(s)$, to both stabilize the predictor filter $F(s)$ and ease the analysis on robust stability.

The set of plants that may be robustly stabilized by the proposed design is extended for larger class of distributed parameter systems. An example on a normalized flexible beam is given to illustrate the stability analysis. As it can be seen within this example, even when the poles of the plant are non-distinct, by using proper modifications, the proposed technique can be applied. Furthermore, the construction process of the haptic feedback $H(s)$ is modified such that the configuration becomes applicable on MIMO systems, under specified conditions. In this case, instead of the classical Nevanlinna-Pick solution, tangential Nevanlinna-Pick interpolation is used to stabilize the predictor filter $F(s)$.

Another crucial aspect of this design is the approximation of infinite dimensional predictor filter to a finite order transfer function, in order to implement it on a practical system. The original filter $F(s)$ consists of an FIR and additional possibly infinite dimensional stable transfer function. During the approximation of this filter by a stable transfer function with finite order, the effect of approximation error on the robust stability of the closed loop system must be taken into consideration. To guarantee stability in such design, a boundary condition obtained by using small gain theorem is defined, which is essential on selecting the order of approximation.

Model order reduction is an extensive field of area of engineering, therefore there exists numerous methods. Approximation of FIR structures, order reduction based on $\mathscr{H}_2$-norm and $\mathscr{H}_\infty$-norm are the most commonly used techniques for this purpose. Since this study mainly focuses on robust stability analysis and optimization of robustness level, most recent $\mathscr{H}_\infty$-norm approximation methods within the literature are deeply investigated and compared during the estimation of $F_{a,r}(s)$, which is the approximation of $F(s)$ by a desired order r. Optimal $\mathscr{H}_\infty$ approximation of high or infinite dimensional structures by a low order transfer function still remains as a challenging unsolved problem. Although recent works in this area return promising results, they are still sub-optimal. Most of these methods use nonlinear optimization algorithms, in which the initial variables exert a substantial influence on the resulting error. Due to their dependence on initial variables, the minimization algorithms employed within these techniques lead to local minima instead of the global minimum, i.e. the optimal solution. A new method that basically uses the main idea behind the Nevanlinna-Pick interpolation to extract linear equations is proposed. As HNA, this method returns the optimal $\mathscr{H}_\infty$ approximation of order $(N-1)$, of an N^{th} order stable function with distinct poles. A recursive minimization algorithm based on this approach is suggested and compared with the state-of-the-art methods in the literature. In addition, the linear equations are extended to return an accurate estimation for initial variables to be used in nonlinear minimization and minimax methods.

Despite several examples are given on the expansion of the set of systems to which this design can be applied, this set may still be extended further. As future work, the feasibility of this configuration with nonlinear systems, time-varying plants, and MIMO structures with internal time delays may be thoroughly examined. Especially systems with time-varying delay are challenging to be stabilized by Smith predictor based structures, due to the necessity of an accurate nominal plant model within the design of the predictor. However, such systems may be stabilized by using a modified version of the proposed configuration, in which the haptic filter and the predictor also vary with time such as the adaptive control designs.

The method proposed within section 4.2 provides a new perspective against $\mathscr{H}_\infty$-norm approximation and returns promising results. This method may clearly be further developed by applying proper optimization techniques. Furthermore, as suggested in section 4.2, various conditions or assumptions can be introduced to achieve more accurate results. Naturally, an appropriate optimization algorithm may also be employed in order to minimize the $\mathscr{H}_\infty$-norm of approximation error, as illustrated in section 4.3.

Bibliography

[1] E. J. Adam, H. A. Latchman and O. D. Crisalle, "Robustness of the Smith predictor with respect to uncertainty in the time-delay parameter," *Proc. of the 2000 American Control Conference*, Chicago IL, pp. 1452–1457, June 2000.

[2] A. C. Antoulas, *Approximation of large-scale dynamical systems*, SIAM, Philadelphia, 2005.

[3] A. C. Antoulas, C. A. Beattie and S. Güğercin, *Interpolatory Methods for Model Reduction*, Society for Industrial and Applied Mathematics, Philadelphia PA, 2020.

[4] P. Apkarian and D. Noll, "Nonsmooth optimization for multiband frequency-domain control design," *Automatica*, vol. 43, pp. 724–731, 2007.

[5] P. Apkarian and D. Noll, "Robust Control of Systems with Hyperbolic Partial Differential Equations," arXiv:2211.08083v1 [math.OC] 15 Nov 2022.

[6] J. A. Ball, I. Gohberg and L. Rodman, *Interpolation of Rational Matrix Functions*, Springer Basel AG, 1990.

[7] B. Beliczynski, I. Kale, and G. D. Cain, "Approximation of FIR by IIR digital filters: An algorithm based on balanced model reduction," *IEEE Transactions on Signal Processing*, pp. 532–542, Mar. 1992.

[8] A. K. Belyaev, A. V. Fedotov, H. Irschik, M. Nader, V. A. Polyanskiy and N. A. Smirnova, "Experimental study of local and modal approaches to active vibration control of elastic systems," *Struct. Control Health Monit.*, vol. 25, e2105, 2018.

[9] P. Benner, S. Grivet-Talocia, A. Quarteroni, G. Rozza, W. Schilders and L. Silveira, *System- and data-driven methods and algorithms*, De Gruyter, Berlin, 2021.

[10] J. Bontsema, R. F. Curtain, J. M. Schumacher, "Robust Control of Flexible Structures: a case study," *Automatica*, vol. 24, pp. 177–186, 1988.

[11] S. Boyd and L. Vandenberghe, *Convex optimization*, Cambridge University Press, 2004.

[12] N. L. Brace, N. B. Andrews, J. Upsal and K. A. Morgansen, "Sensor Placement on a Cantilever Beam Using Observability Gramians," *Proc. 61st IEEE Conference on Decision and Control (CDC)*, Cancun, Mexico, pp. 388–395, Dec. 2022.

[13] E. Crépeau and C. Prieur, "Control of a Clamped-Free Beam by a Piezoelectric Actuator," *ESAIM: Control, Optimisation and Calculus of Variations*, vol. 12, pp. 545–563, July 2006.

[14] R. Curtain and K. Morris, "Transfer functions of distributed parameter systems: A tutorial," *Automatica*, vol. 45, pp. 1101–1116, 2009.

[15] R. Curtain and H. Zwart, *An Introduction to Infinite-Dimensional Linear Systems Theory*, Springer-Verlag, New York, 1995.

[16] V. de Oliveira, A. Nicoletti and A. Karimi, "Robust Smith predictor design for time-delayed systems with H_∞ performance," *Recent Results on Time Delay Systems*, E. Witrant, E. Fridman, O. Sename, L. Dugard Eds., Advances in Delays and Dynamics, vol. 5, no. 15, pp. 287–307, Springer, Cham, 2016.

[17] J. Doyle, B. Francis and A. Tannenbaum, *Feedback Control Theory*, Macmillan, NY, 1990.

[18] C. Foias, H. Özbay and A. Tanennbaum, *Robust Control of Infinite Dimensional Systems: Frequency Domain Methods*, Springer-Verlag, London, 1996.

[19] P. Garcia and P. Albertos, "Robust tuning of a generalized predictor-based controller for integrating and unstable systems with long time-delay," *Journal of Process Control*, vol. 23, no. 8, pp. 1205–1216, Sep. 2013.

[20] K. Glover, "All optimal Hankel-norm approximations of linear multi-variable systems and their L_∞-error bounds," *International Journal of Control*, vol. 39, no. 6, pp. 1115–1193, 1984.

[21] M. Golomb, "Lectures on theory of approximation," *Argonne National Laboratory*, Applied Mathematics Division, 1962.

[22] M. Green, "A relative error bound for balanced stochastic truncation," *IEEE Transactions on Automatic Control*, vol. 33, no. 10, 1988.

[23] B. Gustavsen, "Rational approximation of frequency domain responses by vector fitting," *IEEE Transactions on Power Delivery*, vol. 14, no.3, pp. 1052–1061, 1999.

[24] S. Güğercin and A. C. Antoulas, "A survey of model reduction by balanced truncation and some new results," *International Journal of Control*, vol. 77, no. 8, pp. 748–766, 2004.

[25] Y. Halevi, "Control of Flexible Structures Governed by the Wave Equation Using Infinite Dimensional Transfer Functions," *ASME. J. Dyn. Sys., Meas., Control.*, vol. 127, No. 4, pp. 579–588, December 2005.

[26] C. Harkort and J. Deutscher, "Finite-dimensional observer-based control of linear distributed parameter systems using cascaded output observers," *International Journal of Control*, Vol. 84, No. 1, pp. 107–122, January 2011.

[27] I. Karafyllis and M. Krstic, "Delay-robustness of linear predictor feedback without restriction on delay rate," *Automatica*, vol. 49, no. 6, pp. 1761–1767, 2013.

[28] I. Karafyllis and M. Krstic, *Predictor feedback for delay systems: Implementations and approximations*, Birkhauser, Basel, 2017.

[29] R. Katz and E. Fridman, "Delayed finite dimensional observer based control of 1D parabolic PDEs via reduced order LMIs," *Automatica*, vol. 142, 110341, 2022.

[30] J. Lam, "Convergence of a class of Padé approximations for delay systems," *International Journal of Control*, pp. 989–1008, 1990.

[31] V. Léchappé, E. Moulay, F. Plestan, A. Glumineau and A. Chriette, “New predictive scheme for the control of LTI systems with input delay and unknown disturbances,” *Automatica*, vol. 52, pp. 179–184, Feb. 2015.

[32] K. Lenz and H. Özbay, “Analysis and robust control techniques for an ideal flexible beam,” *Multidisciplinary Engineering Systems: Design and Optimization Techniques and their Applications*, C. T. Leondes ed., Academic Press Inc., pp. 369–421, 1993.

[33] K. Lenz, H. Özbay, A. Tannenbaum, J. Turi and B. Morton, “Frequency domain analysis and robust control design for an ideal flexible beam,” *Automatica*, vol. 7, No. 6, pp. 947–961, November 1991.

[34] S. Levin and Y. Halevi, “Finite Dimension Models of Flexible Structures,” *Proceedings of the 2023 European Control Conference (ECC)*, Bucharest, Romania, June 2023, doi: 10.23919/ECC57647.2023.10178293

[35] H. Lhachemi and C. Prieur, “Predictor-based output feedback stabilization of an input delayed parabolic PDE with boundary measurement,” *Automatica*, vol. 137, 110115, 2022.

[36] M. R. Matausek and A. D. Micic, “A modified Smith predictor for controlling a process with an integrator and long dead-time,” *IEEE Trans. on Automatic Control*, vol. 41, no. 8, pp. 1199–1203, Aug. 1996.

[37] G. Meinsma, and H. Zwart, “On H_∞ control for dead-time systems”, *IEEE Trans. on Automatic Control*, vol. 45, no. 2, pp. 272–285, 2000.

[38] W. Michiels and H. U. Ünal, “Evaluating and Approximating FIR Filters: An Approach Based on Functions of Matrices,” *IEEE Transactions on Automatic Control*, pp. 463–468, 2015.

[39] L. Mirkin and N. Raskin, “Every stabilizing dead-time controller has an observer–predictor-based structure,” *Automatica*, vol. 39, no. 1, pp. 1747–1754, Oct. 2003.

[40] B. C. Moore, “Principal component analysis in linear systems: Controllability observability and model reduction,” *IEEE Transactions on Automatic Control*, pp. 17–31, 1981.

[41] K. A. Morris, *Controller Design for Distributed Parameter Systems*, Springer, Cham, 2020.

[42] M. Nagahara and Y. Yamamoto, “FIR digital filter design by sampled-data $\mathscr{H}_\infty$ discretization,” *IFAC Proceedings Volumes*, vol. 47, Issue 3, pp. 3110–3115, 2014.

[43] J. E. Normey-Rico and E. F. Camacho, “A unified approach to design dead-time compensators for stable and integrative processes with dead-time,” *IEEE Trans. on Automatic Control*, vol. 47, no. 2, pp. 299–305, Aug. 2002.

[44] J. E. Normey-Rico and E. F. Camacho, “Dead-time compensators: A survey,” *Control Engineering Practice*, vol. 16, no. 4, pp. 407–428, Apr. 2008.

[45] H. Özbay, S. Gümüşsoy, K. Kashima and Y. Yamamoto, *Frequency Domain Techniques for H-Infinity Control of Distributed Parameter Systems*, SIAM, Philadelphia, PA, 2018.

[46] J. R. Partington, “Some frequency-domain approaches to the model reduction of delay systems,” *Annual Reviews in Control*, pp. 65–73, 2004.

[47] D. L. Russell, “On mathematical models for the elastic beam with frequency-proportional damping,” *Control and Estimation in Distributed Parameter Systems* H. T. Banks (Ed.), SIAM, Philadelphia PA, 1992.

[48] R. Sanz, P. Garcia and P. Albertos, “A generalized Smith predictor for unstable time-delay SISO systems,” *ISA Transactions*, vol. 72, pp. 197–204, Jan. 2018.

[49] G. Scarciotti, Z. Jiang and A. Astolfi, “Data-driven constrained optimal model reduction,” *European Journal of Control*, vol. 53, pp. 68–78, 2020.

[50] M. F. Shakib, G. Scarciotti, M. Jungers, A. Y. Pogromsky, A. Pavlov and N. van de Wouw, “Optimal $\mathscr{H}_\infty$ LMI-based model reduction by moment matching for linear time-invariant models,” *60th IEEE Conference on Decision and Control*, Austin, TX, USA, pp. 6914–6919, 2021.

[51] A. A. Siranosian, M. Krstic, A. Smyshlyaev and M. Bement, “Motion Planning and Tracking for Tip Displacement and Deflection Angle for Flexible Beams,” *ASME. J. Dyn. Sys., Meas., Control*, vol. 131, No. 3, 031009, May 2009.

[52] O. J. M. Smith, “Closer control of loops with dead time,” *Chemical Engineering Progress.*, vol. 53, no. 5, pp. 217–219, 1957.

[53] A. Smyshlyaev, B-Z. Guo and M. Krstic, “Arbitrary decay rate for Euler-Bernoulli beam by backstepping boundary feedback,” *IEEE Trans. Automatic Control*, vol. 54, No 5, pp 1134–1140, May 2009.

[54] O. Toker and H. Özbay, “$\mathscr{H}_\infty$ optimal and suboptimal controllers for infinite dimensional siso plants,” *IEEE Trans. Automatic Control*, vol. 40, pp. 751–755, 1995.

[55] L. N. Trefethen, “Rational Chebyshev approximation on the unit disk,” *Numerische Mathematik*, vol. 37, pp. 297–320, 1981.

[56] K. Watanabe and M. Ito, “A process-model control for linear systems with delay,” *IEEE Trans. on Automatic Control*, vol. 26, no. 6, pp. 1261–1269, Dec. 1981.

[57] N. Wong, and C. Lei, “IIR Approximation of FIR Filters Via Discrete-Time Vector Fitting.” *IEEE Transactions on Signal Processing*, pp. 1296–1302, 2008.

[58] M. O. Yeğin and H. Özbay, “Numerical computation of $\mathscr{H}_\infty$ optimal controller for time delay systems using Yalta,” *IFAC-PapersOnLine*, vol. 49, no. 10, pp. 182–187, 2016.

[59] M. O. Yeğin and H. Özbay, “On Smith predictor based controllers for plants with time delay and multiple unstable modes,” *Systems & Control Letters*, vol. 172, 105453, 2023.

[60] Q.-C. Zhong, “Unified Smith predictor for dead-time systems,” *IFAC Proceedings Volumes*, vol. 36, no. 19, pp. 83–86, (Proc. of the 4th IFAC Workshop on Time Delay Systems), Rocquencourt, France, Sep. 2003.

[61] Q. Zhong and G. Weiss, “A unified Smith predictor based on the spectral decomposition of the plant,” *Int. Journal of Control*, vol. 77, no. 15, pp. 1362–1371, 2004.